Investigation of Keratin and Keratin-Containing Composite Biomaterials: Applications in Peripheral Nerve Regeneration

Nils Andrew Potter

Dissertation Submitted to the Faculty of
Virginia Polytechnic Institute and State University
in partial fulfillment of the requirements for the degree of

Doctor of Philosophy
in
Biomedical Engineering

Mark Van Dyke, Chair
Kevin J. Edgar
Earl Johan Foster
Blake Johnson
Thomas L. Smith

October 17, 2019
Blacksburg, Virginia

Keywords: Keratin, Purification, Hydrogel, Type I Collagen, Schwann Cell, Peripheral Nerve Regeneration

Investigation of Keratin and Keratin-Containing Composite Biomaterials: Applications in Peripheral Nerve Regeneration

Nils A. Potter

Abstract

Keratins are a family of structural proteins that can be extracted from a variety of sources including wool, nails, skin, hooves, and hair. Keratin can be processed into different constructs such as coatings, scaffolds, and hydrogels, and has shown favorable results when placed in *in vitro* and *in vivo* settings for different tissue regeneration applications.

Over three decades, keratin extraction technology has been continuously modified, and these differences in extraction processes have distinct effects on the characteristics of the end product. In this work, we examine the effect of keratin aggregation during a widely-used purification step, dialysis ultra-filtration, on material characteristics of the final keratin product when fabricated into a hydrogel. Two distinct dialysis procedures were applied during the extraction of oxidized keratin (keratose): one promoting protein aggregation and the other mitigating it. Analyses of material properties such as mechanical and enzymatic stability were conducted in addition to observing the differences in solution behavior between products. Data revealed that protein aggregation during the extraction process has a profound effect on keratose hydrogel material properties.

After determination of the effect of protein aggregation during extraction on keratose hydrogels, investigation of how a blended material comprised of said keratose and type I collagen was undertaken. It was hypothesized that a blend would result in mixing at the molecular level, resulting in improved properties compared to either pure material alone. A

protocol was created to make stable keratose/type I collagen blends and material characterization techniques were applied to determine the inherent properties of samples with differing ratios. Crosslinking density, mechanical properties, enzymatic degradation properties, water uptake capacity, structural architecture, and thermal properties were all assessed. In addition, the ability of this material to maintain cell viability was conducted. Results showed that the addition of type I collagen has a significant effect on the properties of hydrogel blends with keratose compared to the pure keratose system. This was mostly evident with hydrogel mechanical stability and material architecture.

Finally, the ability to use this hybrid material as a luminal filler for a nerve conduit during peripheral nerve regeneration was explored in an *in vitro* setting. The ability of this blend to promote Schwann cell viability was assessed in addition to determining the ability of these cells to attach and migrate through the material matrix. These experiments demonstrate proof-of-concept for the application of using keratose/type I collagen matrices as a luminal filler in peripheral nerve guidance conduits.

Investigation of Keratin and Keratin-Containing Composite Biomaterials: Applications in Peripheral Nerve Regeneration

Nils A. Potter

General Audience Abstract

Keratins are a family of structural proteins that can be extracted from wool, skin, nails, and hair, and that have been investigated in the field of tissue regeneration. Humans make several types of keratins, so it has a natural acceptance by the body and its inflammatory and immune systems. However, keratins can be hard to make and process into useful products. Many methods for producing keratin biomaterials have been developed over the past 30 years, but most of them are not ideal. This work sought to explore a production method that addresses a particular problem, that of protein aggregation during purification. In so doing, methods can be optimized to create more useful keratin biomaterials.

Experiments comparing preparation methods that maximize and minimize protein aggregation were compared. Data showed that minimizing aggregation leads to better biomaterial characteristics, thus demonstrating the potential impact of targeting this processing step. However, even after optimization of purification, keratins still have limitations. Most notably their mechanical strength is not as great as some other materials. A typical approach to address this in other systems has been by blending. In the present work, we explored a blend made from keratin and type 1 collagen.

A method was developed to effectively blend keratin and collagen and create stable mixtures that yielded protein-to-protein coordination. Such interactions typically yield beneficial material characteristics such as increased strength. Data showed that intimate mixing of the two

proteins was achieved, and resulting characteristics were improved compared to either pure material.

Finally, studies were conducted to assess the potential for keratin/collagen blends to be used to regenerate injured nerves. A common method is to enclose the ends of a cut nerve into a tube and let the nerve re-grow through the tube to its target muscle. An important characteristic is an ability for cells to populate the interior of the tube and help the nerve fibers grow. In the present study, we investigated the behavior of a particularly important cell, the Schwann cell, to attach, move and grow through a keratin/collagen biomaterial. Data showed good cell behavior, suggesting that the material could be used in a medical product for nerve repair.

Table of Contents

Acknowledgements

I would like to acknowledge all my friends, family, colleagues, and mentors for their roles in getting me to this point in my academic career. Looking back at myself from when I was entering Virginia Tech as a first-year graduate student and comparing that to now, the differences are certainly evident in a positive way. I have undoubtedly grown as a student, researcher, and person, and you all have been a great influence on my overall growth. To my parents, thank you for your love and encouragement throughout this entire process. I know it must have been quite the change to see that your oldest son would no longer be within earshot of you all as I had been for my entire life, but you all took that in stride and continued to cheer me on. To my brother, Anders, I am extremely grateful to see what our relationship has turned into throughout my graduate career. Thank you for always being the person I know I could always talk to about anything no matter how serious or stupid. My time at VT has allowed me to meet and befriend some fantastic people. Eamon, Megan B., Jaclyn, Jake, Davy, Evan M. – thank you for your near immediate and continued friendship. You all made the transition from Tennessee to VT smooth and painless. Nora, Amanda, Emily, Sabah, Lauren, Ryan, Ty, Evan W., Megan C., Tim, Rob, Jamelle, and so many others along the way, thank you all for your friendship. You all made life better throughout my time here. For my friends in the lab Michele, Alexis, Marc, and Scott – you all always made days fun even when experiments would not want to work. For my committee members Dr. Kevin Edgar, Dr. Johan Foster, Dr. Blake Johnson, and Dr. Thomas Smith – thank you for your guidance and expertise. For my advisor Dr. Mark Van Dyke – thank you for your unparalleled patience and always offering your knowledge and wisdom to me whenever I needed it. It has truly aided me in becoming a better scientist.

Although my time here is coming to an end, the future does not seem so frightening. For me, it seems hopeful, and all the people mentioned above and more have more than contributed to that hopeful feeling. So again, with my deepest gratitude, I thank you all for everything you have done for me.

List of Figures and Tables

Chapter 1: Introduction

Chapter 2: Effects of Differing Purification Methods on Properties of Keratose Biomaterials

Chapter 3: Fabrication and Characterization of a Novel Keratose-Type I Collagen Biomaterial

Chapter 4: Schwann Cell Behavior and Interaction with a Keratose/Type I Collagen Material

Abbreviations (Alphabetized)

ACS	Absorbable Collagen Sponge
ANOVA	Analysis of Variance
APB	Abductor Pollicis Brevis
BDDE	1,4-Butanediol Diglycidyl Ether
BEAM	Biomedical Engineering and Mechanics
bFGF	Basic Fibroblast Growth Factor
BKOS	Buffer Dialyzed Keratose
BMP	Bone Morphogenetic Protein
BMSC	Bone Mesenchymal Stem Cell
BSA	Bovine Serum Albumin
CMAP	Compound Muscle Action Potential
CNS	Central Nervous System
COL	Type I Collagen
DAPI	4′,6-Diamidino-2-Phenylindole
DLS	Dynamic Light Scattering
DMEM	Dulbecco's Modified Eagle Media
DMSO	Dimethyl Sulfoxide
ECM	Extracellular Matrix
EDC	1-Ethyl-3-Dimethylaminopropyl Carbodiimide Hydrochloride
FBS	Fetal Bovine Serum
FITC	Fluorescein Isothiocyanate
FTIR	Fourier-Transform Infrared Spectroscopy
GATA6	GATA Binding Protein
Gly	Glycine
HA	Hyaluronic Acid
hCSC	Human Cardiac Stem Cell
HDF	Human Dermal Fibroblast
IF	Intermediate Filament

IGF-1	Insulin-Like Growth Factor
IgG	Immunoglobulin
KAP	Keratin Associated Protein
KOS	Keratose
KTN	Kerateine
LVEF	Left Ventricular Ejection Fraction
LVER	Linear Viscoelastic Region
MI	Myocardial Infarction
MPC	Muscle Progenitor Cell
MRSA	Methicillin-Resistant *S. Aureus*
MW	Molecular Weight
NGF	Nerve Growth Factor
PAA	Peracetic Acid
PBS	Phosphate Buffered Saline
PCL	Poly(ε-caprolactone)
PEG	Poly(ethylene glycol)
PEO	Poly(ethylene oxide)
PFA	Paraformaldehyde
PLA	Poly(L-lactic acid)
PLGA	Poly(lactic-co-glycolic acid)
PNS	Peripheral Nervous System
Pro	Proline
qPCR	Quantitative Polymerase Chain Reaction
rhBMP	Recombinant Bone Morphogenetic Protein
RT	Room Temperature
SC	Schwann Cell
SD	Standard Deviation
SEC	Size-exclusion Chromatography
SEM	Scanning Electron Microscopy
SM-MHC	Smooth Muscle - Myosin Heavy Chain

SSD	Silver Sulfadiazine Cream
TA	Tibialis Anterior
TCP	Tissue Culture Plastic
TERM	Tissue Engineering and Regenerative Medicine
TFF	Tangential Flow Filtration
TGA	Thioglycolic Acid
TGF-β	Transforming Growth Factor Beta
VSMC	Vascular Smooth Muscle Cell
WKOS	Water Dialyzed Keratose

Specific Aims

In contrast to the central nervous system (CNS), the peripheral nervous system (PNS) has the inherent ability to repair itself following injury. To promote peripheral nerve regeneration, nerve autografts or nerve conduit devices have been utilized. Autografts are currently recognized as the clinical gold standard because they have been shown to promote functional recovery, but numerous limitations are present with this approach such as tissue availability and loss of sensation when a donor nerve is harvested. To provide an alternative that does not require graft harvest, nerve conduits have been created from either synthetic polymers such as polyglycolic acid (PGA) or from natural polymers like collagen (NeuraGen®). As an extension of the conduit concept, luminal fillers have been investigated to augment outcomes toward the level of function obtained from autograft. While filling a conduit with a matrix has shown improvements over empty conduits in preclinical testing, only one filler material has achieved outcomes equivalent to autograft, and no product has translated into clinical use.

The only matrix filler to achieve functional outcomes equivalent to autograft is a keratin-based biomaterial. In previous testing, functional and histologic outcomes similar to or better than autograft were obtained in mouse, rat, and rabbit models. The oxidized keratin (KOS) matrix used in these studies was further tested successfully in non-human primates but has not been used in humans. Recently, our group has improved the process for making keratin, which resulted in KOS hydrogels with improved mechanical properties (made from so-called "keratin nanomaterial"). The KOS can be combined with a small amount of type I collagen (COL) to provide a luminal filler with optimized mechanical properties, porosity for cell infiltration and remodeling, as well as a controlled degradation rate. We hypothesize that this KOS/COL composite matrix can serve as an effective filler for conventional nerve conduits. Reaching this goal will facilitate further investigation of a medical device for peripheral nerve repair that may simplify surgical techniques compared to autograft, and produce patient outcomes similar to the current clinical gold standard

Our long-term goal is to develop a medical device capable of simplifying peripheral nerve repair while producing functional outcomes for patients that are equivalent to or better than autograft. We hypothesize that a KOS/COL matrix, used to fill the lumen of a conventional conduit, will provide structural support and routes for infiltrating regenerative cells, while at the same time resisting rapid enzyme-mediated degradation such that degradation rate can be more closely matched to the rate of nerve regeneration. This hypothesis will be tested by the following aims:

Aim 1: Compare and contrast the mechanical and enzyme-mediated degradation properties of KOS hydrogels made from conventional keratin and keratin nanomaterial

Aim 2: Investigate the mechanical and enzyme-mediated degradation properties of a KOS/COL composite and assess its potential to be used as a conduit filler

Aim 3: Investigate the capacity of a KOS/COL composite matrix to support nerve cell infiltration, migration, attachment and growth in vitro

Introduction

Nils A. Potter

1.1. Introduction

Facilitating tissue regeneration typically requires the use of a support system for cells. Tissue engineering and regenerative medicine (TERM) approaches have historically utilized biomaterials of different types, broadly characterized as either natural or synthetic. There are benefits and challenges with either broad category of biomaterial, and both have found utility in numerous TERM technologies. One successful approach uses either autografts or allografts, but issues such as tissue availability and potential loss of sensation (for autografts) and immunological responses and donor rejection (for allografts) remain as unsolved challenges. In particular, modification of allografts has been viewed as a potential solution. By extension, the components of allografts, or extracellular matrix (ECM)-based biomaterials, have been extensively investigated as allograft surrogates in which composition, properties, and biological response can be better controlled.

1.2. Allografts and Xenografts

Allografts have been widely used as a solution to various tissue regeneration problems and are specifically popular in orthopedic reconstructive surgeries such as anterior cruciate ligament (ACL) repair [1]. Common allografts used for this purpose are typically prepared as fresh-frozen grafts, which are sterilely explanted from donors, cultured, soaked in antibiotic solution, and then frozen [26]. Disadvantages of fresh-frozen grafts, however, are that the residing cellular environment of the allograft can interfere with the indigenous tissue and ultimately lead to a faulty implant. Decellularized, fresh-frozen allografts for ACL repair were used in a rabbit model and compared to controls of normal fresh-frozen samples. From these comparisons, it was shown that the decellularized samples allowed for a statistically significant

improvement in ultimate load and stiffness after 12 weeks of implantation; in addition, vascularity was denser in the decellularized samples [9].

To attempt to circumvent the issues associated with allografts, grafts taken from animals, known as xenografts, have been explored as potential solutions since the early 20th century [27]. Advantages xenografts have over autografts and allografts are there is no availability shortage and the host species that the graft is taken from can be genetically altered to improve compatibility [28]. Prior to exploring genetic modification of donor species, attempts were made to use animal organs as replacements for human organs with minimal success. Reemtsma *et al.* attempted to perform chimpanzee kidney xenotransplantation surgeries into human patients, but most of the surgeries resulted in failure after 4-8 weeks, and the one patient who managed to survive after this initial period died after 9 months [29]. For xenografts, the most common animal species used are pigs due to a multitude of factors such as constant availability, comparable organ size to humans, close anatomical and physiological resemblance to humans, and low risk of xenozoonosis [27]. Heart valves from porcine sources have been popular candidates for heart valve replacement and have shown promise in clinical settings with older patients (>70 y) [30]. With pigs as the host species, however, the risk of introducing the alpha-gal epitope (Galalpha1-3Galbeta1-(3)4GlcNAc-R) into humans is undesirable and can lead to adverse immunological responses due to the function of the alpha-gal antibody found in humans [31]. To avoid this, genetic alteration of pigs has been explored by aiming to create Gal knockout pigs. These have demonstrated some success when organs from these pigs were transplanted into primates, but more work needs to be conducted in this field to create more viable pig xenografts [32].

1.3. Extracellular Matrix-Based Biomaterials

When autografts, allografts, and xenografts are not seen as feasible solutions for tissue regeneration purposes, the next course of action is to apply biomaterials to the site of interest. Biomaterials consist of many different material makeups including metals, ceramics, and plastics. ECM-based biomaterials have gained a large amount of traction in TERM as they closely resemble the cellular and tissue environment *in vivo* and are highly tunable depending on the purpose [33]. Common ECM-based biomaterials for tissue regeneration purposes include collagen, hyaluronic acid (HA), cellulose, and fibrin [34-37].

Like allografts and xenografts, however, issues remain with ECM-based biomaterials pertaining to disease transmission and immunological response. Similar to allografts, it is imperative that endogenous cells, cytosolic proteins, nucleic acids, and organelles must be removed from the ECM material prior to implantation to mitigate the potential for adverse immune response [38]. In contrast, however, these biomaterials and their inherent characteristics can be highly manipulated through applying different extraction processes to enhance purity, loading with drug molecules and/or cells to provide therapeutic effects, and adding crosslinking molecules to improve mechanical properties and degradation kinetics. Another issue that arises is the cost of these biomaterials. Frequently, these biomaterials are purchased from lab quality suppliers such as Thermo Fisher Scientific and Millipore Sigma, and the price per milligram of popular biomaterials such as collagen and laminin is not ideal. Recombinant synthesis of these biomaterials could aid in alleviating problems associated with implant immune response as the synthesis procedure acts to exactly copy the molecular makeup of the indigenous materials in the body [39]. Unfortunately, this is not much of a solution at this time as the cost of recombinant synthesis is exorbitant compared to obtaining these materials from commercial sources. **Table**

1.1 lists common ECM-based biomaterials, their molecule class, extraction sources, and price/milligram.

Table 1.1: Common ECM biomaterials used in tissue regeneration and their extraction sources along with their commercial price per mg. Prices were taken from lab quality suppliers including Thermo Fisher Scientific and Millipore Sigma.

ECM Material	**Molecule Class**	**Extraction Sources**	**Price/mg**
Cellulose	Polysaccharide	Plant	$
Collagen	Protein	Bovine, human, marine, murine, porcine	$$$-$$$$
Recombinant Collagen	Protein	Bacteria	$$$$$$
Elastin	Protein	Bovine, human, murine	$$-$$$$$
Fibrin/Fibrinogen	Protein	Bovine, human, murine	$$$
Hyaluronic Acid	Glycosaminoglycan	Bovine, galline	$$$-$$$$
Laminin	Protein	Human, murine	$$$$$

Of the materials listed in **Table 1.1**, cellulose has the lowest price/mg, but it is not the ideal choice as a degradable biomaterial for tissue regeneration. Cellulose is extracted from plants and not animals and consequently is not biodegradable in humans [36]. A material that has gained traction for usage in TERM applications is keratin. Regarding price, keratin extracted from human sources is on the same level as cellulose, and it is readily degradable when implanted *in vivo* [5,6]. Keratins have shown notable cell and tissue compatibility, but historically have been difficult to process and offer a limited range of properties. Modification or blending keratin with other materials may offer advantages, and this has been done in limited cases. Examples of materials keratin has been blended with include silk, poly(ε-caprolactone)

(PCL), alginate, and poly(ethylene oxide) (PEO) [11-13, 52]. Keratin blends with other protein biomolecules such as type I collagen (COL) have not been explored. Since COL makes up a large portion of the ECM, contributes as a primary load bearing component within the ECM, and has shown to be unharmful to indigenous tissue as a biomaterial, the blending of keratin and COL together could prove to be advantageous when attempting to overcome the deficiencies of keratin.

1.4. Biomaterials for Nerve Regeneration

A popular area for the use of biomaterials has been in peripheral nerve regeneration. Many differing approaches have been applied to this including using biomaterials as hydrogels for peripheral nerve conduit luminal fillers [39]. During peripheral nerve injury, a void area is created between the distal and proximal injury sites. If the void area has a length less than 3 cm between injury sites, a common treatment method is to use conduits to bridge this gap and allow for facilitated regeneration. The primary motivation for using biomaterial hydrogels as luminal fillers to aid in regeneration is to improve conduit efficacy by potentially extending the operational distance during surgery along with providing a physical environment to guide the migration of SCs and axons [40].

Numerous biomaterials have been implemented as luminal fillers for peripheral nerve conduits, and a few instances are listed in **table 1.2**.

Table 1.2: Prior peripheral nerve conduit luminal filler materials along with the type of conduit used, animal model, and repaired nerve.

Filler Material	Conduit	Animal Model	Repaired Nerve	Reference
Fibrin	Silicone	Rat	Sciatic	[41]
Laminin	Silicone	Rat	Sciatic	[42]
Collagen	Silicone	Rat	Sciatic	[43]
Collagen	PGA	Rat	Peroneal	[44]
Polyamide Filaments	Silicone	Rat	Sciatic	[45]
Bioglass 45S5	Silastic	Rat	Sciatic	[46]

Biomaterials used as luminal fillers have been reviewed in great detail elsewhere [40,47-49]. The most popular of ECM biomaterials used for this purpose primarily include fibrin, laminin, and collagen [40]. To attempt to mimic the body's natural response to peripheral nerve injury, Williams *et al.* filled silicone conduits with dialyzed plasma to allow for the formation of a fibrin matrix. This addition of dialyzed plasma to the conduit system allowed for greater migration of SCs along with a greater length of axonal regeneration and myelination after 17 days in a 10 mm rat sciatic nerve model [41]. Madison *et al.* found that laminin could be used as a viable luminal filler material. In this study, Sprague-Dawley rats had a 20-25 mm nerve defect created, which was bridged using a silicone conduit filled with either nothing, 80% laminin gel, or a collagen matrix. Results showed that laminin gels allowed for a greater amount of dorsal root ganglia (DRG) to migrate from the proximal injury site compared to the other treatment groups [42]. Rosen *et al*. explored the effect of a collagen filled PGA conduit when repairing a rat peroneal nerve over a 5 mm gap. Collagen filled conduits and autografts were the two

treatments in this study. Following the 11-12 months allotted for long term regeneration, the collagen filled conduits were compared to the autograft group, and it was determined that the axon count and integrated monophasic compound action potential were statistically similar suggesting that collagen can be used as a viable luminal filler [44]. To assess the effect of luminal filler concentration, Labrador *et al*. explored using different concentrations of collagen gels and laminin gels. Results of using these differing concentrations in a sciatic mouse animal model revealed that a lower concentration of collagen (1.28 mg/ml) resulted in greater levels of reinnervation than higher concentrated samples (1.92 and 2.56 mg/ml). Also, the same trend was observed with laminin gels (4 mg/ml compared to 12 mg/ml) [50]. Different materials have also been applied as luminal fillers, and one material that has gained more traction in this field is keratin from human hair.

1.5. Keratin Biomaterials for Nerve Regeneration

Keratin biomaterials have been used as conduit luminal fillers to repair defects in peripheral nerves following crushing or laceration injuries. Sierpinski *et al*. investigated this regenerative potential in a Webster mouse animal model [23]. For *in vitro* work, qPCR was used to monitor gene expression changes in Schwann cells (SCs) when cultured in KOS-containing media. 1 mg/ml of KOS-containing media resulted in significant upregulation of S100β and CD104, which are responsible for calcium homeostasis and SC-axon communication, respectively. In the *in vivo* model, animals were implanted with empty conduits, KOS hydrogel filled conduits, or autografts. Following 6 weeks of regeneration, the KOS group was found to exhibit a significantly shorter conduction delay and a significantly greater amount of amplitude recovery of the nerve impulse compared to the empty control group. Also, the KOS groups resulted in significantly greater nerve area, axon density, and amount of blood vessels compared

to both the empty control and the autograft groups. In addition to this, Apel *et al.* observed the effects of KOS as a luminal filler using a mouse model for a long-term regeneration study. After 6 months post-surgery, KOS filled conduits were shown to exhibit statistically equivalent compound motor action potential (CMAP) measurements to sural nerve autograft treatments. In addition, KOS filled conduits resulted in greater axon density and larger axon average diameter at 6 months compared to the sural nerve autograft and saline control treatments [51].

To build upon these studies, Pace *et al*. looked into the effects of KOS hydrogels on early cellular response in a Sprague Dawley rat animal model [24]. In this model, it was determined that P75 expression after 3 days following conduit implantation was upregulated within the proximal nerve in KOS hydrogel group compared to the saline control group. Also, SC migration in the proximal nerve was significantly enhanced in the KOS group compared to the saline control group. P75 expression was also significantly increased in the distal portion of the nerve after 3 days compared to the saline control. To further validate the effect that KOS hydrogels have on peripheral nerve regeneration, Pace *et al*. looked to use a more clinically relevant animal model of non-human primates [25]. KOS hydrogels in this animal model were shown to allow for a significantly greater amount of axons in the middle and distal nerve sections compared to saline controls. KOS hydrogels were also found to enhance abductor pollicis brevis (APB) muscle regeneration through measurements of the myofiber area and density.

1.6. Keratin Chemistry

Keratin proteins are found in wool, skin, nails, hooves, and hair and can also be produced recombinantly. These macromolecules belong to a small family of intermediate filament (IF) forming proteins, which form the structural component in many biological systems. Keratins can be separated into two broad groups, depending on where they originate. Nails and hair are made

of up of so-called “hard” keratins, while skin is made up of “soft” keratins. A delineating factor in hard and soft keratins is the sulfur content. Hard keratins possess more sulfur content in the form of cysteine amino acid residues while soft keratins have less. The greater sulfur content increases the amount of disulfide crosslinks within the keratin matrix, and more disulfide crosslinks leads to a greater rigidity that is observed in hair and nails while less crosslinks leads to more elasticity as seen in skin [2].

Extraction of keratin from human hair and fabrication of biomaterials from the resulting isolates has gained popularity in recent years. Keratins that reside in the cortex of the hair fiber consist of two protein categories: low-sulfur, α-Keratin monomers and high-sulfur matrix proteins at a 2:1 ratio [3]. α-keratins are between a molecular weight (MW) of 40-60 kDa and self-assemble to form IF structures that provide mechanical stability to the hair fiber. Matrix proteins, also referred to as keratin associated proteins (KAPs), act as a disulfide crosslinking agent to hold the IF-based superstructure together [4]. α-keratins can be further categorized into type I (acidic) and type II (neutral-basic) subcategories. These keratins polymerize to form heterodimers and undergo further self-assembly to form IF structures on the scale of ~10 nm.

For extraction of keratin proteins from human hair fibers, two primary methodologies are utilized: oxidation or reduction chemistries to obtain keratose (KOS) or kerateine (KTN), respectively. For oxidation methods, an agent such as peracetic acid (PAA) has been used to cleave disulfide bonds formed between cysteine amino acid residues (R-S-S-R) and result in the generate sulfonic acid groups ($R\text{-}SO_3^-$) [5]. For reduction methods, a reducing agent such as thioglycolic acid (TGA) is used to break disulfide bonds, but in contrast to oxidation, free thiol groups (R-SH) are formed. These free thiols can then oxidize and reform disulfide bonds [6].

Figure 1 illustrates the differences observed between KOS and KTN-based biomaterial hydrogels [7].

	Reduced keratin (kerateine; KTN)	Oxidized keratin (keratose; KOS)
Protein composition	Cortical hair keratins (mostly type I: K31, K33A, K33B, K34 & type II: K81, K83, K85, K86) with keratin-associated proteins (KAPs)	
Cysteine and cystine modification	Reduced disulfide (R-S-S-R) to sulfhydryls (R-SH)	Oxidized R-S-S-R and R-SH to sulfonic acids ($R\text{-}SO_3^-$)
Disulfide and covalent network assembly	Yes 	No 
Charge at pH 7.4	Negative	More negative

Figure 1: Differences between KOS and KTN biomaterials [7]

Extraction of both material types is conducted by the same general process. Once the cortical proteins are either oxidized or reduced, and the network covalent bonds are severed, proteins can be solubilized using a denaturing solution. This extract is clarified, typically by centrifugation and filtration, followed by purification by dialysis. One form of dialysis that performs both purification of processing reagents and selection of molecular weight fractions is tangential flow filtration (TFF). TFF has been successfully used to remove processing reagents, matrix proteins, as well as damaged protein fragments in a single step [5,6,8]. Purified materials are typically frozen and freeze dried before use.

1.7. Keratin Characterization

Because KOS and KTN undergo differing extraction chemistries, the material properties that manifest in biomaterials made from keratin derivatives are dominated by conversion of disulfide bonds into either cysteic acid or thiol. KOS hydrogels and scaffolds were first characterized by de Guzman *et al*. 20% KOS hydrogels were found to behave like elastic gels with low storage modulus values as determined by rheological measurements. Solubilized KOS

in media found that macrophages maintained their morphology and viability compared to untreated media up to 750 μg/ml of KOS. KOS-based porous implants in CD-1 mice were found to undergo 80% degradation over a period of 2 weeks while also resulting in a significantly less fibrous capsule thickness over the course of 8 weeks compared to the poly(lactic-co-glycolic acid) (PLGA) control. In addition, KOS scaffolds resulted in a significantly higher blood vessel density over 2, 5, and 8 weeks than the PLGA counterparts [5]. Potter and Van Dyke [8] explored the effects on KOS material properties when subjected to a phosphate buffer dialysis agent during the dialysis step of extraction. Extensive protein aggregation can occur in solution, even when using strong buffer solutions. As described by Van Dyke and Rahmany, aggregation can be overcome using phosphate buffers, which promotes effective separation in TFF as the actual molecular dimensions of solution constituents can be maintained [Van Dyke M, Rahmany MB. Keratin nanomaterials and methods of production. US Pat appl 15/308285. May 1, 2015]. Potter and Van Dyke revealed through dynamic light scattering (DLS) that reconstituting KOS in a 10 mM Na_2HPO_4-100 mM NaCl buffer solution resulted in less aggregation than ultrapure water, which is typically used as a dialysate for KOS isolation. Size-exclusion chromatography (SEC) confirmed that the KOS isolated using water dialysate was lower in weight average MW than KOS purified using phosphate buffer. Biomaterial hydrogel made from purer KOS material was shown to exhibit greater structural integrity than water-dialyzed KOS as it had double the storage modulus at 0.1, 1, and 10 Hz, but unexpectedly demonstrated a faster rate of enzyme-mediated degradation.

KTN biomaterials have been characterized by Hill *et al*. [6]. These investigators were able to show that KTN coatings supported NIH 3T3 fibroblast adhesion and proliferation. KTN degraded over a significantly longer time scale compared to KOS. KTN showed 65% hydrolytic

(i.e. saline; no enzyme added) degradation *in vitro* after 90 days, which remained stable at the 110 and 165 day time points. *In vivo* degradation in a CD-1 mouse model showed that implants still retained adequate structure after 6 months of implantation. In addition, KTN samples did not elicit the formation of a fibrous capsule. Richter *et al*. [10] investigated the effects that altering the ratios of α-KTN and low molecular weight fraction KTN had on KTN hydrogels and scaffolds. Increasing the α-KTN fraction resulted in a greater storage modulus along with decreasing its susceptibility to hydrolytic degradation.

Keratin biomaterials have also been used in making composite materials such as blending keratin with other proteins, synthetic materials, and polysaccharides. The central theme for blending is to overcome keratin's poor mechanical properties. Bhardwaj *et al*. [11] explored blending keratin and silk fibroin into a composite material. Keratin-silk fibroin scaffolds were shown to have a significantly greater compressive modulus than strictly silk fibroin scaffolds. Also, keratin-silk fibroin scaffolds allowed for significantly more L929 fibroblast proliferation along with cell viability after 5 days of culture. Edwards *et al*. [12] looked into blending keratin and poly(ε-caprolactone) (PCL) to create electrospun nanofibers. Mixing the synthetic PCL with natural keratin allowed for the creation of a blended material, which was confirmed through observation of the amine peak at 1544 cm^{-1} from Fourier transform infrared spectroscopy (FTIR) measurements. FTIR measurements also revealed that keratin was separating from the PCL when subjected to immersion in phosphate buffered saline (PBS) between time points of 3-7 weeks. The addition of keratin to PCL resulted in lower Young's moduli values as more keratin was added into the system. 70/30 ratios of PCL:keratin were able to support 3T3 fibroblast cell viability. Hartrianti *et al*. [13] investigated blending keratin with alginate and observe the effects of a protein-polysaccharide material. Chemical crosslinking was utilized to couple the materials

together by using 1-ethyl-3-dimethylaminopropyl carbodiimide hydrochloride (EDC), taking advantage of alginate's carboxylic groups and keratin's amine groups. Alginate on its own was shown to not promote L929 fibroblast viability, but the addition of keratin allowed for the promotion of viability especially at a 2:1 and 4:1 ratio of keratin:alginate. Addition of alginate was also shown to improve compressive and tensile properties when compared to only keratin.

1.8. Keratin Biomaterials for Tissue Regeneration

1.8.1. Bone

Keratin's effects on bone regeneration have been studied in great detail. Dias *et al* [14] observed the effect keratin biomaterials have on bone regeneration in an ovine model. This group utilized differing techniques for fabrication of keratin scaffolds that control for porosity, the pH treatment prior to scaffold formation, and the addition of 4% hydroxyapatite into the material matrix. In their model, 8 defect sites per animal were drilled into the mid-shaft femur, distal femur, proximal tibia, and mud-shaft tibia, and animals were kept alive for up to 24 weeks. After 12 and 24 week time points, histological outcomes revealed distinctive bone growth through the biomaterial. Keratin on its own was found to adequately aid in bone regeneration, but the keratin/hydroxyapatite complex was shown to result in the most favorable regeneration. The effect of keratin scaffolds on bridging proximal and distal portions of bone after excision was looked at by de Guzman *et al*. [15]. A CD-1 mouse animal model was used, and bone defects were created by excising an 8-mm defect to create an injury site with well-defined proximal and distal ends. Collagen scaffolds infused with bone morphogenetic protein 2 (BMP-2), KOS scaffolds, and KOS scaffolds infused with BMP-2 were investigated as experimental groups. KOS without BMP-2 did not bridge the proximal and distal injury sites together, but the BMP-2 infused collagen (known commercially as Infuse®) and KOS scaffolds succeeded in bridging

these sites. KOS with BMP-2 allowed for similar development of bone volume, bone mineral density, and bone mineral content as the Infuse® scaffolds after 8 and 16 week time points. Kowalczewski *et al*. [16] investigated the effects of KTN scaffolds with recombinant BMP-2 (rhBMP-2) on ectopic bone growth within a Sprague Dawley rat mandible animal model. Circular sized defects were made in the rats, which were injected with absorbable collagen sponges (ACS) and KTN hydrogels and scaffolds each impregnated with rhBMP-2. After time points of 8 and 16 weeks, KTN gels and scaffolds with rhBMP-2 resulted in similar bone regeneration and bone mineral density values as ACSs. Also, it was shown that KTN gels and scaffolds with rhBMP-2 allowed for significantly less ectopic bone formation than ACSs. This was attributed to the fact that ACSs had significantly greater burst release rates of rhBMP-2 over a period of 2 weeks than each KTN counterpart.

1.8.2. Skin

Keratin biomaterials have also been administered in skin regeneration environments specifically for burn injuries. Because keratin is a primary component of skin, it may be an ideal candidate to serve as a burn wound dressing. Initially, Xu *et al*. observed the effects that keratin biomaterials have on repairing skin defects in a Wistar rat animal model [17]. Skin defects were created by excusing the dorsum of each rat, and the resulting wound was dressed with a sterilized 4% keratin scaffold disc compared to no wound dressing as a control group. After 3 weeks, histological outcomes revealed that keratin treated injuries allowed for greater angiogenesis after 2 weeks and a thicker epidermis after 3 weeks compared to the untreated control. In a study specifically on burn injury, Poranki *et al*. looked into the efficacy of using KOS as a burn wound treatment in a swine animal model [18]. Pigs were burned with cylindrical brass blocks and treated with “crude” KOS, modified KOS (differing amounts of α and γ-keratin fractions), a

commercial collagen hydrogel known as Coloplast, and silver sulfadiazine cream (SSD). Both crude and modified KOS were able to close the wound faster than SSD treatment and allowed for similar total wound closure time compared to the Coloplast treatment. Both KOS groups resulted in quicker epithelialization during the early stages of the recovery period (3 and 6 days) than the Coloplast treatment while the SSD treatment resulted in a negatively trending pattern. In addition to documenting the effect of keratin on burns, observing the effect keratin can have on mitigating infection following burn injury is paramount. Roy *et al*. aimed to use ciprofloxacin-loaded KOS hydrogels to combat bacterial growth and infection following burn injury [19]. Pigs were burned with a brass cylinder and the injury sites were subjected to *P. aeruginosa* or Methicillin-resistant *S. aureus* (MRSA) over a time period of 15 days. Injuries were treated with KOS gel, KOS + ciprofloxacin gel, SSD, or left untreated. At time points of 4, 7, 11, and 15 days, KOS + ciprofloxacin gels were found to significantly reduce the amount of *P. aeruginosa* and MRSA at the injury site. KOS + ciprofloxacin gels also allowed for full similar healing patterns to uninfected burns such as full epithelialization, adequate macrophage recruitment, and collagen deposition.

1.8.3. Muscle

Keratin biomaterials have also been employed to aid in regeneration of different types of muscle including cardiac, smooth, and skeletal. Shen *et al.* investigated the effect of keratin hydrogels on alleviating cardiac dysfunction after inducing myocardial infarction (MI) in Sprague-Dawley rats [20]. After induction of MI by ligation of the left anterior descending artery, saline controls and KOS hydrogels were injected intramyocardially to the infarct site. Assessment of extracted hearts revealed that saline and KOS treatments allowed for the same amount of macrophage recruitment, but KOS allowed for significantly greater

neovascularization. KOS treatment also resulted in a significantly lower scar size and a greater amount of viable cardiac tissue while also improving left ventricular ejection fraction (LVEF) and fractional shortening. At time points of 3, 14, and 28 days, KOS groups resulted in greater expression of nerve growth factor (NGF), transforming growth factor-beta (TGF-β), and bone morphogenetic protein 4 (BMP4) than the saline controls. Ledford *et al*. explored the capabilities of KOS hydrogels to promote vascular smooth muscle cell (VSMC) differentiation from human cardiac stem cells (hCSCs) [21]. In this study, hCSCs were plated atop blank coverslips or KOS hydrogel coated coverslips for 3-5 days, and differentiation patterns were observed by using quantitative polymerase chain reaction (qPCR) to gauge cardiac, endothelial, and vascular smooth muscle markers. Results showed that following differentiation, vascular smooth muscle markers such as smooth muscle myosin heavy chain (SM-MHC) and GATA binding protein 6 (GATA6) were significantly upregulated on cells plated on KOS hydrogels compared to the untreated controls. The hCSCs seeded on KOS hydrogels were also shown to form "endothelial cell tube-like" structures, which suggests that KOS hydrogels may promote angiogenesis of VSMCs differentiated from hCSCs. To observe the effect that keratin biomaterials had on skeletal muscle regeneration, Passipieri *et al.* induced a volumetric muscle loss injury in a female Lewis rat animal model by removing ~20% of the tibialis anterior (TA) muscle and replacing the void with keratin hydrogels that were impregnated with insulin-like growth factor (IGF-1), basic fibroblast growth factor (bFGF), and/or skeletal muscle progenitor cells (MPCs) [22]. After 8 weeks, regenerated TA muscles had a significantly greater isometric torque value in the keratin + bFGF and keratin + IGF-1 + bFGF group compared to the unrepaired control, and after 12 weeks, strictly keratin biomaterial along with the groups previously mentioned had a significantly greater isometric torque value compared to the unrepaired control. Histological

outcomes revealed that all keratin groups allowed for significantly greater muscle tissue formation within the void space compared to the unrepaired control group.

1.9. Conclusion

Numerous extraction methods have been employed to produce keratin biomaterials. Characterization has shown many compositional differences, as well as ranges of chemical and physical properties of the resulting biomaterials, which have been explored in a bevy of tissue regeneration environments and have demonstrated significant success. A general theme has arisen from this body of work that keratin biomaterials, in a variety of forms, appear to generally support tissue regeneration responses rather than inflammatory or immunogenic responses. However, challenges to the use of keratin biomaterial as a scaffold or payload delivery system still exist and no ideal keratin-based platform has been identified. A major limitation, identified by numerous investigators, is the narrow range of physical properties, especially ductility of processed keratins. In the present work, we explore the feasibility of blending KOS with type I collagen to use as a peripheral nerve luminal filler in order to overcome limitations of prior work in this field.

References

[1] Paschos, N. K., & Howell, S. M. (2016). Anterior cruciate ligament reconstruction: principles of treatment. *Efort Open Reviews, 1*(11), 398-408. doi:10.1302/2058-5241.1.160032

[2] Edsall, J. T., Bailey, K., & Anson, M. L. (1954). *Advances in Protein Chemistry - Volume 9*. Academic Press.

[3] Crewther, W. G., Fraser, R. D., Lennox, F. G., & Lindley, H. (1965). The chemistry of keratins. *Adv Protein Chem, 20*, 191-346.

[4] Schweizer, J., Bowden, P. E., Coulombe, P. A., Langbein, L., Lane, E. B., Magin, T. M., . . . Wright, M. W. (2006). New consensus nomenclature for mammalian keratins. *Journal of Cell Biology, 174*(2), 169-174. doi:DOI 10.1083/jcb.200603161

[5] de Guzman, R. C., Merrill, M. R., Richter, J. R., Hamzi, R. I., Greengauz-Roberts, O. K., & Van Dyke, M. E. (2011). Mechanical and biological properties of keratose biomaterials. *Biomaterials, 32*(32), 8205-8217. doi:10.1016/j.biomaterials.2011.07.054

[6] Hill, P., Brantley, H., & Van Dyke, M. (2010). Some properties of keratin biomaterials: Kerateines. *Biomaterials, 31*(4), 585-593. doi:10.1016/j.biomaterials.2009.09.076

[7] de Guzman, R. C., Tsuda, S. M., Ton, M. T., Zhang, X., Esker, A. R., & Van Dyke, M. E. (2015). Binding Interactions of Keratin-Based Hair Fiber Extract to Gold, Keratin, and BMP-2. *PLoS One, 10*(8), e0137233. doi:10.1371/journal.pone.0137233

[8] Potter, N. A., & Van Dyke, M. (2018). Effects of Differing Purification Methods on Properties of Keratose Biomaterials. *Acs Biomaterials Science & Engineering, 4*(4), 1316-1323. doi:10.1021/acsbiomaterials.7b00964

[9] Dong, S. K., Huangfu, X. Q., Xie, G. M., Zhang, Y., Shen, P., Li, X. X., . . . Zhao, J. Z. (2015). Decellularized Versus Fresh-Frozen Allografts in Anterior Cruciate Ligament Reconstruction: An In Vitro Study in a Rabbit Model. *American Journal of Sports Medicine, 43*(8), 1924-1934. doi:10.1177/0363546515585314

[10] Richter, J. R., de Guzman, R. C., Greengauz-Roberts, O. K., & Van Dyke, M. (2012). Structure-property relationships of meta-kerateine biomaterials derived from human hair. *Acta Biomater, 8*(1), 274-281. doi:10.1016/j.actbio.2011.08.020

[11] Bhardwaj, N., Sow, W. T., Devi, D., Ng, K. W., Mandal, B. B., & Cho, N. J. (2015). Silk fibroin-keratin based 3D scaffolds as a dermal substitute for skin tissue engineering. *Integrative Biology, 7*(1), 53-63. doi:10.1039/c4ib00208c

[12] Edwards, A., Jarvis, D., Hopkins, T., Pixley, S., & Bhattarai, N. (2015). Poly(epsilon-caprolactone)/keratin-based composite nanofibers for biomedical applications. *J Biomed Mater Res B Appl Biomater, 103*(1), 21-30. doi:10.1002/jbm.b.33172

[13] Hartrianti, P., Nguyen, L. T. H., Johanes, J., Chou, S. M., Zhu, P., Tan, N. S., . . . Ng, K. W. (2017). Fabrication and characterization of a novel crosslinked human keratin-alginate sponge. *J Tissue Eng Regen Med, 11*(9), 2590-2602. doi:10.1002/term.2159

[14] Dias, G. J., Peplow, P. V., McLaughlin, A., Teixeira, F., & Kelly, R. J. (2010). Biocompatibility and osseointegration of reconstituted keratin in an ovine model. *J Biomed Mater Res A, 92*(2), 513-520. doi:10.1002/jbm.a.32394

[15] de Guzman, R. C., Saul, J. M., Ellenburg, M. D., Merrill, M. R., Coan, H. B., Smith, T. L., & Van Dyke, M. E. (2013). Bone regeneration with BMP-2 delivered from keratose scaffolds. *Biomaterials, 34*(6), 1644-1656. doi:10.1016/j.biomaterials.2012.11.002

[16] Kowalczewski, C. J., Tombyln, S., Wasnick, D. C., Hughes, M. R., Ellenburg, M. D., Callahan, M. F., . . . Saul, J. M. (2014). Reduction of ectopic bone growth in critically-sized rat mandible defects by delivery of rhBMP-2 from kerateine biomaterials. *Biomaterials, 35*(10), 3220-3228. doi:10.1016/j.biomaterials.2013.12.087

[17] Xu, S., Sang, L., Zhang, Y., Wang, X., & Li, X. (2013). Biological evaluation of human hair keratin scaffolds for skin wound repair and regeneration. *Mater Sci Eng C Mater Biol Appl, 33*(2), 648-655. doi:10.1016/j.msec.2012.10.011

[18] Poranki, D., Goodwin, C., & Van Dyke, M. (2016). Assessment of Deep Partial Thickness Burn Treatment with Keratin Biomaterial Hydrogels in a Swine Model. *Biomed Research International*. doi:Artn 1803912

[19] Roy, D. C., Tomblyn, S., Isaac, K. M., Kowalczewski, C. J., Burmeister, D. M., Burnett, L. R., & Christy, R. J. (2016). Ciprofloxacin-loaded keratin hydrogels reduce infection and support healing in a porcine partial-thickness thermal burn. *Wound Repair Regen, 24*(4), 657-668. doi:10.1111/wrr.12449

[20] Shen, D., Wang, X., Zhang, L., Zhao, X., Li, J., Cheng, K., & Zhang, J. (2011). The amelioration of cardiac dysfunction after myocardial infarction by the injection of keratin biomaterials derived from human hair. *Biomaterials, 32*(35), 9290-9299. doi:10.1016/j.biomaterials.2011.08.057

[21] Ledford, B. T., Simmons, J., Chen, M., Fan, H., Barron, C., Liu, Z., . . . He, J. Q. (2017). Keratose Hydrogels Promote Vascular Smooth Muscle Differentiation from C-kit-Positive Human Cardiac Stem Cells. *Stem Cells Dev, 26*(12), 888-900. doi:10.1089/scd.2016.0351

[22] Passipieri, J. A., Baker, H. B., Siriwardane, M., Ellenburg, M. D., Vadhavkar, M., Saul, J. M., . . . Christ, G. J. (2017). Keratin Hydrogel Enhances In Vivo Skeletal Muscle Function in a Rat Model of Volumetric Muscle Loss. *Tissue Eng Part A, 23*(11-12), 556-571. doi:10.1089/ten.TEA.2016.0458

[23] Sierpinski, P., Garrett, J., Ma, J., Apel, P., Klorig, D., Smith, T., . . . Van Dyke, M. (2008). The use of keratin biomaterials derived from human hair for the promotion of rapid regeneration of peripheral nerves. *Biomaterials, 29*(1), 118-128. doi:10.1016/j.biomaterials.2007.08.023

[24] Pace, L. A., Plate, J. F., Smith, T. L., & Van Dyke, M. E. (2013). The effect of human hair keratin hydrogel on early cellular response to sciatic nerve injury in a rat model. *Biomaterials, 34*(24), 5907-5914. doi:10.1016/j.biomaterials.2013.04.024

[25] Pace, L. A., Plate, J. F., Mannava, S., Barnwell, J. C., Koman, L. A., Li, Z., . . . Van Dyke, M. (2014). A human hair keratin hydrogel scaffold enhances median nerve regeneration in nonhuman primates: an electrophysiological and histological study. *Tissue Eng Part A, 20*(3-4), 507-517. doi:10.1089/ten.TEA.2013.0084

[26] Busam, M. L., Rue, J. P. H., & Bach, B. R. (2007). Fresh-frozen allograft anterior cruciate ligament reconstruction. *Clinics in Sports Medicine, 26*(4), 607-+. doi:10.1016/j.csm.2007.06.001

[27] Cooper, D. K. (2012). A brief history of cross-species organ transplantation. *Proc (Bayl Univ Med Cent), 25*(1), 49-57. doi:10.1080/08998280.2012.11928783

[28] Vadori, M., & Cozzi, E. (2015). The immunological barriers to xenotransplantation. *Tissue Antigens, 86*(4), 239-254. doi:10.1111/tan.12669

[29] Reemtsma, K., McCracken, B. H., Schlegel, J. U., Pearl, M. A., Pearce, C. W., Dewitt, C. W., . . . Creech, O., Jr. (1964). Renal Heterotransplantation in Man. *Ann Surg, 160*, 384-410. doi:10.1097/00000658-196409000-00006

[30] Lehmann, S., Merk, D. R., Etz, C. D., Oberbach, A., Uhlemann, M., Emrich, F., . . . Mohr, F. W. (2016). Porcine xenograft for aortic, mitral and double valve replacement: long-term results of 2544 consecutive patients. *European Journal of Cardio-Thoracic Surgery, 49*(4), 1150-1156. doi:10.1093/ejcts/ezv383

[31] Galili, U. (2005). The alpha-gal epitope and the anti-Gal antibody in xenotransplantation and in cancer immunotherapy. *Immunology and Cell Biology, 83*(6), 674-686. doi:10.1111/j.1440-1711.2005.01366.x

[32] Zhong, R. (2007). Gal knockout and beyond. *American Journal of Transplantation, 7*(1), 5-11. doi:10.1111/j.1600-6143.2006.01615.x

[33] Cornwell, K. G., Landsman, A., & James, K. S. (2009). Extracellular matrix biomaterials for soft tissue repair. *Clin Podiatr Med Surg, 26*(4), 507-523. doi:10.1016/j.cpm.2009.08.001

[34] Parenteau-Bareil, R., Gauvin, R., & Berthod, F. (2010). Collagen-Based Biomaterials for Tissue Engineering Applications. *Materials, 3*(3), 1863-1887. doi:10.3390/ma3031863

[35] Hussain, Z., Thu, H. E., Katas, H., & Bukhari, S. N. A. (2017). Hyaluronic Acid-Based Biomaterials: A Versatile and Smart Approach to Tissue Regeneration and Treating Traumatic, Surgical, and Chronic Wounds. *Polymer Reviews, 57*(4), 594-630. doi:10.1080/15583724.2017.1315433

[36] Hickey, R. J., & Pelling, A. E. (2019). Cellulose Biomaterials for Tissue Engineering. *Front Bioeng Biotechnol, 7*, 45. doi:10.3389/fbioe.2019.00045

[37] Park, C. H., & Woo, K. M. (2018). Fibrin-Based Biomaterial Applications in Tissue Engineering and Regenerative Medicine. *Biomimetic Medical Materials: From Nanotechnology to 3d Bioprinting, 1064*, 253-261. doi:10.1007/978-981-13-0445-3_16

[38] Kim, W. (2013). Recombinant protein polymers in biomaterials. *Frontiers in Bioscience-Landmark, 18*, 289-304. doi:10.2741/4100

[39] Madduri, S., Papaloizos, M., & Gander, B. (2010). Trophically and topographically functionalized silk fibroin nerve conduits for guided peripheral nerve regeneration. *Biomaterials, 31*(8), 2323-2334. doi:10.1016/j.biomaterials.2009.11.073

[40] Chen, M. B., Zhang, F., & Lineaweaver, W. C. (2006). Luminal fillers in nerve conduits for peripheral nerve repair. *Ann Plast Surg, 57*(4), 462-471. doi:10.1097/01.sap.0000237577.07219.b6

[41] Williams, L. R. (1987). Exogenous Fibrin Matrix Precursors Stimulate the Temporal Progress of Nerve Regeneration within a Silicone Chamber. *Neurochemical Research, 12*(10), 851-860. doi:Doi 10.1007/Bf00966306

[42] Madison, R. D., Dasilva, C. F., & Dikkes, P. (1988). Entubulation Repair with Protein Additives Increases the Maximum Nerve Gap Distance Successfully Bridged with Tubular Prostheses. *Brain Research, 447*(2), 325-334. doi:Doi 10.1016/0006-8993(88)91135-3

[43] Satou, T., Nishida, S., Hiruma, S., Tanji, K., Takahashi, M., Fujita, S., . . . Hashimoto, S. (1986). A morphological study on the effects of collagen gel matrix on regeneration of severed rat sciatic nerve in silicone tubes. *Acta Pathol Jpn, 36*(2), 199-208.

[44] Rosen, J. M., Padilla, J. A., Nguyen, K. D., Padilla, M. A., Sabelman, E. E., & Pham, H. N. (1990). Artificial Nerve Graft Using Collagen as an Extracellular-Matrix for Nerve Repair Compared with Sutured Autograft in a Rat Model. *Annals of Plastic Surgery, 25*(5), 375-387. doi:Doi 10.1097/00000637-199011000-00006

[45] Lundborg, G., Dahlin, L., Dohl, D., Kanje, M., & Terada, N. (1997). A new type of "bioartificial" nerve graft for bridging extended defects in nerves. *Journal of Hand Surgery-British and European Volume, 22b*(3), 299-303. doi:Doi 10.1016/S0266-7681(97)80390-7

[46] Bunting, S., Di Silvio, L., Deb, S., & Hall, S. (2005). Bioresorbable glass fibres facilitate peripheral nerve regeneration. *Journal of Hand Surgery-British and European Volume, 30b*(3), 242-247. doi:10.1016/j.jhsh.2004.11.003

[47] Gaudin, R., Knipfer, C., Henningsen, A., Smeets, R., Heiland, M., & Hadlock, T. (2016). Approaches to Peripheral Nerve Repair: Generations of Biomaterial Conduits Yielding to Replacing Autologous Nerve Grafts in Craniomaxillofacial Surgery. *Biomed Research International*. doi:Artn 3856262

[48] Wang, S. F., & Cai, L. (2010). Polymers for Fabricating Nerve Conduits. *International Journal of Polymer Science*. doi:Artn 138686

[49] Lackington, W. A., Ryan, A. J., & O'Brien, F. J. (2017). Advances in Nerve Guidance Conduit-Based Therapeutics for Peripheral Nerve Repair. *Acs Biomaterials Science & Engineering, 3*(7), 1221-1235. doi:10.1021/acsbiomaterials.6b00500

[50] Labrador, R. O., Buti, M., & Navarro, X. (1998). Influence of collagen and laminin gels concentration on nerve regeneration after resection and tube repair. *Experimental Neurology, 149*(1), 243-252. doi:DOI 10.1006/exnr.1997.6650

[51] Apel, P. J., Garrett, J. P., Sierpinski, P., Ma, J. J., Atala, A., Smith, T. L., . . . Van Dyke, M. E. (2008). Peripheral Nerve Regeneration Using a Keratin-Based Scaffold: Long-Term Functional and Histological Outcomes in a Mouse Model. *Journal of Hand Surgery-American Volume, 33a*(9), 1541-1547. doi:10.1016/j.jhsa.2008.05.034

[52] Aluigi, A., Vineis, C., Varesano, A., Mazzuchetti, G., Ferrero, F., & Tonin, C. (2008). Structure and properties of keratin/PEO blend nanofibres. *European Polymer Journal, 44*(8), 2465-2475. doi:10.1016/j.eurpolymj.2008.06.004

Chapter 2

Effects of Differing Purification Methods on Properties of Keratose Biomaterials

Nils A. Potter and Mark Van Dyke

Virginia Polytechnic Institute and State University, Department of Biomedical Engineering and Mechanics, School of Biomedical Engineering and Sciences, Blacksburg, VA 24061

This manuscript was published in ACS Biomaterials Science & Engineering: 1316-1323 (2018), which is an open access journal. Organizational differences are due to the requirements of this journal. Nils Potter prepared the manuscript. Mark Van Dyke acted in an advisory and editorial capacity.

Abstract

Keratin is a natural polymer found in hair fibers, skin, and nails. It has been investigated as a biomaterial since the 1970's and has more recently been shown to have applications in healthcare such as medical devices and tissue engineering. Keratins are one of few intermediate filament forming proteins and demonstrate a propensity to self-assemble. Keratins extracted and purified from natural sources such as human hair fibers and wool tend to have weak mechanical properties but can be crosslinked to form more robust structures. When extracting and purifying keratin proteins from natural fibers, the method of extraction is paramount to obtaining materials that retain the ability to self-assemble and form network structures with appreciable mechanical strength. Here, we compare and contrast two methods for purifying keratin extracts – one in which conventional purification methods are used and a second in which solution aggregation is minimized to promote purification of the molecular entities with the highest propensity for self-assembly, dimers of type I and type II hard keratins. Material that underwent the latter, novel extraction method exhibited higher purity in the form of a lower peptide content. Moreover, hydrogels formed from this material were found to demonstrate greater resistance to shear, and interestingly, increased susceptibility to enzymatic degradation in comparison to hydrogels formed from conventionally extracted material. This novel keratin purification method allows for enrichment of compounds with increased self-assembly behavior and has the potential to overcome limitations noted in other studies where biomaterials fabricated from purified keratins demonstrated inferior mechanical characteristics.

Keywords: keratin, hydrogel, aggregation, rheology, degradation

2.1. Introduction

Biomaterials that originate from natural protein sources have been shown to demonstrate successful results in biomedical applications. A large number of these materials, however, are derived from animal sources or are synthetically produced; relatively few are from human sources. Many natural proteins are derived from tissues or fluids and their associated isolation and purification processes can lead to protein denaturation and inclusion of contaminants. Batch-to-batch consistency can also be problematic and translation of such technologies into products intended for human clinical use has been hindered by issues related to sourcing, batch sizes, and lot release criteria. Keratin proteins are unique, in part because they can be easily sourced from humans and do not rely on cadaveric donors or invasive tissue harvest methods. Consistency of purified keratin production methods has not previously been addressed but is an important topic for translation of keratin biomaterials-based technologies.

Keratin proteins are primary components in the composition of hair fibers and contribute to their structural integrity by providing shape and strength [1]. These proteins can be manipulated for many biomaterial applications such as coatings, hydrogels, as well as scaffolds for regenerative medicine applications. In tissue engineering applications, keratin biomaterials have been shown to aid in bone, peripheral nerve, and cardiac regeneration [2-5]. The purity of extracted keratin is an important issue when using this material in biomedical applications since contaminants and inconsistent material properties can lead to unwanted biologic responses. Importantly, keratins are two of only seven types of intermediate filament forming proteins, which as a class of compounds, show a strong propensity for self-assembly. It is this property of self-assembly, combined with the complex composition of molecular species generated by

numerous, published keratin extraction/purification methods, that complicates the purification process.

Most published keratin extraction/purification methods follow the same general methodology: Oxidation or reduction to cleave disulfide bonds, dissolution of cortical proteins using denaturing solutions, purification by dialysis, followed by freeze drying to isolate the product. Various oxidation and reduction methods have been extensively studied and published early in the genesis of keratin biomaterials technology development [10]. To date, however, the critical step of dialysis has not been studied, particularly with respect to the natural self-assembly behavior of keratin proteins, even while in solution. Many keratin purification methods still dialyze against ultrapure water [5-8,14]. We have investigated the solution aggregation behavior of keratin extracts and determined the essential role this behavior has on the purification processes, particularly membrane dialysis separation. In the present study, we investigated two keratin biomaterial preparations, one in which solution aggregation was exacerbated and one in which it was minimized. We hypothesized that the degree of solution aggregation would affect sample purity, which would in turn affect network formation in hydrogels subsequently produced from these samples. To explore this question, we investigated molecular weight and solution behavior of isolated/purified keratin samples, as well as rheological properties and degradation assays of hydrogels formed from these isolated purified keratin samples.

2.2. Methods

2.2.1. Keratose Preparation

Keratose (KOS) was prepared based on a previously published method, with modifications [11]. Briefly, clean, dry human hair fibers were obtained from a commercial source and were oxidized using a 2% (w/v) solution of peracetic acid (PAA) in ultrapure water.

The hair fiber weight to liquid volume ratio was 1:20 and the oxidation was carried out at 37ºC with continuous, gentle stirring for 12 hours. Oxidized fibers were recovered by passing the suspension through a 500 μm sieve and were rinsed with deionized water until no residual PAA was detectable with a test strip. Fibers were extracted twice with a 1:40 ratio of dry fiber weight to 100 mM tris base at 37ºC for 2 hours with continuous, gentle stirring. After each extraction, fibers were recovered by sieve and the liquid retained. Extracts were combined, centrifuged and filtered for solids removal, and the KOS purified by tangential flow filtration (TFF) using a custom-designed system. In one case, the sample was dialyzed in the TFF system against ultrapure water (i.e. 18 MΩ); this sample is referred to as water dialyzed or "WKOS" and represents a highly aggregated system. In a second case, the sample was dialyzed first against phosphate buffer (10 mM Na_2HPO_4/100 Mm NaCl, pH 7.4), then ultrapure water; this sample is referred to as buffer dialyzed or "BKOS" and represents a case wherein aggregation was minimized during the TFF process. In both cases, following dialysis, the sample was concentrated, frozen, lyophilized, and ground into a coarse powder prior to use.

2.2.2. Keratose Peptide Preparation

Low molecular weight contaminants removed by the TFF system were collected and a KOS "peptide" fraction was purified and isolated as a dry powder. To accomplish this, the first wash from the TFF system, performed using a 100K Da nominal low molecular weight cutoff membrane, was collected. This sample was then re-dialyzed on the TFF system against ultrapure water using a 5K Da nominal low molecular weight cutoff membrane, such that the peptides had molecular weights between 100K and 5K Da. The purified peptide solution was concentrated and a dry powder produced by lyophilization.

2.2.3. Size-Exclusion Chromatography Analysis

KOS extracts from both processing methods were reconstituted in 10 mM Na_2HPO_4/100 mM NaCl at a concentration of 0.2 mg/ml. 20 µl of sample was injected into the injection loop, and samples were run for 20 min each. The SEC system consisted of a Dionex Ultimate 3000 quaternary analytical pump, Rheodyne manual injection loop, and Ultimate 3000 UV/Vis detector. The mobile phase, flowing at 0.5 mL/min, was 10 mM Na_2HPO_4/100 mM NaCl at pH 7.4, and a BioBasic SEC-1000 column, 7.8mm x 150 mm, 5 µm particle size (ThermoFisher), was used. Detection was at 280 nm and data collected using a laptop computer running Chromeleon v6.8 chromatography software. The system was standardized against bovine albumin.

2.2.4. Dynamic Light Scattering

KOS extracts from both processing methods were reconstituted in ultrapure water or 10 mM Na_2HPO_4/100 mM NaCl at a concentration of 1 mg/ml. 1 ml of samples were transferred into cuvettes and placed in the Zetasizer Nano ZS (Malvern Instruments). Each sample went through 7 measurement cycles and intensity, volume, and correlation plots were generated for each. Each measurement cycle took 2 min, and each measurement cycle immediately went into the next one to minimize any potential time loss.

2.2.5. Keratose Hydrogel Preparation and Rheological Analysis

KOS powders from both processing methods were reconstituted with ultrapure water along with a 20 mg/ml solution of 1,4-butanediol diglycidyl ether (BDDE) in ultrapure water to create a solution of 12% (w/w) KOS that was crosslinked with 12% (w/w) of BDDE relative to the KOS mass. The resulting mixture was vortexed and centrifuged at 1000 rpm for 1 min. For a 1 g KOS sample, 6 ml of 20 mg/ml BDDE solution and 1.333 ml of ultrapure water would be

added to the KOS powder, which would then be vortexed to ensure a homogenous solution and then centrifuged to remove air bubbles. **Figure 2.1** shows an illustration of how the hydrogels were created. The KOS mixture was then distributed into 2.5 ml aliquots, transferred into cylindrical silicone molds (33.5 mm in diameter and 3.175 mm thick) resting on top of individual sheets of parafilm by use of a positive displacement pipette, and incubated at room temperature for 72 h to allow for curing. After curing, samples were removed from the silicone molds, removed from the parafilm, and placed onto the Peltier plate of the ARG2 rheometer (TA Instruments). A 25 mm diameter stainless steel parallel plate geometry was used for testing. The upper plate was lowered onto the samples until a reading for normal force greater than 0 N was observed. Samples were trimmed and set to a gap height of 90% of the trim height to ensure for proper filling. Stress sweep tests were administered from 0.1 – 600 Pa to determine the linear viscoelastic region (LVER) at a constant frequency of 1 Hz. Frequency sweeps from 0.1 – 10 Hz were performed at a constant stress of 25 Pa, which was found to reside within the LVER.

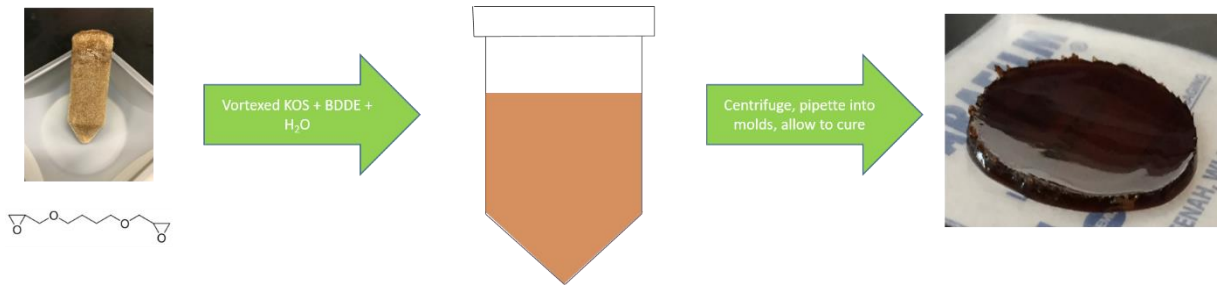

Figure 2.1: Diagram of how KOS hydrogels are made. Lyophilized KOS is combined with ultrapure water and BDDE and thoroughly mixed. The resulting mixture is then centrifuged to remove air bubbles. After centrifugation, the mixture is transferred via positive displacement pipette into silicone molds resting on top of sheets of parafilm. After curing, the disks are removed from the molds, and the parafilm is lifted off.

2.2.6. Enzymatic Degradation

12% (w/w) sterile KOS (25 Gy X-ray irradiated) plus 12% (w/w) BDDE (relative to KOS mass; sterile filtered) were reconstituted in sterile ultrapure water (similar to sample preparation

for rheological testing as described above) and placed in sterile 2 ml microcentrifuge tubes (KOS mass ~ 60 mg). Samples were cured at room temperature for 72 h. KOS hydrogels were subjected to enzyme-containing solutions (type I collagenase, elastase, trypsin, chymotrypsin, keratinase, and PBS control; sterile filtered through 0.22 μm pore filter cartridge) at concentrations of 0.5 U/ml and a 2:1 ratio of enzyme solution to hydrogel volume. 500 μl of the sample supernatant was removed and replenished with fresh enzyme solution at time points of 1 h, 2 h, 4 h, 8 h, 1 day, 3 days, and 1 week. Protein quantification in the supernatant was carried out using Bradford-Lowry assays to determine the percent degradation of hydrogel. Samples were handled in a sterile manner to mitigate against the chance of aided degradation from microbial enzymes.

2.2.7. Peptide-Containing KOS Hydrogel Degradation

Enzymatic degradation for the peptide infused samples was carried out in a similar fashion to the prior enzymatic degradation methods listed above. Briefly, 12% (w/w) BKOS containing 0%, 10%, 20%, and 40% weight percent peptide fraction (added together as dry powders, prior to hydration; relative to BKOS mass) and 12% (w/w) BDDE (relative to BKOS plus peptide mass) were reconstituted in sterile ultrapure water in 2 ml microcentrifuge tubes and cured at room temperature for 72 h. BKOS gels with infused peptide were subjected to the same enzymes, concentrations, and volume ratios as listed above at time points of 6 h, 3 days, and 6 days. Bradford-Lowry assays were performed on supernatant samples to quantify degradation.

2.2.8. Statistical Analysis

All quantitative results are reported as means ± standard deviation unless otherwise stated. Statistical analyses were carried out by performing one-way analysis of variance

(ANOVA) and a Tukey's *post hoc* test for significance. P-values less than 0.05 were considered statistically significant. All statistical analyses were performed in JMP 12.0.1.

2.3. Results

2.3.1. Size-Exclusion Chromatography

Size-exclusion chromatography results revealed that KOS dialyzed against phosphate buffer retained more high-molecular weight keratin (referred to as "keratin nanomaterial" or KN) while KOS dialyzed against ultrapure water resulted in a higher fraction of retained peptide fragment as shown by **Figure 2.2**. The peak times for BKOS and WKOS were 9.993 and 10.58 min, respectively. Numerical integration of each peak showed that the WKOS material consisted of 52% peptide fragment, and the BKOS material consisted of 37% peptide fragment. The cutoff between KN and peptide is assumed to be the molecular weight of bovine serum albumin (BSA) at 66.6 kDa, which corresponds to the approximate mass of an intact keratin monomer.

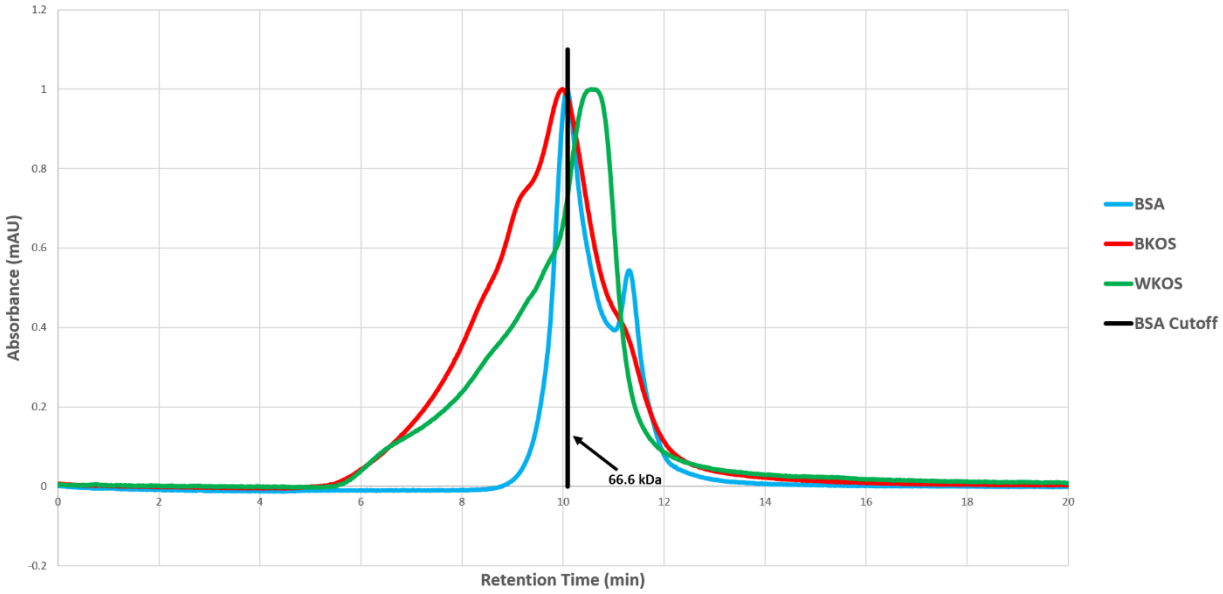

Figure 2.2: Size-exclusion chromatography of water dialyzed KOS, buffer dialyzed KOS, and bovine serum albumin (BSA). The molecular weight of BSA (66.6 kDa) represents the cutoff between peptide and keratin nanomaterial.

2.3.2. Dynamic Light Scattering

WKOS and BKOS solution profiles reconstituted in either ultrapure water or phosphate buffer are shown by **Figure 2.3**. WKOS powder reconstituted in ultrapure water was shown to be the most dynamically unstable in solution while BKOS powder reconstituted in water as well as phosphate buffer was shown to be more dynamically stable in solution compared to WKOS powder in either solvent, as illustrated by the plots for correlation coefficient. Both WKOS and BKOS powder in ultrapure water exhibited protein aggregation in solution as demonstrated by the rightward shift on the volume plot, but BKOS exhibited a more consistent aggregation profile as shown by intensity, volume, and correlation plots. Phosphate buffer mitigated aggregation in both WKOS and BKOS samples, but again, BKOS powder demonstrated more consistent repeat measurements of the same sample as shown by the volume and correlation plots.

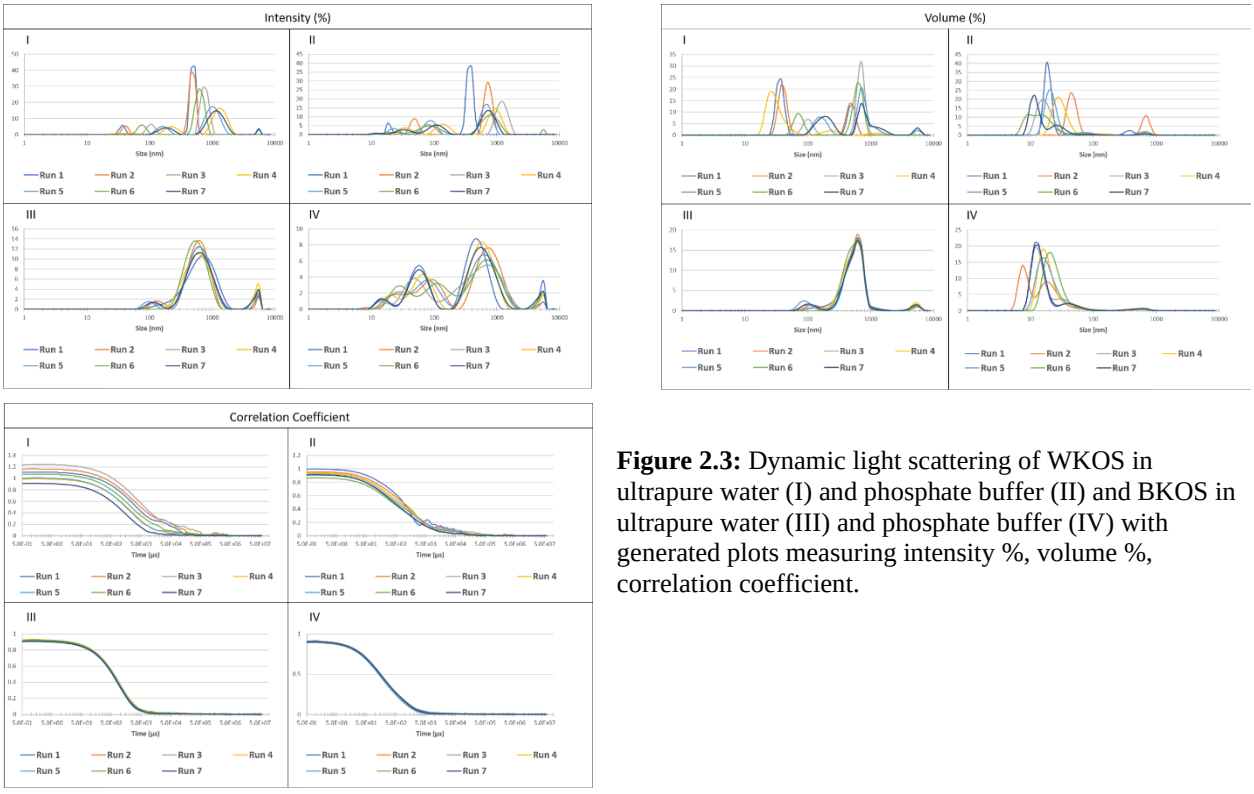

Figure 2.3: Dynamic light scattering of WKOS in ultrapure water (I) and phosphate buffer (II) and BKOS in ultrapure water (III) and phosphate buffer (IV) with generated plots measuring intensity %, volume %, correlation coefficient.

2.3.3. Rheology

Stress sweep analyses conducted from 0.1-600 Pa revealed the LVER for WKOS and BKOS hydrogels. An oscillation stress of 25 Pa resided in the LVER for both samples and was used as the input stress for subsequent frequency sweep tests. Results from this are found in the supplementary information.

Frequency sweep analysis (**Figures 2.4a-d**) illustrate the profiles for storage moduli (G'), loss moduli (G"), dynamic viscosity (η'), and phase angle (δ) of both BKOS and WKOS hydrogels as a function of frequency. BKOS hydrogels exhibited more resistance to shear under differing frequencies (0.1, 1, 10 Hz) as evident by the differences in G' for each group ($p < 0.001$ for 0.1 and 1 Hz, $p < 0.01$ for 10 Hz) (**Figure 2.4e**). BKOS hydrogels also displayed a more elastic structure at differing frequencies as validated by the differences in δ between each group ($p < 0.001$) (**Figure 2.4f**). G" and dynamic viscosity (η') were shown to be greater for WKOS hydrogels at 0.1, 1, and 10 Hz, but statistical significance ($p < 0.05$) was only observed for samples at 1 Hz.

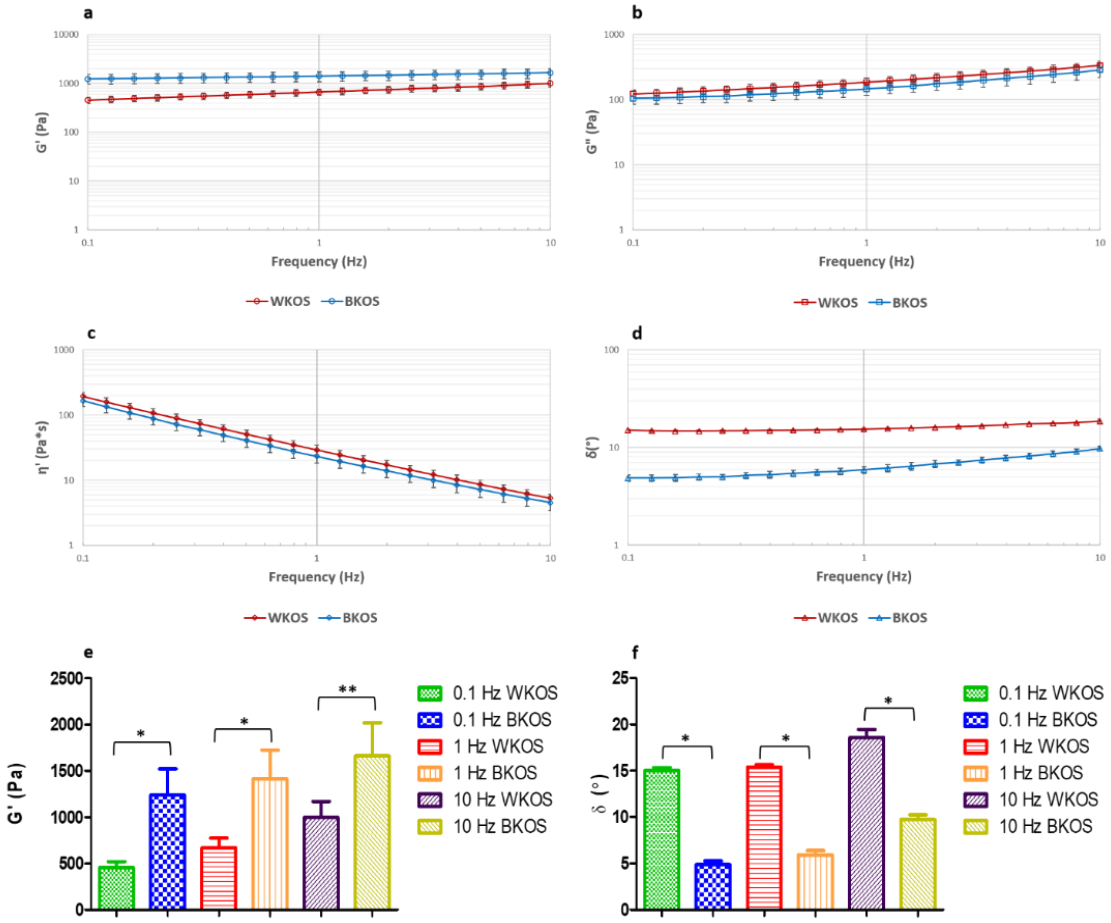

Figure 2.4: Rheological assessment of KOS hydrogels. Frequency sweep test of WKOS and BKOS hydrogels showing (a) storage modulus, (b) loss modulus, (c) dynamic viscosity, and (d) phase angle (mean ± SD, n = 8). (e) Bar chart reflecting differences in storage modulus. (f) Bar chart reflecting differences in phase angle (* indicates $p < 0.001$. ** indicates $p < 0.01$).

2.3.4. Enzymatic Degradation

Results gathered from Bradford-Lowry assays revealed that degradation of BKOS hydrogels occurred at a significantly faster rate than WKOS hydrogels for every enzyme over the course of 1 week with the exception of type I collagenase (**Figure 2.5**). After 2 weeks of enzyme-hydrogel contact, hydrogels in all BKOS groups were observed to be completely degraded. WKOS hydrogels, however, did not experience full degradation after 2 weeks and continued to retain their structure after 2 months of immersion in enzyme solution. For BKOS

hydrogels, elastase was observed to degrade them at the fastest rate. After 3 days, the weight percent of BKOS hydrogels dissolved into the elastase solution was found to be 101% ± 15.1%.

Results gathered from Bradford-Lowry assays for the peptide infused BKOS hydrogels revealed a fairly consistent trend of the material having more enzymatic resistance than samples that did not have any additional peptide component. The instance where this was not observed was when the hydrogels were subjected to type I collagenase and the 10 wt% peptide hydrogel was shown to experience more degradation than the control group of no peptide after 6 days (**Figure 2.6**).

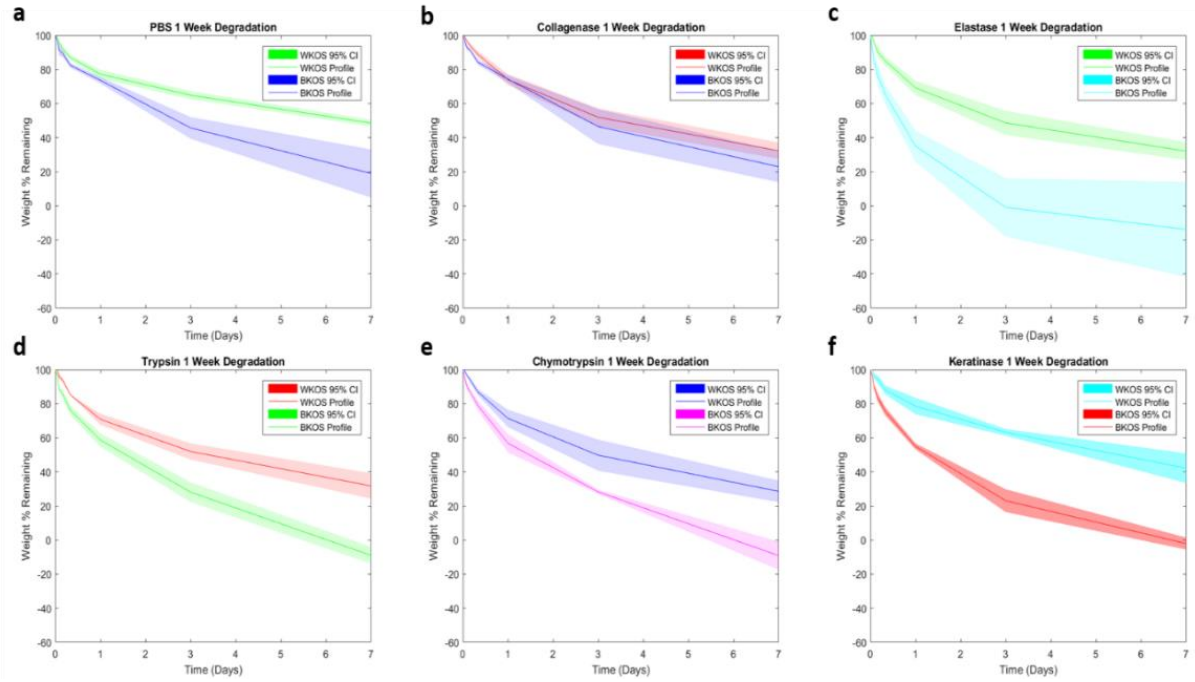

Figure 2.5: Enzymatic degradation of BKOS and WKOS hydrogels after 1 week. Degradation profiles and 95% confidence intervals of hydrogels in (a) PBS, (b) type I collagenase, (c) elastase, (d) trypsin, (e) chymotrypsin, and (f) keratinase (n = 3).

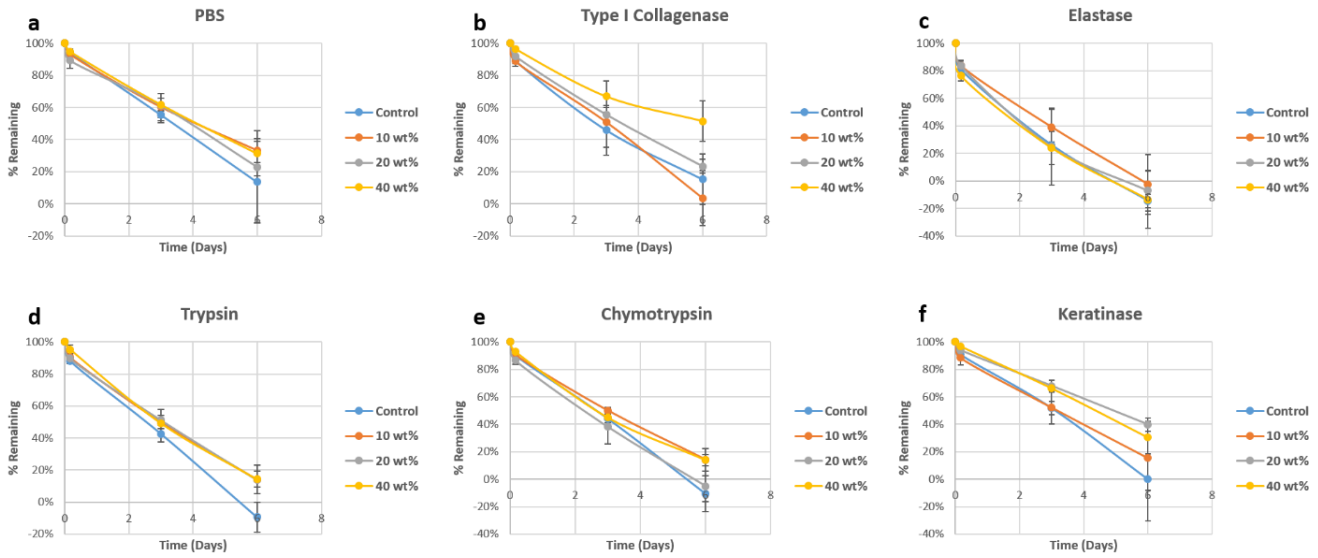

Figure 2.6: Enzymatic degradation of BKOS hydrogels with added peptide (10, 20, and 40 wt%). The control group consisted of BKOS hydrogels with no peptide added. Degradation profiles of hydrogels in (a) PBS, (b) type I collagenase, (c) elastase, (d) trypsin, (e) chymotrypsin, and (f) keratinase (n = 3).

Table 2.1: List of the cleavage sites for type I collagenase, elastase, trypsin, and chymotrypsin for all 17 keratin protein amino acid sequences.

Keratins	Sequence Length (# of AA's)	# of Sites			
		Type I Collagenase	Elastase	Trypsin	Chymotrypsin
K31	416	1	52	38	20
K32	448	0	74	40	19
K33a	404	0	55	41	19
K33b	404	1	52	39	22
K34	436	0	55	42	20
K35	455	0	84	48	22
K36	467	0	84	46	25
K37	449	0	78	40	17
K38	456	0	74	40	14
K39	491	0	62	50	22
K40	431	0	57	33	19
K81	505	0	118	58	26
K82	513	0	108	61	30
K83	493	0	112	56	27
K84	600	0	151	69	37
K85	507	0	112	66	30
K86	486	0	112	60	26

2.4. Discussion

The effect of solutes on protein stability while in solution is well-known in protein biochemistry. Altering the type of buffer system can impact the denaturation time as well as the ability for aggregation to occur [17,18]. During the KOS extraction process, dialysis plays a crucial step in obtaining a pure final product. Ultrapure water as a dialysis agent during KOS purification results in excessive amounts of protein aggregation as shown by **Figure 2.3**, which is to be expected for a self-assembling protein like keratin. Due to this aggregation, the effective molecular weight of an aggregate is higher than keratin monomer or dimer, thus allowing larger amount of peptide to be retained during the dialysis step. Therefore, the end product is less pure than desired. Substituting phosphate buffer for ultrapure water allows for considerably less protein aggregation within the TFF system, leading to greater peptide removal as shown by **Figure 2.2**. The WKOS product exhibits a less stable behavior when reconstituted in either water or phosphate buffer in comparison to the BKOS product, suggesting that the mere presence of peptide contamination exacerbates a dynamic state of aggregation-disaggregation in solution. This is demonstrated by the near constant correlation coefficient generated by consecutive analyses of the same sample. Clearly, the mitigation of protein aggregation during the purification process, along with a more stable protein-in-solution behavior, has implications to the properties of the resulting KOS hydrogels.

In previous investigations, gelation of KOS has typically required greater than 15 wt% keratin content [1,3,19]. This can be attributed to the fact that unlike the reduced form of keratin (referred to as kerateine - KTN), KOS cannot create disulfide bonds with itself due to the oxidation steps employed during the extraction process. Oxidation of keratin leads to the creation of sulfonic acid groups (SO_3^-) from initial disulfide bonds, whereas reduction of keratin leads to

the creation of thiol groups from initial disulfide bonds [21,22]. These sulfonic acid groups in KOS cannot form bonds with each other unlike the free thiols. Preliminary experiments in the present study showed that BKOS could form a stable hydrogel at as low as 8 wt% in ultrapure water (data not shown). BKOS hydrogels were fabricated at 12 wt% with 12% BDDE relative to the KOS mass to compare to WKOS hydrogels because WKOS material would not allow for such low gelation concentrations. The increased peptide contamination present in WKOS hydrogels leads to lower shear resistance of the KOS matrix as well as a more viscous rather than elastic final product as shown by **Figure 2.4**.

To further explore enzyme-mediated degradation of KOS hydrogels, each of the 17 different human hair keratin protein amino acid sequences were inspected and possible cleavage sites quantified for each of the enzymes used in this study. Type I collagenase recognizes the specific amino acid sequence of -R-Pro-X-Gly-Pro-R- where 'R' represents any amino acid residue, and 'X' represents a neutral amino acid [20]. Elastase recognizes small amino acid residues such as glycine, alanine, and valine and cleaves at the C-terminus of these residues. Trypsin recognizes a positively charged amino acid residue such as lysine or arginine and cleaves on the carboxyl side unless ether residue is bound to a C-terminal proline. Chymotrypsin cleaves at aromatic amino acid residues such as phenylalanine, tyrosine, and tryptophan. The mechanism for how keratinase degrades protein has not been extensively published. In the present study, the 17 human hair keratin protein amino acid sequences were analyzed in MATLAB R2015b to determine the cleavage sites for each of the enzymes mentioned above. The number of potential cleavage sites (**Table 2.1**) for elastase on every human hair keratin amino acid sequence was more than any other enzyme tested. Type I collagenase cleavage sites were observed to be sparse among the keratin protein amino acid sequences, with only 1

cleavage site appearing in K31 and K33b. This may explain why the degradation profile for BKOS hydrogels exposed to type I collagenase was the slowest out of all the enzyme groups. Surprisingly, keratinase did not cleave as many potential sites as many of the other enzymes. Keratinase is commonly extracted from bacterial strains and has been used to digest feather keratins in the poultry industry [16]. The specific source of the keratinase used in this study is not known, and it may be that its activity is better suited to applications in feather keratin degradation.

It was hypothesized that reducing peptide contamination would result in improvements in hydrogel properties, but the increased enzyme-mediated degradation rate of BKOS hydrogels was not expected. This may be due to the exposure of active sites in BKOS hydrogels that may be sterically blocked in a WKOS gel by the increased presence of aggregated peptide. We explored this postulate by adding peptide back in to buffer-dialyzed samples. The addition of peptide appeared to increase the resistance to enzyme attack as demonstrated by **Figure 2.6**, where the general trend is a rate increase over no-added-peptide hydrogels. However, there was no statistical significance among any of the groups at the same times points, and adding peptide back into the BKOS sample did not recapitulate the WKOS degradation results shown in **Figure 2.5**, suggesting that coordination of peptide within the keratin network may be more complex than appreciated.

Optimizing extraction processes for biomaterials to obtain high yields as well as pure product has been investigated for a multitude of materials. Collagen extraction processes have been studied in great detail, and three primary methods are currently used for extraction. These include neutral salt-solubilized collagen, acid-solubilized collagen, and pepsin-solubilized collagen extraction [23]. In the pepsin-solubilized extraction method, centrifugation speed as

well as extraction temperature has been investigated to determine whether these had positive effects on collagen yield. Noitup *et al.* [24] investigated using centrifuge speeds of 30,000 rpm at 4-6°C, which resulted in a collagen yield of 90% from silver-line grunt and albacore tuna. After this initial study, the kinetics of collagen self-assembly were studied, and it was determined that self-assembly greatly relies on pH as well as temperature and concentration [25]. Hyaluronic acid (HA) is another material frequently used as a biomaterial, and purity and molecular weight (MW) of this material is paramount in many applications. A primary issue with HA extraction and purification is elimination of proteins from the proteoglycan matrix [26]. HA is taken from three distinct sources, which include bacteria, animals, and enzymatic synthesis [27]. MW is an important feature of HA, as different molecular weights have different properties and lend themselves to different applications. Thus, the extraction process of HA must be tailored in a way to recover the most suitable MW. This has previously been investigated by subjecting *Streptococcus zooepidemicus* to differing amino acid concentrated media. Post extraction, the more concentrated media resulted in an average HA MW of 2600 ± 100 kDa compared to the less concentrated media with an average HA MW of 2200 ±100 kDa [15].

Altering the parameters of extraction processes has also been shown to affect properties of other proteins in solution, as well as when fabricated into hydrogels. Mechanical properties such as gel strength and viscosity of pig gelatin were shown to fluctuate when extraction temperature and acetic acid concentration were changed. Samples extracted with a higher concentration of acetic acid were shown to exhibit a higher gel strength and a lower viscosity, and samples extracted at a higher temperature were shown to exhibit higher gel strength and viscosity [9]. Much like keratin, silk also exhibits a great propensity to undergo self-assembly in solution with the end result being self-assembled micelles. Different dialysis methods have been

applied to the purification of silk fibroin extracted from cocoons. The most common dialysis method includes dialyzing against water, which has been shown to result in the formation of silk fibroin aggregates [12]. Another dialysis method used with silk has involved dialyzing against polyethylene glycol solution (PEG), which allowed for the extraction of more concentrated silk fibroin [13].

2.5. Conclusions

In this study, we set out to investigate the differences between oxidized keratin samples (KOS) that underwent identical extraction methods, but different purification steps that specifically targeted solution aggregation behavior. We hypothesized that the amount of protein aggregation would have a significant effect on the purity of the final purified product and that the purity would, in turn, affect the structural integrity of hydrogel networks formed, both from a mechanical perspective and an enzymatic degradation perspective. From the gathered data, we determined that alteration of the conventional KOS extraction method by changing the dialysis process from the use of purified water to an appropriate buffer system, results in a KOS material that is less dominated by peptide fragments and more dominated by keratin nanomaterial. Because of the reduced peptide content, the structural integrity of KOS hydrogels was increased, but unexpectedly, the susceptibility to enzymatic degradation was increased. The results from this study suggest that the mechanical and biochemical properties of KOS biomaterials can be manipulated by alterations to purification techniques.

2.6. Acknowledgements

The authors thank Dr. Rick Davis of Virginia Tech Department of Chemical Engineering for allowing the use of the ARG2 rheometer as well as the Zetasizer Nano ZS, as well as Laura Wichin for her assistance in the KOS peptide degradation studies and preparation of the

MATLAB code used for determination of the enzyme cleavage sites within the keratin amino acid sequences. Funding was provided by Virginia Tech Biomedical Engineering and Mechanical (BEAM) departmental and overhead funds.

References

[1] de Guzman, R. C., Merrill, M. R., Richter, J. R., Hamzi, R. I., Greengauz-Roberts, O. K., & Van Dyke, M. E. (2011). Mechanical and biological properties of keratose biomaterials. *Biomaterials, 32*(32), 8205-8217. doi:10.1016/j.biomaterials.2011.07.054

[2] Apel, P. J., Garrett, J. P., Sierpinski, P., Ma, J., Atala, A., Smith, T. L., . . . Van Dyke, M. E. (2008). Peripheral nerve regeneration using a keratin-based scaffold: long-term functional and histological outcomes in a mouse model. *J Hand Surg Am, 33*(9), 1541-1547. doi:10.1016/j.jhsa.2008.05.034

[3] Lin, Y. C., Ramadan, M., Van Dyke, M., Kokai, L. E., Philips, B. J., Rubin, J. P., & Marra, K. G. (2012). Keratin gel filler for peripheral nerve repair in a rodent sciatic nerve injury model. *Plast Reconstr Surg, 129*(1), 67-78. doi:10.1097/PRS.0b013e3182268ae0

[4] Shen, D., Wang, X., Zhang, L., Zhao, X., Li, J., Cheng, K., & Zhang, J. (2011). The amelioration of cardiac dysfunction after myocardial infarction by the injection of keratin biomaterials derived from human hair. *Biomaterials, 32*(35), 9290–9299. doi:10.1016/j.biomaterials.2011.08.057

[5] de Guzman, R. C., Saul, J. M., Ellenburg, M. D., Merrill, M. R., Coan, H. B., Smith, T. L., & Van Dyke, M. E. (2013). Bone regeneration with BMP-2 delivered from keratose scaffolds. *Biomaterials, 34*(6), 1644-1656. doi:10.1016/j.biomaterials.2012.11.002

[6] Nakamura, A., Arimoto, M., Takeuchi, K., & Fujii, T. (2002). A rapid extraction procedure of human hair proteins and identification of phosphorylated species. *Biol Pharm Bull, 25*(5), 569-572.

[7] Schrooyen, P. M., Dijkstra, P. J., Oberthur, R. C., Bantjes, A., & Feijen, J. (2000). Partially carboxymethylated feather keratins. 1. Properties in aqueous systems. *J Agric Food Chem, 48*(9), 4326-4334.

[8] Hartrianti, P., Nguyen, L. T., Johanes, J., Chou, S. M., Zhu, P., Tan, N. S., . . . Ng, K. W. (2016). Fabrication and characterization of a novel crosslinked human keratin-alginate sponge. *J Tissue Eng Regen Med*. doi:10.1002/term.2159

[9] Sompie, M., Surtijono, S. E., Pontoh, J. H. W., & Lontaan, N. N. (2015). The Effects of Acetic Acid Concentration and Extraction Temperature on Physical and Chemical Properties of Pigskin Gelatin. *First International Symposium on Food and Agro-Biodiversity Conducted by Indonesian Food Technologists Community, 3*, 383-388. doi:10.1016/j.profoo.2015.01.042

[10] Crewther, W. Frase, R., Lennox F.,et al. The chemistry of keratins. Advances in protein chemistry. New York: Academic Press 1965;191-346.

[11] Sierpinski, P., Garrett, J., Ma, J., Apel, P., Klorig, D., Smith, T., . . . Van Dyke, M. (2008). The use of keratin biomaterials derived from human hair for the promotion of rapid regeneration of peripheral nerves. *Biomaterials, 29*(1), 118-128. doi:10.1016/j.biomaterials.2007.08.023

[12] Lu, Q., Zhu, H., Zhang, C., Zhang, F., Zhang, B., & Kaplan, D. L. (2012). Silk self-assembly mechanisms and control from thermodynamics to kinetics. *Biomacromolecules, 13*(3), 826-832. doi:10.1021/bm201731e

[13] Kim, U. J., Park, J., Li, C., Jin, H. J., Valluzzi, R., & Kaplan, D. L. (2004). Structure and properties of silk hydrogels. *Biomacromolecules, 5*(3), 786-792. doi:10.1021/bm0345460

[14] Kakkar, P., Madhan, B., & Shanmugam, G. (2014). Extraction and characterization of keratin from bovine hoof: A potential material for biomedical applications. *Springerplus, 3*, 596. doi:10.1186/2193-1801-3-596

[15] Armstrong, D. C., Cooney, M. J., & Johns, M. R. (1997). Growth and amino acid requirements of hyaluronic-acid-producing Streptococcus zooepidemicus. *Applied Microbiology and Biotechnology, 47*(3), 309-312.

[16] Cai, C., Xu, X., & Zheng, X. (2011). Keratin Degradation and Dehairing Application of Keratinase from a New Bacillus subtilis Strain. *2011 5th International Conference on Bioinformatics and Biomedical Engineering*. doi:10.1109/icbbe.2011.5781470

[17] Asakura, T., Adachi, K., & Schwartz, E. (1978). Stabilizing Effect of Various Organic Solvents on Protein. *Journal of Biological Chemistry, 253*(18), 6423-6425.

[18] Kastelic, M., Kalyuzhnyi, Y. V., Hribar-Lee, B., Dill, K. A., & Vlachy, V. (2015). Protein aggregation in salt solutions. *Proceedings of the National Academy of Sciences of the United States of America, 112*(21), 6766-6770. doi:10.1073/pnas.1507303112

[19] Pace, L. A., Plate, J. F., Smith, T. L., & Van Dyke, M. E. (2013). The effect of human hair keratin hydrogel on early cellular response to sciatic nerve injury in a rat model. *Biomaterials, 34*(24), 5907-5914. doi:10.1016/j.biomaterials.2013.04.024

[20] Extracellular Matrix: A Practical Approach, Haralson, M., and Hassell, J., eds., IRL Press at Oxford University Press (Oxford, England: 1995), p. 31.

[21] Hill, P., Brantley, H., & Van Dyke, M. (2010). Some properties of keratin biomaterials: Kerateines. *Biomaterials, 31*(4), 585-593. doi:10.1016/j.biomaterials.2009.09.076

[22] de Guzman, R. C., Tsuda, S. M., Ton, M. T. N., Zhang, X., Esker, A. R., & Van Dyke, M. E. (2015). Binding Interactions of Keratin-Based Hair Fiber Extract to Gold, Keratin, and BMP-2. *Plos One, 10*(8). doi:ARTN e0137233

[23] Zhang, Y., Liu, W. T., Li, G. Y., Shi, B., Miao, Y. Q., & Wu, X. H. (2007). Isolation and partial characterization of pepsin-soluble collagen from the skin of grass carp

(Ctenopharyngodon idella). *Food Chemistry, 103*(3), 906-912. doi:10.1016/j.foodchem.2006.09.053

[24] Noitup, P., Garnjanagoonchorn, W., & Morrissey, M. T. (2005). Fish Skin Type I Collagen: Characteristic Comparison of Albacore Tuna (Thunnus Alalunga) and Silver-Line Grunt (Pomadasys Kaakan). *Journal of Aquatic Food Product Technology,14*(1), 17-28. doi:10.1300/j030v14n01_03

[25] Noitup, P., Morrissey, M. T., & Garnjanagoonchorn, W. (2006). In vitro self-assembly of silver-line grunt type I collagen: Effects of collagen concentrations, pH and temperatures on collagen self-assembly. *Journal of Food Biochemistry, 30*(5), 547-555. doi:DOI 10.1111/j.1745-4514.2006.00081.x

[26] Murado, M. A., Montemayor, M. I., Cabo, M. L., Vazquez, J. A., & Gonzalez, M. P. (2012). Optimization of extraction and purification process of hyaluronic acid from fish eyeball. *Food and Bioproducts Processing, 90*(C3), 491-498. doi:10.1016/j.fbp.2011.11.002

[27] Sze, J. H., Brownlie, J. C., & Love, C. A. (2016). Biotechnological production of hyaluronic acid: a mini review. *3 Biotech, 6*. doi:ARTN 67

Supplemental Figures

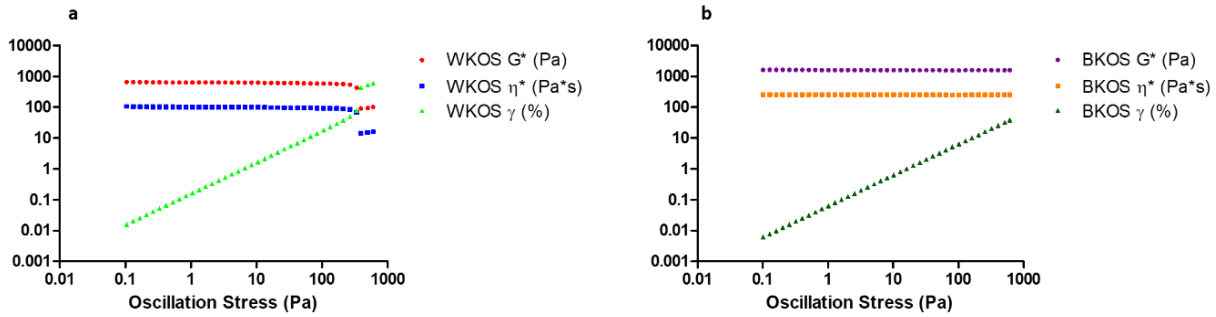

Supplemental Figure S2.1: Stress sweep analysis for both WKOS and BKOS hydrogels. From these data, the LVER was determined. 25 pa was used for subsequent frequency sweep tests as this value resided in the LVER for both hydrogel types.

Chapter 3

Fabrication and Characterization of a Novel Keratose-Type I Collagen Biomaterial

Nils A. Potter and Mark Van Dyke

Virginia Polytechnic Institute and State University, Department of Biomedical Engineering and Mechanics, School of Biomedical Engineering and Sciences, Blacksburg, VA 24061

Abstract

Keratin is a natural biopolymer that resides in skin, nails, and hair fibers and is typically extracted through oxidative or reductive chemistries. Keratins belong to the intermediate filament family of proteins and they exhibit a great propensity to undergo self-assembly. Extracted oxidized keratin biomaterials, however, display poor mechanical properties and can only form stable hydrogel constructs at very high concentrations on the order of 15-20 wt%. These poor gelation properties can render the biomaterial ineffective when exposed to a tissue regeneration environment. Material blends have been created to combine favorable qualities of two or more biomaterials while aiming to mitigate the less desirable qualities of said materials. Taking advantage of the inherent self-assembly characteristics of type I collagen to promote hydrogel formation when subjected to a neutral pH is an innovative way to allow for oxidized keratin to be incorporated into a hydrogel network structure at much lower total protein concentrations. Here, we examine and characterize the formation of a novel protein biomaterial blend resulting from the coupling of type I collagen extracted from rat tail with oxidized keratin extracted from human hair through numerous means including enzymatic degradation, structural architecture observation, and rheological measurements. KOS/COL blends were able to be fabricated at 0.5 wt% total protein content while determining optimal chemical crosslinking density. Rheological measurements revealed that resistance to shear increased as the COL concentration was increased. A more connective network was shown in the microarchitecture in samples with greater KOS content. Cell viability was shown the be similar in 80/20 KOS/COL ratios compared to COL hydrogel controls.

Keywords: keratin, type I collagen, self-assembly, hydrogel

3.1. Introduction

Biomaterials derived from natural sources have experienced notable success in the field of tissue regeneration. Many of these biomaterials fall into the protein category and are primarily derived (e.g. acellular grafts) or extracted from animal sources. One protein biomaterial that has gained more traction in the field of tissue regeneration is keratin. Keratin is a protein commonly found in nails, hooves, skin, and hair fibers. Many methods are practiced for extracting keratin proteins such as oxidative chemistries, reductive chemistries, microwave irradiation, alkali extraction, sulfitolysis, and ionic liquid extraction. Oxidative and reductive chemistries are the most prevalent of the methods, yielding keratose (KOS) and kerateine (KTN), respectively [3, 29-34]. Keratins are characterized by containing a high concentration of cysteine amino acid residues, which allow for a greater amount of disulfide linkages to occur between monomers due to the free thiol groups (R-SH) on their side chains which, when combined with self-assembly, yields particularly strong materials [27]. Following extraction, however, KOS has disulfide bonds and free thiol groups oxidized into sulfonic acid residues ($R\text{-}SO_3^-$) while KTN has the disulfide bonds reduced into free thiols [41]. Because of this chemical change following extraction, KOS is not as stable as the KTN counterpart due to its inability to reform disulfide linkages.

Like other natural biomaterial constructs, keratin biomaterials have been formed into hydrogels, scaffolds, and coatings, and characterization of these constructs have been carried out at great lengths [1, 33-34, 41]. These have been used in a multitude of *in vitro* investigations such as hepatocyte attachment and macrophage polarization along with *in vivo* tissue regeneration applications including burn, cardiac, bone, muscle, and peripheral nerve regeneration, demonstrating success in each application [4-12, 42-45].

Type I collagen (COL) is another protein-based biomaterial that is used frequently in tissue regeneration applications. COL is the most abundant component in the extracellular matrix (ECM) and is distinguished by its triple helical structure along with an abundance of glycine, proline, and hydroxyproline amino acid residues in its protein chain [13]. COL also contributes greatly to the mechanical stability of tissues such as bones, tendons, ligaments, and skin [47]. Common sources for this material in research include rat tail, bovine skin, and porcine skin, which can be extracted through numerous means including enzymatic hydrolysis such as digestion with pepsin in an acidic solution or chemical hydrolysis with organic acids such as acetic acid [2, 28, 35-39]. COL is also well recognized for its ability to undergo self-assembly when adjusted to neutral pH, which is also referred to as fibrillogenesis [17]. This self-assembly characteristic allows for COL to form stable hydrogels when introduced to a neutral pH and body temperature environment. Hydrogels consisting of COL have been characterized in great depth by observing the effects that variables such as COL concentration, polymerization temperature, pH, and ionic strength have on overall hydrogel structure and mechanics [48-55]. COL has also been utilized in numerous applications much like keratin including peripheral nerve, bone, and corneal regeneration [14-16].

Depending on the molecular composition of each biomaterial, different characteristics vary such as mechanical integrity, degradation kinetics, and self-assembly characteristics. Due to these variations and inherent limitations of any one pure biomaterial system, biomaterials are commonly combined with the primary goal of harnessing positive qualities from each biomaterial while mitigating deficiencies of the pure material. Keratin has been widely used in connection with other materials from different molecular families for this purpose. Commonly, the goal for combining keratin with another material is to improve upon mechanical properties of

oxidized keratin hydrogels, fibers, and scaffolds, which are inherently weak when hydrated and can be brittle when dried. This has been done previously with the incorporation of poly(ethylene oxide) (PEO), poly(L-lactic acid) (PLA), chitosan, poly(ε-caprolactone) (PCL), and alginate [18-21]. COL has also been used in creating blended biomaterials, including mixtures with poly(D, L-lactide-co-glycolide) (PLGA), PCL, PEO, agarose, and chitosan [22-26]. Often, the primary objectives of these blended biomaterials are to improve the mechanical properties through incorporation of, for example, synthetic polymers, improve tissue compatibility by introducing natural collagen, and improving thermal properties. COL's well-defined self-assembly characteristics have to potential to improve the mechanical properties of KOS hydrogels, which characteristically require large amounts of protein to achieve desired characteristics in unblended systems [1,8,10-12,33].

3.2. Methods

3.2.1. Extraction of Keratose from Human Hair

KOS was extracted as described previously [1]. In brief, dry human hair fibers were received from a commercial source and oxidized using a 2% (w/v) solution of peracetic acid (PAA) in ultrapure water. Oxidation was carried out at 37 °C with continuous stirring for 12 h at a 1:20 ratio of hair fiber weight to liquid volume. The oxidized fibers were recovered after stirring by passing them through a 500 μm sieve and were rinsed with deionized water until no PAA was detectable with a test strip. Hair fibers were then extracted twice at a 1:40 ratio of dry hair fiber weight to 100 mM tris base at 37 °C for 2 h with continuous stirring. Following each extraction, the fibers were recovered via sieve and the liquid was retained. The liquid extracts were then combined, centrifuged, and filtered to allow for solids removal. KOS was further purified through use of a custom tangential flow filtration (TFF) system. The sample was first

dialyzed against a phosphate buffer solution (10 mM Na_2HPO_4/ 100 mM NaCl, pH 7.4) then ultrapure water. Following dialysis, the sample was concentrated, frozen, lyophilized, and ground into a powder for application.

3.2.2. Extraction of Type I Collagen from Rat Tails

Using an adapted protocol, COL was extracted from the tails of Sprague-Dawley rats [2]. Briefly, Sprague-Dawley rat tails were purchased from BioIVT (Westbury, NY) and cleaned thoroughly with 70% ethanol. Using a #22 blade attached to a #4 scalpel, the rat tail skin was removed to expose the tendon. Following this, 2 pairs of surgical clamps were used to separate the knuckle regions on the tail and remove the collagen strands. The strands were then placed in 70% ethanol for 15 min, removed, air dried, and weighed. Tendon strands were then placed in a solution of 0.1% acetic acid at a concentration of 200 ml/g of tendon for 72 h at 4 °C with occasional stirring. After dissolving in 0.1% acetic acid, the solution was centrifuged at 33,000g for 45 min at 4°C to separate the insoluble fraction from the soluble fraction. The soluble fraction was separated, frozen at -80°C, and lyophilized with the aid of an acid trap attachment (Labconco).

3.2.3. KOS/COL Material Fabrication

KOS was dissolved in 1X phosphate buffered saline (PBS) at a concentration of 28 mg/ml, and COL was dissolved in 0.1 M acetic acid at a concentration of 3 mg/ml. 10X PBS was added to ensure the final solution had a salt concentration of 1X PBS, 1 M NaOH was added to titrate the solution pH to 7.4, and ultrapure water was added to correct for the final calculated target volume. COL was added to this solution, and then a 20 mM stock solution of genipin (Wako Chemicals) in 1X PBS was added to provide for crosslinking of the resulting protein network. KOS was added last, and all the components were mechanically mixed using a plastic

spatula while making sure visually that the KOS did not precipitate from solution due to its insolubility in acidic media. Samples were all made at a consistent 0.5 wt% total protein content to allow for proper mixing of all components. Following mixing, pH of 7.4 was confirmed with a pH test strip, and the mixture was incubated at 37 °C for 72 h to allow for protein self-assembly and full genipin crosslinking. Immediately after curing, the newly formed gel was frozen at -80°C overnight and lyophilized for 72 h. Pure COL hydrogels were fabricated in a similar fashion by mixing 10X PBS, 1 M NaOH, ultrapure water, and a 3 mg/ml COL solution together where a neutral pH was achieved. The final pH was determined by pH test strips, and the final concentration of COL in the hydrogel was 2.4 mg/ml. Curing of the COL hydrogel was induced by placing the COL solution at 37 °C for 45 min. For cell culture, each biomaterial was sterilized using a protocol adapted from Sigma [59]. Briefly, KOS and COL were solubilized and placed atop a layer of chloroform 10% in volume to the entire suspension in separate glass containers. Each suspension was placed at 4 °C overnight to allow the chloroform vapor to travel upward and sterilize the material. The next day, the solution was aspirated off aseptically and carefully to avoid reintroducing any potential bacterial cells and/or residual chloroform.

3.2.4. Degree of Crosslinking

The amount of crosslinking between KOS and COL was determined by quantifying free amine groups in the combined material matrix. The crosslinking mechanism of genipin primarily involves binding to free primary amine groups, which are found in abundance on the N-terminus portion of an amino acid chain along with numerous side chains of amino acids such as lysine or arginine [46]. Briefly, 1 ml of ninhydrin solution (0.4% in water) was added to 10 mg of KOS/COL sample and incubated in a 90 °C bead bath for 20 min. The samples were cooled down to room temperature (RT), the supernatant was removed, and absorbance was read at 570

nm using a microplate reader. The degree of crosslinking was determined by comparing the absorbance reading from a crosslinked sample and comparing it to a non-crosslinked sample.

3.2.5. Scanning Electron Microscopy

The architecture of KOS/COL material was observed using scanning electron microscopy (SEM) (LEO (Zeiss) 1550 field-emission scanning electron microscope – Virginia Tech Nanoscale Characterization and Fabrication Laboratory). Prior to imaging, samples were cut with a razor blade to obtain pieces that fit the size requirements for the instrument along with obtaining a discernible cross-section. Samples were mounted on doubled-sided carbon tape and coated with approximately 7 nm of platinum/palladium. Samples were then imaged at an accelerating voltage of 5 kV.

3.2.6. Water Uptake Capacity

The water uptake capacity was determined by immersing lyophilized samples in ultrapure water at RT for 60 s. Samples were placed in individual wells and allowed to air dry for 3 h, and the masses before and after water immersion were documented. Water uptake capacity was calculated as follows:

$$Water\ Uptake\ Capacity\ (\%) = \frac{W_h - W_0}{W_0}\ x\ 100$$

W_0 is the mass of a dried sample, and W_h is the mass of the hydrated sample.

3.2.7. Rheological Testing

The rheological properties of KOS/COL material were determined using an ARG2 rheometer (TA Instruments). 12 ml of each cured gel type was lyophilized, and the resulting samples were cut in half with a razor blade, submerged in ultrapure water for 60 s, and placed on

the Peltier plate. A stainless steel 25 mm diameter parallel plate was used for testing. All tests were performed at a 1000 μm gap height and 37 °C. Prior to testing, samples were trimmed and underwent a conditioning step for 60 s to allow for stress relaxation after being compressed with the parallel plate geometry. Stress sweep tests were conducted within a stress range of 0.1-600 Pa at a constant frequency of 1 Hz to determine the linear viscoelastic region (LVER). Following stress sweep tests, frequency sweep tests were conducted within a frequency range of 0.1-10 Hz. For these tests, a constant stress of 10 Pa was used for all samples as this was found to reside within the LVER for each stress sweep test.

3.2.8. Enzymatic Degradation

Degradation of crosslinked KOS/COL material was done in a 48-well plate format. Between 5-10 mg of sample was weighed out and placed in individual wells. Prior to immersing in enzyme solution, dry samples were sterilized through X-ray irradiation at a dose of 100 Gy to prevent any bacteria from secreting enzymes that would unwantedly contribute to material degradation. Following irradiation, samples were immersed in 600 μl of enzyme solution with a concentration of 0.5 U/ml in PBS. Samples were kept at 37 °C and the well plates were wrapped with parafilm to negate any possible evaporation. The enzymes used for these experiments include type I collagenase, elastase, and keratinase while using PBS as a control. Enzyme solution was aspirated off and replaced every 4 days. Following every time point, samples were removed, frozen at -80 °C, and lyophilized. Sample masses were recorded and compared to their initial masses to calculate degradation.

3.2.9. Differential Scanning Calorimetry

Lyophilized samples were weighed between 1-10 mg, placed into tzero, pans and covered with tzero lids using a hydraulic press (TA Instruments). Covered samples were placed opposite

to the reference pan in the DSC Q20 (TA Instruments). The instrument was equilibrated to 25 °C, and a scan was run from 25-300 °C at a heating rate of 10 °C/min. KOS and lyophilized neutralized COL were used as controls.

3.2.10. Cell Viability

Cell viability when exposed to KOS/COL hydrogels was assessed using an alamarBlue assay. COL hydrogels and KOS coatings were used as comparison groups. KOS/COL hydrogels were prepared as mentioned previously. To prevent drying of the hydrogels, 1X PBS was added atop the gels after 12 h of curing time and remained for the next 60 h. KOS coatings were made using 200 μg/ml of KOS in 1X PBS, adding sufficient solution volume to cover the surface of the well, and incubating at 37°C for 2 h. Following incubation, the solution was aspirated out of each well, and all wells were washed 3 times with 1X PBS for 5 min prior to cell seeding. Human dermal fibroblasts (HDFs) were seeded at a density of 50,000 cells/well in Dulbecco's modified eagle medium (DMEM) supplemented with 10% fetal bovine serum (FBS) and 1% penicillin/streptomycin in a polystyrene, tissue culture treated 24 well plate and incubated at 37°C in 5% CO_2. Time points of 24, 48, and 72 h were used to assess viability. Before alamarBlue treatment, the medium was removed and replaced with fresh medium containing alamarBlue reagent. After treatment, the plates were incubated at 37 °C for 24 h. To mitigate any potential fluorescence interference from the KOS/COL gels, 100 μl of media after alamarBlue treatment was taken from the 24 well plate and placed into a separate 96 well plate, and that plate was read for fluorescence using a Synergy H1 microplate reader (BioTek®) at 560/590 nm. A positive control of cells seeded on tissue culture plastic (TCP) was used for comparison.

3.2.11. Statistical Analysis

All quantitative results are reported as means ± standard deviation unless otherwise stated. Statistical analyses were carried out in JMP 13.0.0 using one-way analysis of variance (ANOVA) and Tukey's post hoc tests to determine significance. Statistical significance was defined as $p < 0.05$.

3.3. Results

3.3.1. Crosslinking Index

Crosslinking index determined by the ninhydrin assay revealed that genipin was able to adequately crosslink KOS and COL together to form a composite biomaterial matrix. These results are depicted by **Figure 3.1a & 3.1b**. The greatest crosslinking indexes observed were expectedly the 5 mM genipin groups at 1 day and 3 days with indexes of 74.44 ± 4.20% and 85.93 ± 3.90%, respectively. Allowing the material to cure for 3 days at 1 mM genipin concentration compared to 1 day showed statistically significant differences ($p < 0.01$). Although 5 mM of genipin at both time points exhibited a greater crosslinking index than samples at 1 mM of genipin, it was deduced that because an addition of 5 times the concentration of crosslinking solution did not even double the crosslinking index compared to the 1 mM 3 day group (53.26 ± 11.05%), much unreacted genipin solution remained within the sample, which would be toxic in a biological setting. From this, a genipin concentration of 1 mM and a cure time of 3 days was used for further experiments.

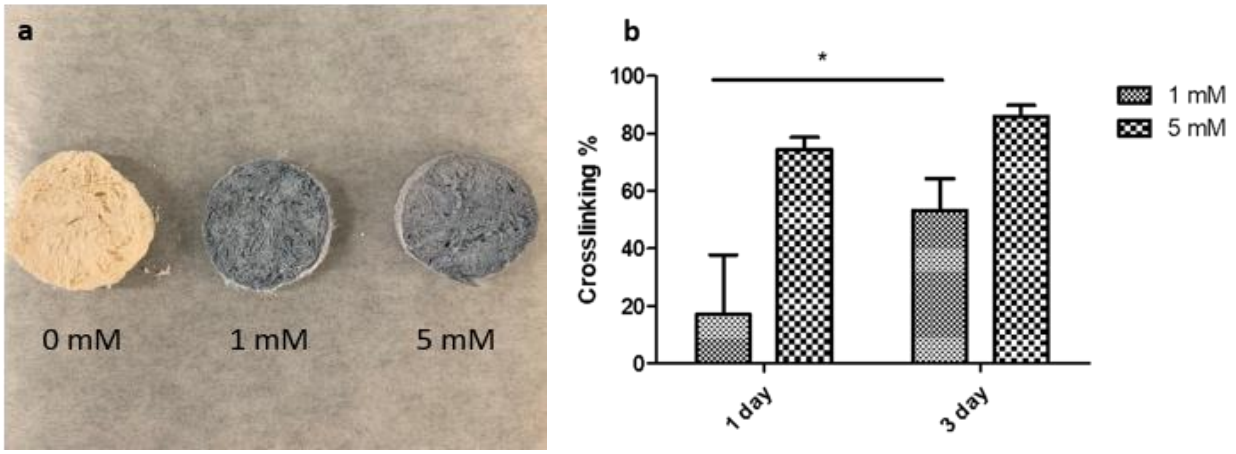

Figure 3.1: Visual representation of the composite KOS/COL material at different genipin concentrations after 3 days of crosslinking (a) and a ninhydrin assay (b) to quantify free amine content (mean ± SD, n = 5). Genipin acts to bind to free amines of protein to carry out crosslinking. * signifies $p < 0.01$.

3.3.2. Water Uptake

Water uptake measurements revealed that samples with higher crosslink density retained more water than those without any crosslinker (**Figure 3.2**). Compared to their uncrosslinked counterparts, the water uptake for each KOS/COL sample at 1 mM of crosslinking was statistically significant. In addition, it was observed that as the KOS concentration increased and the COL concentration decreased within the samples crosslinked with 1 mM genipin, the water uptake increased as well. The water uptake between the 60/40 1 mM and 70/30 1 mM samples along with the uptake between the 60/40 1 mM and the 80/20 1 mM samples was shown to be statistically significant ($p < 0.05$ and $p < 0.005$, respectively). Uptake between the 70/30 1 mM and 80/20 1 mM samples was not significant, although an increasing trend was observed. This pattern was also observed within the 0 mM and 5 mM genipin crosslinked series, but no statistically significant difference was found between different KOS/COL ratios.

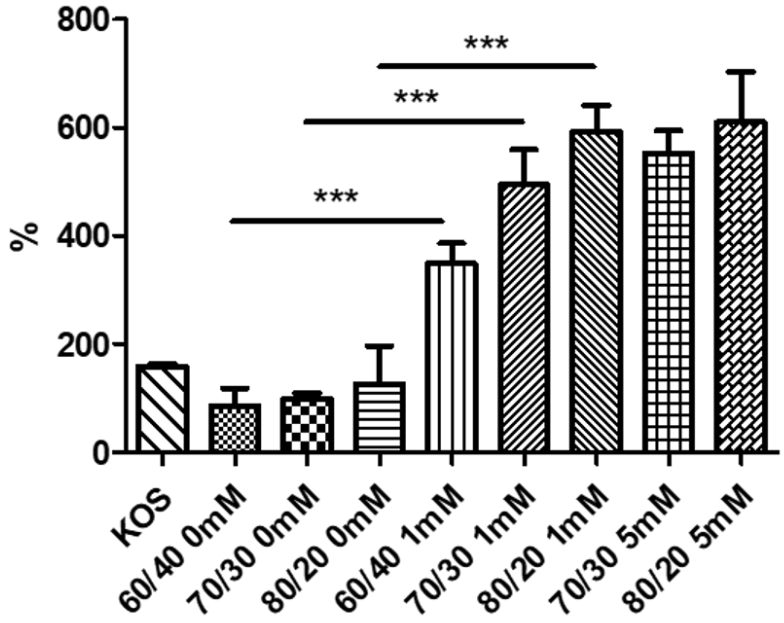

Figure 3.2: Water uptake capacity after 3 h of air drying of KOS/COL ratios of 60/40, 70/30, and 80/20 with differing amounts of genipin (mean ± SD, n = 3). 60/40 5mM samples were not fabricated due to volume restrictions. KOS with no genipin was used as a control. *** signifies $p < 0.001$.

3.3.3. Rheology

Rheological measurements revealed a strong trend of the hydrated sample becoming stronger as the ratio of COL increased. The complex modulus (G*) increased as the ratio of COL increased as illustrated by the stress sweep analysis (**Figure 3.3a**). Each material type retained similar LVERs over the range of 0.1-600 Pa at a constant frequency of 1 Hz. From these LVERs, a constant stress of 10 Pa was at which to conduct frequency sweeps. Frequency sweep tests (**Figure 3.3b & 3.3c**) also confirmed that the addition of COL led to an increase in shear resistance over a range of 0.1-10 Hz. At each order of magnitude for frequency (0.1, 1, and 10 Hz), the storage modulus (G') was found to be significantly different between 70/30 and 80/20 ratios of KOS/COL ($p < 0.05$) and between 60/40 and 80/20 ratios ($p < 0.001$). Peak storage

modulus values for each KOS/COL blend were all found at 10 Hz (1201 ± 111.3 Pa for 80/20, 1677 ± 269.9 Pa for 70/30, and 3546 ± 346.2 Pa for 60/40).

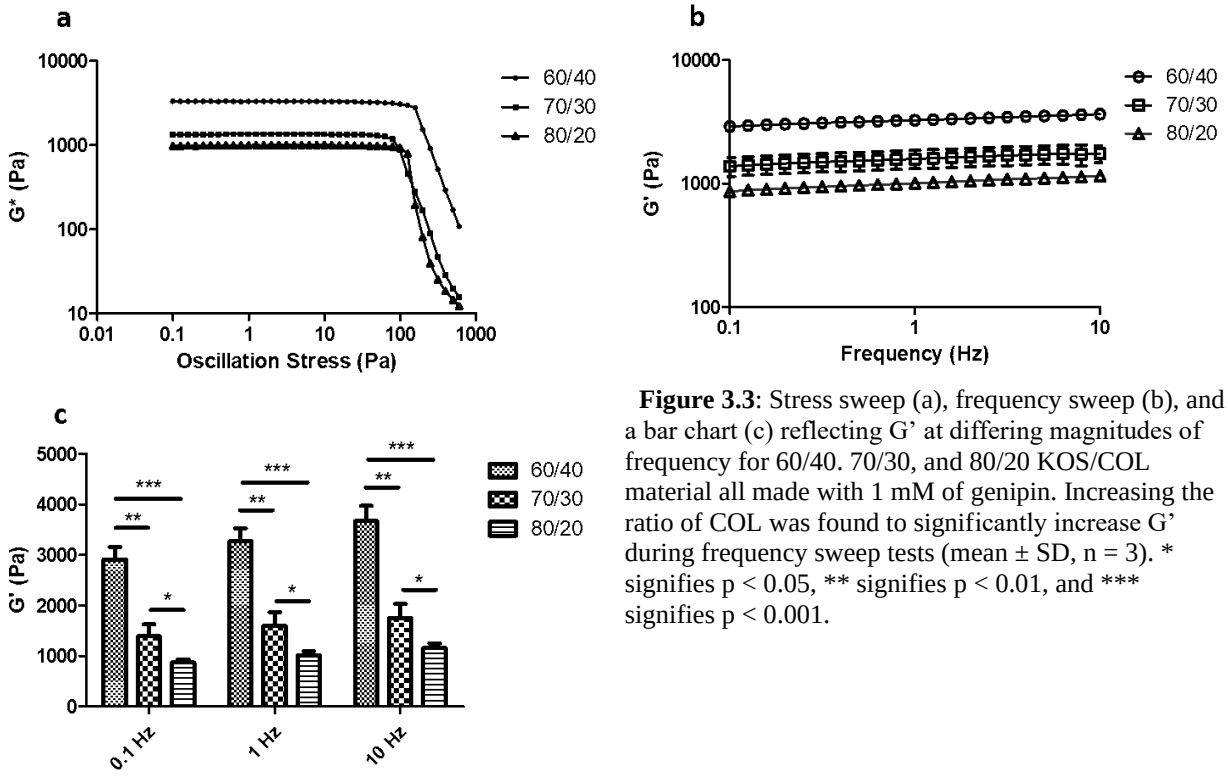

Figure 3.3: Stress sweep (a), frequency sweep (b), and a bar chart (c) reflecting G' at differing magnitudes of frequency for 60/40. 70/30, and 80/20 KOS/COL material all made with 1 mM of genipin. Increasing the ratio of COL was found to significantly increase G' during frequency sweep tests (mean ± SD, n = 3). * signifies $p < 0.05$, ** signifies $p < 0.01$, and *** signifies $p < 0.001$.

3.3.4. Scanning Electron Microscopy

SEM micrographs show an increase in interconnected architecture as more KOS was added to the matrix (**Figure 3.4**). At lesser KOS ratios, seen in the 60/40 micrographs (left), the structure contained a more random, sheet-like architecture. The structure of the 70/30 micrographs (middle) closely resembles the microstructure of lyophilized 20% KOS hydrogels [33]. At the greatest KOS ratio, displayed by the 80/20 micrographs (right), a highly interconnected and porous architecture was observed with notably less planar structure and more fibrous connections between planes.

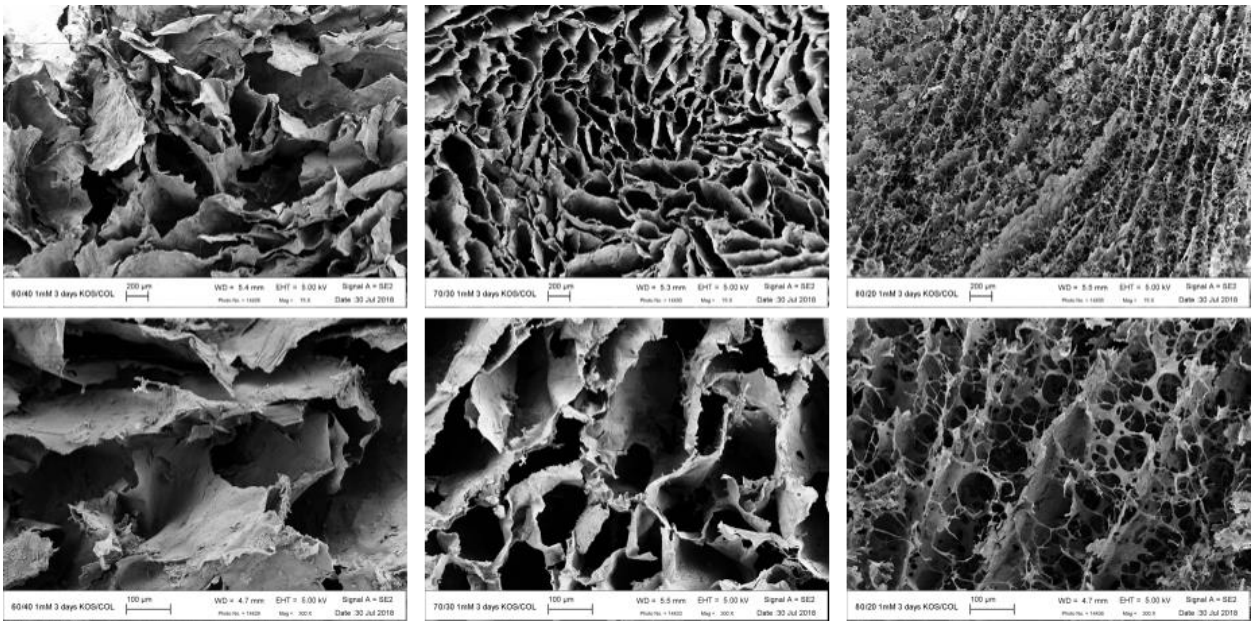

Figure 3.4: SEM micrographs showing architecture of KOS/COL ratios of 60/40, 70/30, and 80/20 (left to right) at 75x (top row) and 300x (bottom row). As the COL concentration decreases and the KOS concentration increases, a more connected network can be observed.

3.3.5. Differential Scanning Calorimetry

Differential scanning calorimetry results (**Figure 3.5**) revealed that the addition of KOS material did not alter the position of first endothermic peak as seen in the COL control group (53.92 ± 0.62 °C). The broad peaks for all samples in the range between 95-110 °C were most likely associated with the evaporation of the unbound water residing within the sample. The KOS control showed a second endothermic peak after the unbound water peak at 233.7 ± 0.50 °C, while the KOS/COL groups did not. The final endothermic peak for each blended material group varied. This peak was observed to be 254.4 ± 3.20, 269.2 ± 0.83, and 260.9 ± 1.46 °C for

60/40, 70/30, and 80/20, respectively. Each of these were shown to be statistically significant compared to the endothermic peak of KOS ($p < 0.001$).

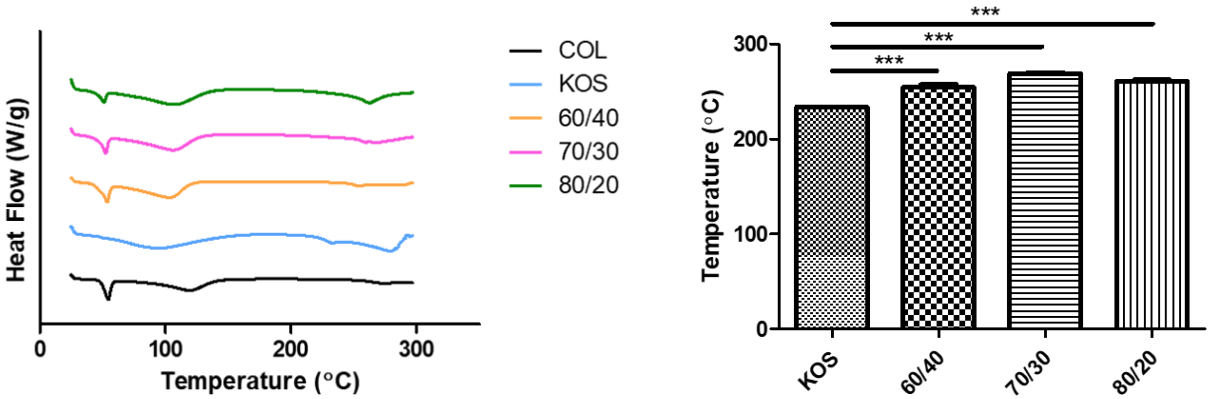

Figure 3.5: Differential scanning calorimetry profiles of COL, KOS, 60/40, 70/30, and 80/20 samples from a temperature range of 25-300 °C and temperatures found for the final endothermic peak of each sample compared to the KOS control endothermic peak (mean ± SD, n = 3). *** signifies $p < 0.001$.

3.3.6. Enzyme Degradation

Enzymatic degradation experiments revealed that for each material ratio, elastase was the most potent enzyme (**Figure 3.6**). After only 6 h with each material, elastase was shown to result in significant degradation compared to the other enzyme treatments (75.54 ± 2.28% for 60/40, 75.47 ± 2.78% for 70/30, and 71.18 ± 2.86% for 80/20; $p < 0.05$ compared to all other enzyme treatment groups at 6 h). Time points beyond 6 h also revealed significant degradation from elastase compared to all other enzyme groups. When comparing by material composition after 16 days, the 60/40 material was shown to result in the most degradation for the PBS, type I collagenase, and keratinase enzyme groups (72.90 ± 1.55%, 71.15 ± 1.23%, and 70.30 ± 0.42%, respectively). While no statistical significance was observed in the type I collagenase degradation among material types, the 60/40 material degradation was significant compared to the 70/30 material in the case of PBS, and the 60/40 material was significant compared to the

70/30 and 80/20 material in the case of keratinase ($p < 0.05$). After 1 day, no significance was observed between any materials in the elastase group.

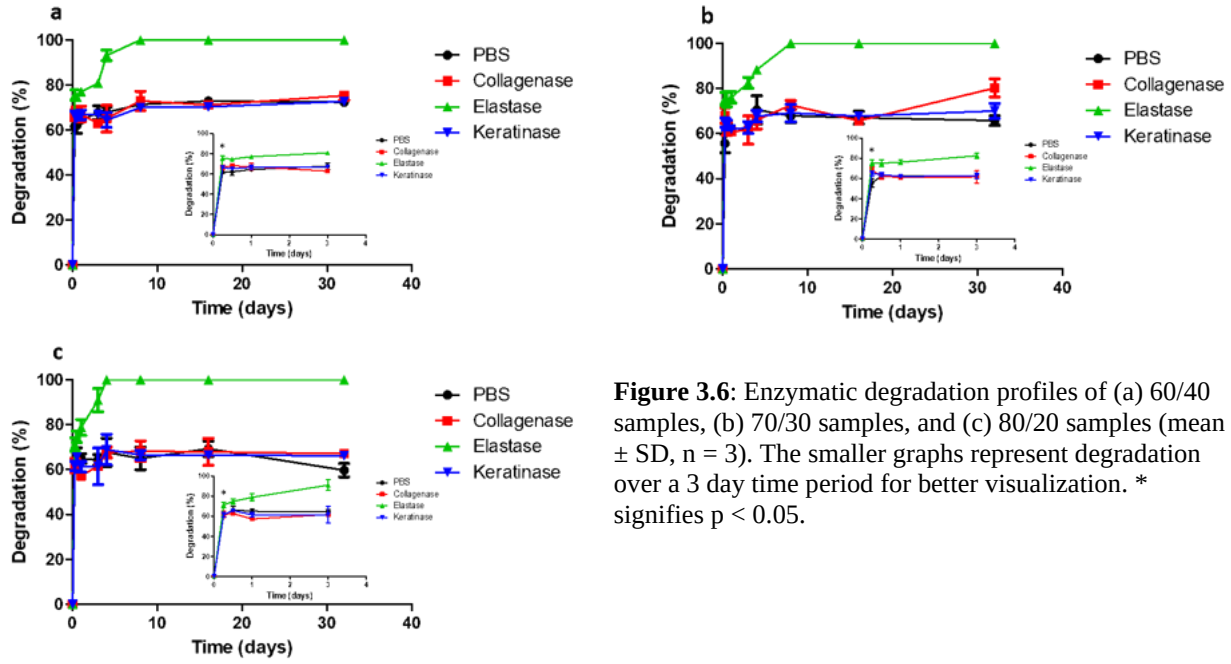

Figure 3.6: Enzymatic degradation profiles of (a) 60/40 samples, (b) 70/30 samples, and (c) 80/20 samples (mean ± SD, n = 3). The smaller graphs represent degradation over a 3 day time period for better visualization. * signifies $p < 0.05$.

3.3.7. Cell Viability

Cell viability experiments (**Figure 3.7**) revealed that some KOS/COL material had comparable cell survival rates to COL hydrogels. The 60/40 and 70/30 materials did not show a similar amount of cell viability compared to COL at each time point, but the 80/20 samples were shown to exhibit viability percentages of 84.27 ± 1.00%, 84.88 ± 0.87%, and 83.94 ± 1.39% at 24, 48, and 72 h time points, respectively. When compared to the results for COL at these time points, no statistical significance was observed.

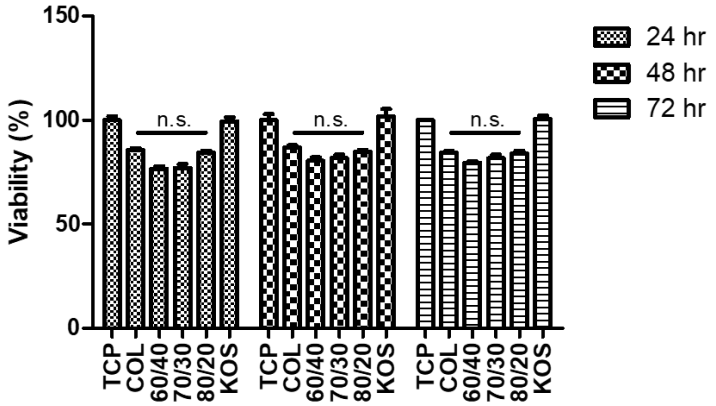

Figure 3.7: Viability profiles of HDFs seeded on top of TCP, KOS/COL hydrogels, COL hydrogels, and KOS coatings (mean ± SD, n = 3). n.s. signifies no statistical significant difference compared to COL hydrogels.

3.4. Discussion

Reduced keratin or "keratose/KOS" is inherently less stable that its reduced counterpart, "kerateine/KTN", due to the absence of reformed disulfide crosslinks. Stability has been imparted to KOS hydrogels by increasing total weight percent of protein, blending with other materials, and addition of exogenous crosslinking agents [8,18-22,58]. COL would seem a natural choice for a material to blend with keratins, having an isoelectric point of approximately 8.2 compared with keratin at approximately 4.6. At neutral pH, the opposing net charge would presumably create strong electrostatic interactions that would act to stabilize the mixture. Despite this, a systematic investigation of COL-keratin systems has not, as yet, been published, and there are no reports of the structure of such blends at the molecular level. The present study was undertaken to demonstrate proof-of-concept for a KOS/COL system wherein, surprisingly, remarkably little COL was required to achieve large changes in the properties of pure KOS hydrogels.

As stated previously, optimal crosslinking conditions in the subject KOS/COL system were at 1 mM of genipin cured for 72 h. This was deemed as the most beneficial because although 5 mM of genipin produced a greater amount of crosslinking, the possibility of unbound

genipin residing within the material even after multiple wash steps was a potential consequence. In addition, the water uptake results showed a direct correlation between crosslinking concentration and the amount of retained water within the material network. Commonly, the higher the degree of crosslinking within a network, the less water uptake is observed due to the formation of a tighter network that does not allow for as much water to reside. In this case, however, the opposite is observed. A possible explanation for this trend could be the weak bonding between materials without crosslinking as mentioned before. KOS is not hydrolytically stable and is very soluble in water. Dissolution of the KOS while being immersed for water uptake studies could have occurred leading to an overall decrease in gel mass.

From a structural standpoint, it was expected that the greater the COL concentration, the greater the strength would be in response to a shear stimulus. This trend was observed in the storage modulus behavior when subjected to differing frequency values. Observation of SEM images reinforces this finding. The 60/40 material exhibits a less porous structure, and as the KOS concentration increases and the COL concentration decreases, the structure becomes more porous with less supportive fibrous content. The microstructure of the 60/40 material seems to translate well to shear resistance while greater porosity does not. From a strictly materials engineering perspective, this is expected since COL is the primary load bearing component within the native extracellular matrix, so more self-assembled COL within a blend would presumably lead to an overall stronger material.

The thermal properties shown by DSC show that the COL denaturation peak was not affected by the combination of KOS and COL, which suggests that mixing at the molecular level did not occur, at least to the point where there is a convergence of thermal behavior. The pure KOS denaturation peak at 233.7 °C was consistent with other DSC profiles of KOS with the

main endothermic peak occurring between 227 and 236 °C [57]. This peak seemed to be shifted slightly to higher temperature with the addition of COL, suggesting that COL contributes to a higher thermal stability for the denaturation of KOS.

Enzymatic degradation showed that elastase was the most potent enzyme to elicit degradation. This is consistent with prior work done on enzymatic degradation of pure KOS hydrogels reported previously [1]. A surprising result was that type I collagenase nor keratinase did not appear to elicit an expected result. That is, a blend high in COL might be expected to degrade faster in collagenase compared to a blend with lower COL content. Similarly, a blend with high KOS content would be expected to show an increase in degradation rate as keratinase concentration increased. However, there appeared to be no such correlations and both proteases were statistically indiscernible from the no-enzyme control, PBS. A possible explanation for this lack of degradation for type I collagenase compared to PBS is that type I collagenase specifically recognizes the amino acid sequence Pro-X-Gly-Pro and cleaves the bond between X and Gly where 'X' is known to be any neutral amino acid [40]. In this material matrix, however, the addition of KOS could be associating closely with COL, blocking the target site of type I collagenase. In the case of keratinase, the enzyme employed in the present work is typically used for the mass digestion of feather keratins in the poultry industry, which differ from human hair keratins [56].

There were no statistically significant differences in cell viability on any of the substrates tested, although some slight trends were observed. In general, and only to a small degree, viability was reduced on all blends and COL itself compared to a pure keratin coating and TCP. Again, this may relate to where cell adhesive receptors are blocked from interacting with their

target ligands within the structure of the network. It is unlikely that this is due to the presence of genipin, since the pure COL control demonstrated a similar outcome.

3.5. Conclusions

This study aimed to create a novel composite material by harnessing the self-assembly characteristics of COL and pairing them with KOS. We hypothesized that the addition of type I collagen would enhance the structural stability of the final product and allow for gelation to occur at concentrations as low as 0.5 wt%. From the gathered data, we were able to determine that the combination of COL and KOS into one material matrix was able to contribute greatly to structural integrity at a low protein content. Also, we observed that the addition of COL to KOS needed the aid of chemical crosslinking since the common bonding mechanisms, with the exception of disulfide bonds, were not sufficient to prevent solid separation. Unexpectedly, the enzymatic susceptibility among differing formulations of KOS/COL material did not differ, and type I collagenase as well as keratinase did not have any major impact on material degradation compared to PBS. The results from this study confirm that COL can be added to KOS to create a stable hydrogel and allows a way to incorporate KOS into hydrogel constructs at lower concentrations than previously reported.

3.6. Acknowledgements

The authors thank Dr. Rick Davis of Virginia Tech Department of Chemical Engineering for allowing the use of the ARG2 rheometer and the Virginia Tech Department of Materials Science for allowing the use of the DSC Q20. Funding was provided by Virginia Tech Biomedical Engineering and Mechanical (BEAM) departmental and overhead funds.

References

[1] Potter, N. A., & Van Dyke, M. (2018). Effects of Differing Purification Methods on Properties of Keratose Biomaterials. *Acs Biomaterials Science & Engineering, 4*(4), 1316-1323. doi:10.1021/acsbiomaterials.7b00964

[2] Szot, C. S., Buchanan, C. F., Freeman, J. W., & Rylander, M. N. (2011). 3D in vitro bioengineered tumors based on collagen I hydrogels. *Biomaterials, 32*(31), 7905-7912. doi:10.1016/j.biomaterials.2011.07.001

[3] Rouse, J. G., & Van Dyke, M. E. (2010). A Review of Keratin-Based Biomaterials for Biomedical Applications. *Materials, 3*(2), 999-1014. doi:10.3390/ma3020999

[4] de Guzman, R. C., Saul, J. M., Ellenburg, M. D., Merrill, M. R., Coan, H. B., Smith, T. L., & Van Dyke, M. E. (2013). Bone regeneration with BMP-2 delivered from keratose scaffolds. *Biomaterials, 34*(6), 1644-1656. doi:10.1016/j.biomaterials.2012.11.002

[5] Dias, G. J., Peplow, P. V., McLaughlin, A., Teixeira, F., & Kelly, R. J. (2010). Biocompatibility and osseointegration of reconstituted keratin in an ovine model. *Journal of Biomedical Materials Research Part A, 92a*(2), 513-520. doi:10.1002/jbm.a.32394

[6] Kowalczewski, C. J., Tombyln, S., Wasnick, D. C., Hughes, M. R., Ellenburg, M. D., Callahan, M. F., . . . Saul, J. M. (2014). Reduction of ectopic bone growth in critically-sized rat mandible defects by delivery of rhBMP-2 from kerateine biomaterials. *Biomaterials, 35*(10), 3220-3228. doi:10.1016/j.biomaterials.2013.12.087

[7] Passipieri, J. A., Baker, H. B., Siriwardane, M., Ellenburg, M. D., Vadhavkar, M., Saul, J. M., . . . Christ, G. J. (2017). Keratin Hydrogel Enhances In Vivo Skeletal Muscle Function in a Rat Model of Volumetric Muscle Loss. *Tissue Engineering Part A, 23*(11-12), 556-+. doi:10.1089/ten.tea.2016.0458

[8] Ledford, B. T., Simmons, J., Chen, M., Fan, H. M., Barron, C., Liu, Z. M., . . . He, J. Q. (2017). Keratose Hydrogels Promote Vascular Smooth Muscle Differentiation from C-kit-Positive Human Cardiac Stem Cells. *Stem Cells and Development, 26*(12), 888-900. doi:10.1089/scd.2016.0351

[9] Sierpinski, P., Garrett, J., Ma, J., Apel, P., Klorig, D., Smith, T., . . . Van Dyke, M. (2008). The use of keratin biomaterials derived from human hair for the promotion of rapid regeneration of peripheral nerves. *Biomaterials, 29*(1), 118-128. doi:10.1016/j.biomaterials.2007.08.023

[10] Pace, L. A., Plate, J. F., Smith, T. L., & Van Dyke, M. E. (2013). The effect of human hair keratin hydrogel on early cellular response to sciatic nerve injury in a rat model. *Biomaterials, 34*(24), 5907-5914. doi:10.1016/j.biomaterials.2013.04.024

[11] Pace, L. A., Plate, J. F., Mannava, S., Barnwell, J. C., Koman, L. A., Li, Z. Y., . . . Van Dyke, M. (2014). A Human Hair Keratin Hydrogel Scaffold Enhances Median Nerve

Regeneration in Nonhuman Primates: An Electrophysiological and Histological Study. *Tissue Engineering Part A, 20*(3-4), 507-517.

[12] Lin, Y. C., Ramadan, M., Van Dyke, M., Kokai, L. E., Philips, B. J., Rubin, J. P., & Marra, K. G. (2012). Keratin Gel Filler for Peripheral Nerve Repair in a Rodent Sciatic Nerve Injury Model. *Plastic and Reconstructive Surgery, 129*(1), 67-78. doi:10.1097/PRS.0b013e3182268ae0

[13] Karsdal, M. A., Leeming, D. J., Henriksen, K., & Bay-Jensen, A. (2016). *Biochemistry of collagens, laminins and elastin: Structure, function and biomarkers*. London, United Kingdom: Elsevier/AP, Academic Press is an imprint of Elsevier.

[14] Labrador, R. O., Buti, M., & Navarro, X. (1998). Influence of collagen and laminin gels concentration on nerve regeneration after resection and tube repair. *Exp Neurol, 149*(1), 243-252. doi:10.1006/exnr.1997.6650

[15] Chamieh, F., Collignon, A. M., Coyac, B. R., Lesieur, J., Ribes, S., Sadoine, J., . . . Rochefort, G. Y. (2016). Accelerated craniofacial bone regeneration through dense collagen gel scaffolds seeded with dental pulp stem cells. *Scientific Reports, 6*. doi:ARTN 38814

[16] McLaughlin, C. R., Fagerholm, P., Muzakare, L., Lagali, N., Forrester, J. V., Kuffova, L., . . . Griffith, M. (2008). Regeneration of corneal cells and nerves in an implanted collagen corneal substitute. *Cornea, 27*(5), 580-589. doi:DOI 10.1097/ICO.0b013e3181658408

[17] Li, Y. P., Asadi, A., Monroe, M. R., & Douglas, E. P. (2009). pH effects on collagen fibrillogenesis in vitro: Electrostatic interactions and phosphate binding. *Materials Science & Engineering C-Biomimetic and Supramolecular Systems, 29*(5), 1643-1649. doi:10.1016/j.msec.2009.01.001

[18] Hartrianti, P., Nguyen, L. T. H., Johanes, J., Chou, S. M., Zhu, P. C., Tan, N. S., . . . Ng, K. W. (2017). Fabrication and characterization of a novel crosslinked human keratin-alginate sponge. *Journal of Tissue Engineering and Regenerative Medicine, 11*(9), 2590-2602. doi:10.1002/term.2159

[19] Aluigi, A., Vineis, C., Varesano, A., Mazzuchetti, G., Ferrero, F., & Tonin, C. (2008). Structure and properties of keratin/PEO blend nanofibres. *European Polymer Journal, 44*(8), 2465-2475. doi:10.1016/j.eurpolymj.2008.06.004

[20] Tanase, C. E., & Spiridon, I. (2014). PLA/chitosan/keratin composites for biomedical applications. *Materials Science & Engineering C-Materials for Biological Applications, 40*, 242-247. doi:10.1016/j.msec.2014.03.054

[21] Edwards, A., Jarvis, D., Hopkins, T., Pixley, S., & Bhattarai, N. (2015). Poly(epsilon-caprolactone)/keratin-based composite nanofibers for biomedical applications. *Journal of Biomedical Materials Research Part B-Applied Biomaterials, 103*(1), 21-30. doi:10.1002/jbm.b.33172

[22] Kreimendahl, F., Köpf, M., Thiebes, A. L., Campos, D. F., Blaeser, A., Schmitz-Rode, T., . . . Fischer, H. (2017). Three-Dimensional Printing and Angiogenesis: Tailored Agarose-Type I Collagen Blends Comprise Three-Dimensional Printability and Angiogenesis Potential for Tissue-Engineered Substitutes. *Tissue Engineering Part C: Methods,23*(10), 604-615. doi:10.1089/ten.tec.2017.0234

[23] Machado, A. A. S., Martins, V. C. A., & Plepis, A. M. G. (2002). Thermal and rheological behavior of collagen - Chitosan blends. *Journal of Thermal Analysis and Calorimetry, 67*(2), 491-498.

[24] Huang, L., Nagapudi, K., Apkarian, R. P., & Chaikof, E. L. (2001). Engineered collagen-PEO nanofibers and fabrics. *Journal of Biomaterials Science-Polymer Edition, 12*(9), 979-993. doi:Doi 10.1163/156856201753252516

[25] Jose, M. V., Thomas, V., Dean, D. R., & Nyairo, E. (2009). Fabrication and characterization of aligned nanofibrous PLGA/Collagen blends as bone tissue scaffolds. *Polymer, 50*(15), 3778-3785. doi:10.1016/j.polymer.2009.05.035

[26] Chakrapani, V. Y., Gnanamani, A., Giridev, V. R., Madhusoothanan, M., & Sekaran, G. (2012). Electrospinning of type I collagen and PCL nanofibers using acetic acid. *Journal of Applied Polymer Science, 125*(4), 3221-3227. doi:10.1002/app.36504

[27] Yu, J. L., Yu, D. W., Checkla, D. M., Freedberg, I. M., & Bertolino, A. P. (1993). Human Hair Keratins. *Journal of Investigative Dermatology, 101*(1), S56-S59. doi:DOI 10.1111/1523-1747.ep12362635

[28] Parenteau-Bareil, R., Gauvin, R., & Berthod, F. (2010). Collagen-Based Biomaterials for Tissue Engineering Applications. *Materials, 3*(3), 1863-1887. doi:10.3390/ma3031863

[29] Zoccola, M., Aluigi, A., Patrucco, A., Vineis, C., Forlini, F., Locatelli, P., . . . Tonin, C. (2012). Microwave-assisted chemical-free hydrolysis of wool keratin. *Textile Research Journal, 82*(19), 2006-2018. doi:10.1177/0040517512452948

[30] Tsuda, Y., & Nomura, Y. (2014). Properties of alkaline-hydrolyzed waterfowl feather keratin. *Anim Sci J, 85*(2), 180-185. doi:10.1111/asj.12093

[31] Katoh, K., Tanabe, T., & Yamauchi, K. (2004). Novel approach to fabricate keratin sponge scaffolds with controlled pore size and porosity. *Biomaterials, 25*(18), 4255-4262. doi:10.1016/j.biomaterials.2003.11.018

[32] Xie, H. B., Li, S. H., & Zhang, S. B. (2005). Ionic liquids as novel solvents for the dissolution and blending of wool keratin fibers. *Green Chemistry, 7*(8), 606-608. doi:10.1039/b502547h

[33] de Guzman, R. C., Merrill, M. R., Richter, J. R., Hamzi, R. I., Greengauz-Roberts, O. K., & Van Dyke, M. E. (2011). Mechanical and biological properties of keratose biomaterials. *Biomaterials, 32*(32), 8205-8217. doi:10.1016/j.biomaterials.2011.07.054

[34] Hill, P., Brantley, H., & Van Dyke, M. (2010). Some properties of keratin biomaterials: Kerateines. *Biomaterials, 31*(4), 585-593. doi:10.1016/j.biomaterials.2009.09.076

[35] Wang, L. Z., Yang, B., Du, X. Q., Yang, Y. F., & Liu, J. L. (2008). Optimization of conditions for extraction of acid-soluble collagen from grass carp (Ctenopharyngodon idella) by response surface methodology. *Innovative Food Science & Emerging Technologies, 9*(4), 604-607. doi:10.1016/j.ifset.2008.03.001

[36] Santos, M. H., Silva, R. M., Dumont, V. C., Neves, J. S., Mansur, H. S., & Heneine, L. G. D. (2013). Extraction and characterization of highly purified collagen from bovine pericardium for potential bioengineering applications. *Materials Science & Engineering C-Materials for Biological Applications, 33*(2), 790-800. doi:10.1016/j.msec.2012.11.003

[37] Nagai, T., Tanoue, Y., Kai, N., & Suzuki, N. (2015). Characterization of collagen from emu (Dromaius novaehollandiae) skins. *Journal of Food Science and Technology-Mysore, 52*(4), 2344-2351. doi:10.1007/s13197-014-1266-1

[38] Liu, D., Wei, G., Li, T., Hu, J., Lu, N., Regenstein, J. M., & Zhou, P. (2015). Effects of alkaline pretreatments and acid extraction conditions on the acid-soluble collagen from grass carp (Ctenopharyngodon idella) skin. *Food Chem, 172*, 836-843. doi:10.1016/j.foodchem.2014.09.147

[39] Schmidt, M. M., Dornelles, R. C. P., Mello, R. O., Kubota, E. H., Mazutti, M. A., Kempka, A. P., & Demiate, I. M. (2016). Collagen extraction process. *International Food Research Journal, 23*(3), 913-922.

[40] Extracellular Matrix: A Practical Approach, Haralson, M., and Hassell, J., eds., IRL Press at Oxford University Press (Oxford, England: 1995), p. 31.

[41] de Guzman, R. C., Tsuda, S. M., Ton, M. T., Zhang, X., Esker, A. R., & Van Dyke, M. E. (2015). Binding Interactions of Keratin-Based Hair Fiber Extract to Gold, Keratin, and BMP-2. *PLoS One, 10*(8), e0137233. doi:10.1371/journal.pone.0137233

[42] Fearing, B. V., & Van Dyke, M. E. (2014). In vitro response of macrophage polarization to a keratin biomaterial. *Acta Biomater, 10*(7), 3136-3144. doi:10.1016/j.actbio.2014.04.003

[43] Waters, M., VandeVord, P., & Van Dyke, M. (2018). Keratin biomaterials augment anti-inflammatory macrophage phenotype in vitro. *Acta Biomater, 66*, 213-223. doi:10.1016/j.actbio.2017.10.042

[44] Richter, J. R., de Guzman, R. C., & Van Dyke, M. E. (2011). Mechanisms of hepatocyte attachment to keratin biomaterials. *Biomaterials, 32*(30), 7555-7561. doi:10.1016/j.biomaterials.2011.06.061

[45] Poranki, D., Whitener, W., Howse, S., Mesen, T., Howse, E., Burnell, J., . . . Van Dyke, M. (2014). Evaluation of skin regeneration after burns in vivo and rescue of cells after thermal stress in vitro following treatment with a keratin biomaterial. *J Biomater Appl, 29*(1), 26-35. doi:10.1177/0885328213513310

[46] Yoo, J. S., Kim, Y. J., Kim, S. H., & Choi, S. H. (2011). Study on genipin: a new alternative natural crosslinking agent for fixing heterograft tissue. *Korean J Thorac Cardiovasc Surg, 44*(3), 197-207. doi:10.5090/kjtcs.2011.44.3.197

[47] Shoulders, M. D., & Raines, R. T. (2009). Collagen structure and stability. *Annu Rev Biochem, 78*, 929-958. doi:10.1146/annurev.biochem.77.032207.120833

[48] Chandran, P. L., & Barocas, V. H. (2004). Microstructural mechanics of collagen gels in confined compression: Poroelasticity, viscoelasticity, and collapse. *Journal of Biomechanical Engineering-Transactions of the Asme, 126*(2), 152-166. doi:10.1115/1.1688774

[49] Gobeaux, F., Mosser, G., Anglo, A., Panine, P., Davidson, P., Giraud-Guille, M. M., & Belamie, E. (2008). Fibrillogenesis in dense collagen solutions: A physicochemical study. *Journal of Molecular Biology, 376*(5), 1509-1522. doi:10.1016/j.jmb.2007.12.047

[50] Cross, V. L., Zheng, Y., Choi, N. W., Verbridge, S. S., Sutermaster, B. A., Bonassar, L. J., . . . Stroock, A. D. (2010). Dense type I collagen matrices that support cellular remodeling and microfabrication for studies of tumor angiogenesis and vasculogenesis in vitro. *Biomaterials, 31*(33), 8596-8607. doi:10.1016/j.biomaterials.2010.07.072

[51] Chrobak, K. M., Potter, D. R., & Tien, J. (2006). Formation of perfused, functional microvascular tubes in vitro. *Microvasc Res, 71*(3), 185-196. doi:10.1016/j.mvr.2006.02.005

[52] Gelman, R. A., Poppke, D. C., & Piez, K. A. (1979). Collagen fibril formation in vitro. The role of the nonhelical terminal regions. *J Biol Chem, 254*(22), 11741-11745.

[53] Achilli, M., & Mantovani, D. (2010). Tailoring Mechanical Properties of Collagen-Based Scaffolds for Vascular Tissue Engineering: The Effects of pH, Temperature and Ionic Strength on Gelation. *Polymers, 2*(4), 664-680. doi:10.3390/polym2040664

[54] Raub, C. B., Suresh, V., Krasieva, T., Lyubovitsky, J., Mih, J. D., Putnam, A. J., . . . George, S. C. (2007). Noninvasive assessment of collagen gel microstructure and mechanics using multiphoton Microscopy. *Biophysical Journal, 92*(6), 2212-2222. doi:10.1529/biophysj.106.097998

[55] Antoine, E. E., Vlachos, P. P., & Rylander, M. N. (2014). Review of collagen I hydrogels for bioengineered tissue microenvironments: characterization of mechanics, structure, and transport. *Tissue Eng Part B Rev, 20*(6), 683-696. doi:10.1089/ten.TEB.2014.0086

[56] Cai, C. G., Chen, J. S., Qi, J. J., Yin, Y., & Zheng, X. D. (2008). Purification and characterization of keratinase from a new Bacillus subtilis strain. *J Zhejiang Univ Sci B, 9*(9), 713-720. doi:10.1631/jzus.B0820128

[57] Esparza, Y., Bandara, N., Ullah, A., & Wu, J. P. (2018). Hydrogels from feather keratin show higher viscoelastic properties and cell proliferation than those from hair and wool keratins. *Materials Science & Engineering C-Materials for Biological Applications, 90*, 446-453. doi:10.1016/j.msec.2018.04.067

[58] Sando, L., Kim, M., Colgrave, M. L., Ramshaw, J. A., Werkmeister, J. A., & Elvin, C. M. (2010). Photochemical crosslinking of soluble wool keratins produces a mechanically stable biomaterial that supports cell adhesion and proliferation. *J Biomed Mater Res A, 95*(3), 901-911. doi:10.1002/jbm.a.32913

[59] Sitterley, G. (2008). Collagen Attachment Protocols, Solubility, and Stability. Retrieved from https://www.sigmaaldrich.com/technical-documents/articles/biofiles/collagen-product-protocols.html

Supplemental Figures

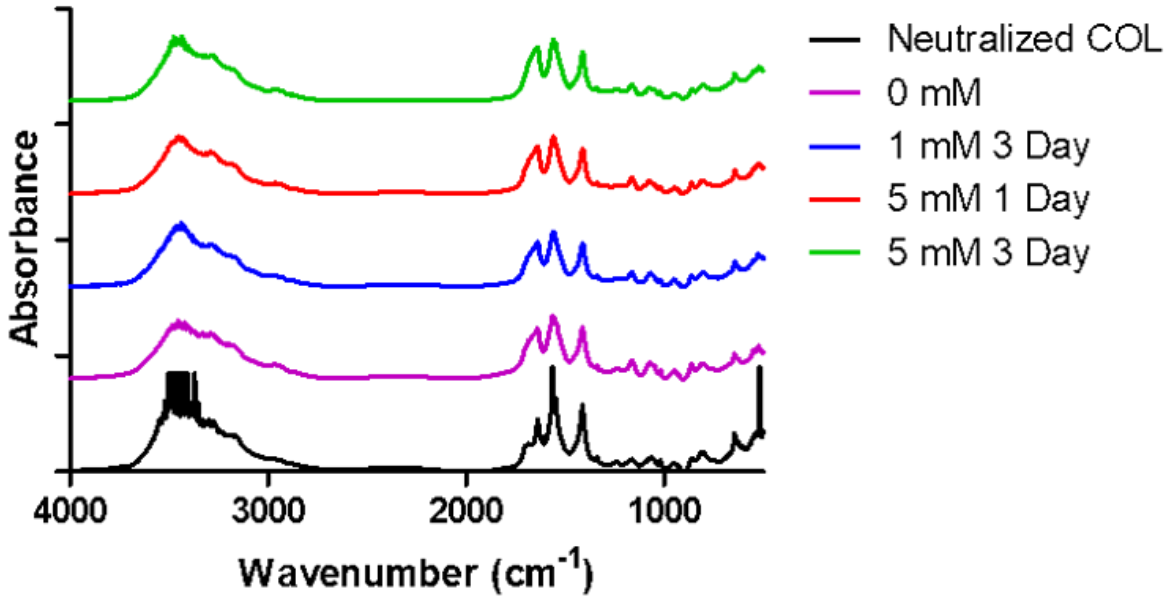

Supplemental Figure S3.1: FTIR spectra for KOS/COL material at different crosslinking concentrations. Data was taken from 4000-400 cm^{-1}.

Chapter 4

Schwann Cell Behavior and Interaction with a Keratose/Type I Collagen Material

Nils A. Potter and Mark Van Dyke

Virginia Polytechnic Institute and State University, Department of Biomedical Engineering and Mechanics, School of Biomedical Engineering and Sciences, Blacksburg, VA 24061

Abstract

Numerous approaches have been taken to aid in peripheral nerve regeneration. One common approach that has been investigated is using a conduit system that bridges the proximal and distal injury sites together following injury. Within this system, conduit luminal fillers have been applied to facilitate the guidance of regenerating axons and Schwann cells and to counteract the possibility of neuroma formation. Keratin hydrogels have been previously used as luminal fillers in *in vivo* models and have demonstrated successes. These hydrogels, however, could only be formulated using 15-20 wt% of total protein content, which may not provide optimal initial porosity for infiltrating cells, or could alter later stages of tissue remodeling. Blends of keratin and collagen formed into hydrogels have shown promising mechanical characteristics such that they can be used as a luminal filler with total protein content of 0.5 wt%. Here, we examine the effect of a keratin/type I collagen blend material on the behavior of Schwann cells though viability assays, focal adhesion studies, and chemoattractant cellular migration assays. Results showed that keratin/collagen blends allow for acceptable Scwhann cell viability and in some cases, surpassed the collagen hydrogel control group. Blended samples were also shown to allow for Schwann cell adhesion through immunofluorescence in comparable amounts to collagen and tissue culture plastic control groups without any inhibition. Finally, blended samples also allowed for Schwann cell migration with steadily increased migration as the keratin concentration increased. Data collected from this was shown to allow for less migration than collagen controls, but the total protein content of the blended samples was 150% more than collagen controls suggesting that total protein content plays an important role in the migratory capabilities of Schwann cells.

Keywords: keratin, type I collagen, schwann cell, adhesion, migration

4.1. Introduction

Unlike the central nervous system (CNS), the peripheral nervous system (PNS) has the inherent ability to undergo self-regeneration [1,2]. Following injury such as a crush or laceration, a void area is created between the proximal and distal injury sites. At the distal end, a process known as Wallerian degeneration occurs where the axons and myelin degenerate, and Schwann cells (SCs), in conjunction with macrophages, migrate to the primary injury site to phagocytize any residual cellular debris left over from the injury along with remyelinating the migrating axons [3-6]. Following Wallerian degeneration, SCs act to form longitudinal bands known as bands of Büngner, and these act to guide axons in addition to creating a region saturated with trophic factors [7].

For treatment of peripheral nerve injury, the first option is direct surgical repair by performing a tensionless neurorrhaphy, a suturing of a divided nerve, but the conditions needed for this to be feasible are uncommon [8,9]. In the instance where tensionless surgery cannot be performed, the suggested gold standard is to use autografts. While these are optimal to use due to their lack of an immunogenic response and instant delivery of viable cells, the lack of available tissue and potential loss of function from the donor site act as deterrents [10]. Nerve allografts can be another treatment method, but these elicit an immune response and instant delivery of viable cells from the body, which requires the patient to undergo immunosuppression regimens that can result in adverse side effects [11]. When autografts and allografts are not seen as viable solutions and the void area is $\leq$ 3 cm, the suggested treatment option is the use of nerve conduits [12-14].

Numerous materials have been used in the fabrication of nerve conduits including synthetic polymers such as polycaprolactone (PCL) and polylactic acid (PLA) in addition to

natural biomaterials such as type I collagen (COL) [15-18]. Along with using different materials to create the nerve conduit itself, many different methods for trying to promote SC and axon migration and improve growth factor and cytokine diffusion have been explored. These methods include surface functionalization of the conduit, performing different fabrication techniques, and intraluminal guidance by filling the lumen of the conduit with a hydrogel material [19-22]. The luminal filler method has been explored as the treatment that exhibits the most potential for peripheral nerve regeneration, and numerous biomaterials have been implemented as luminal fillers including fibrin, COL, laminin, and keratose (KOS) [23-32].

Numerous factors play pivotal roles when choosing the optimal material to serve as a luminal filler including mechanical strength, material architecture to support adequate cellular migration, ability to allow for cell survival, and degradation kinetics. A material with preferred mechanical strength characteristics can withstand the inherent regeneration environment in addition to the extra strain applied to the area due to common movements such as wrist and elbow flexion and extension [35,36]. Material architecture is paramount in this environment because SCs and axons need some sort of medium to migrate through without 1) the possibility to form a neuroma due to too much free space or 2) the possibility to not migrate at all due to the architecture being too dense. Many studies have observed SC migration, but a majority of these studies have either been conducted *in vivo* where the environment can be more favorable than an *in vitro* environment due to an abundance of trophic factors or *in vitro* but with the goal to measure the effect of different chemoattractants rather than the effect of a material barrier [37-44]. Observing the effect that a material barrier has on the invasion and migration of SCs is paramount to understanding the efficacy of a material to function as a conduit luminal filler in a peripheral nerve regeneration setting, if the material in question does not support adequate

migration in addition to cell survival, then it cannot be deemed as an appropriate candidate for this purpose.

As mentioned previously, KOS has been used as a luminal filler for peripheral nerve regeneration, but the composition of the material has been very concentrated in these studies at 15-20 wt%, which results in a dense network that is not optimal for cellular migration [23,24,32]. We hypothesized that coupling KOS with COL to form a blended material would allow for a material matrix that requires less total protein, and thus would promote cell survival along with adequate migration. In this work, we observe the effect a novel KOS/COL material has with SCs through viability, focal adhesion, and invasion and migration assays.

4.2. Methods

4.2.1. Keratose Extraction

KOS was extracted as mentioned previously [33]. In brief, dry human hair fibers were received from a commercial source and oxidized using a 2% (w/v) solution of peracetic acid (PAA) in ultrapure water. Oxidation was carried out at 37°C with continuous stirring for 12 h at a 1:20 ratio of hair fiber weight to liquid volume. The oxidized fibers were recovered after stirring by passing them through a 500 μm sieve and were rinsed with deionized water until no PAA was detectable with a test strip. Hair fibers were then extracted twice at a 1:40 ratio of dry hair fiber weight to 100 mM tris base at 37°C for 2 h with continuous stirring. Following each extraction, the fibers were recovered via sieve and the liquid was retained. The liquid extracts were then combined, centrifuged, and filtered to allow for solids removal. KOS was further purified through use of a custom tangential flow filtration (TFF) system. The sample was first dialyzed against a phosphate buffer solution (10 mM Na_2HPO_4/100 mM NaCl, pH 7.4) then

ultrapure water. Following dialysis, the sample was concentrated, frozen, lyophilized, and ground into a powder for application.

4.2.2. Collagen Extraction

COL was extracted as mentioned previously [34]. In brief, Sprague-Dawley rat tails were purchased from BioIVT (Westbury, NY) and cleaned thoroughly with 70% ethanol. Using a #22 blade attached to a #4 scalpel, the rat tail skin was removed to expose the rat tail tendon. Following this, 2 pairs of surgical clamps were used to separate the knuckle regions on the tail to remove the collagen strands. These strands were then placed in 70% ethanol, removed, air dried, and weighed. Collagen strands were then placed in a solution of 0.1% acetic acid at a concentration of 200 ml/g of collagen for 72 h at 4 °C with occasional stirring. After dissolving in 0.1% acetic acid, the solution was centrifuged at 33,000 g for 45 min at 4 °C to separate the insoluble fraction from the soluble fraction. The soluble fraction was extracted, frozen at -80 °C, and lyophilized with the aid of an acid trap attachment (Labconco).

4.2.3. Cell Culture

The RT4-D6P2T rat Schwann cell line was used for all experiments (American Type Culture Collection). SCs were cultured in GIBCO® Dulbecco's Modified Eagle Media (DMEM) supplemented with 10% fetal bovine serum (FBS) and 1% Penicillin/Streptomycin. All cell cultures were incubated in a humidified incubator of 95% air and 5% CO_2 at 37°C. For all experiments, cell passages below 10 were used.

4.2.4. Keratin/Collagen Hydrogels

KOS was dissolved in 1X phosphate buffered saline (PBS) at a concentration of 28 mg/ml, and COL was dissolved in 0.1 M acetic acid at a concentration of 3 mg/ml. Prior to solution mixing and hydrogel formation, the stock KOS and COL solutions were sterilized by

placing 10% of the total solution volume of chloroform on the bottom of a Pyrex glass bottle. The stock KOS or COL was then carefully layered atop the chloroform and placed at 4°C for 24 h to allow the chloroform vapor to sterilize the solution. After 24 h, the sterilized protein solutions were removed and used for hydrogel fabrication. 10X PBS was added to balance salt content, 1 M NaOH was added to balance the solution pH to 7.4, and ultrapure water was added to correct for the proper calculated volume. COL was added to this solution, and then a 20 mM stock solution of genipin (Wako Chemicals) in 1X PBS was added to provide a crosslinking agent between the two proteins. KOS was added last, and all the components were mechanically mixed using a plastic spatula while making sure that the KOS did not precipitate in solution due to its propensity to do so when exposed to acidic solutions. All hydrogel samples were prepared at 0.5 wt% total protein to allow for proper mixing of all components. The final salt concentration was that of 1X PBS. Following mixing, pH of 7.4 was confirmed through pH test strips, and the solution was incubated at 37 °C for 72 h to allow for COL self-assembly and full genipin crosslinking. To prevent hydrogel drying during the incubation step, 1X PBS was placed atop the hydrogels after 6 h of curing. COL hydrogels were fabricated in a similar fashion by mixing 10X PBS, 1 M NaOH, ultrapure water, and a 3 mg/ml COL solution together where a neutral pH was achieved. The final pH was determined by pH test strips, and the final concentration of COL in the hydrogel was 2.4 mg/ml. Curing of the COL hydrogel was induced by placing the COL solution at 37 °C for 45 min.

4.2.5. Cell Viability

Cell viability was assessed using an alamarBlue assay. COL hydrogels and KOS coatings were used as comparison groups. KOS/COL hydrogels and COL hydrogels were prepared as mentioned previously. For KOS coatings, 200 μg/ml of KOS in 1X PBS was incubated for 2 h at

37 °C in a 24 well plate formant. Following incubation, the solution was aspirated. Wells were washed 3 times with 1X PBS after their respective incubation times. Rat SCs were seeded atop the treatment groups at a density of 30,000 cells/well. Time points of 24, 48, and 72 h were used to determine cell viability. At each respective time point, medium was removed and replaced with fresh medium containing alamarBlue reagent. This was incubated for an additional 24 h at 37 °C. To mitigate any potential fluorescence interference from the underlying substrate, 100 µl of media was taken from the 24 well plate and transferred to a 96 well plate following alamarBlue treatment. The 96 well plate was read for fluorescence using a Synergy H1 microplate reader (BioTek®) at 560/590 nm. Tissue culture plastic (TCP) was used as a positive control group.

4.2.6. Focal Adhesion Immunochemistry

Rat SCs were stained for the focal adhesion proteins vinculin and F-actin. SCs were seeded in 24 well plates at a density of 50,000 cells/well in serum free media atop COL and KOS/COL hydrogels and a TCP control. Hydrogels were prepared as mentioned previously to allow for a gel height of ~ 1 mm and washed 3x with PBS following completion of curing. After 24 h of incubation, cells were fixed with 4% paraformaldehyde (PFA) for 20 min, washed 2x with PBS, permeabilized with 0.1% Triton X-100, and then stained for the respective focal adhesion proteins. For vinculin, cells were first blocked in 1% bovine serum albumin (BSA) for 30 min. Next, they were labeled with a primary antibody for vinculin (1:250) in 1% BSA for 60 min, washed with 0.05% Tween-20, and labeled with FITC-conjugated goat anti-mouse immunoglobulin G (IgG) secondary antibody (1:100) for 60 min. For actin, cells were stained with Alexa Fluor 488 phalloidin (1:40) and washed 2x with PBS. For both staining procedures, cells were stained with 4′,6-diamidino-2-phenylindole (DAPI, 1:100) for 5 min, washed 3x with

PBS, and covered with PBS prior to imaging. Fluorescent images were taken using a Zeiss LSM 800 confocal microscope. Each focal adhesion protein was stained in its own well plate due to the inherent red autofluorescence of genipin. Immunofluorescence was quantified by measuring the area of immunofluorescence per cell through the use of ImageJ software.

4.2.7. Schwann Cell Invasion

Rat SCs were seeded in a 12 transwell well plate format. The transwell membranes were made from polyethylene terephthalate with a pore size of 8 μm. 1 mg/ml COL hydrogels and 0.25 wt% KOS/COL hydrogels were prepared as mentioned previously. Untreated transwell membranes were used as a control group. Cells were seeded at a density of 100,000 cells/transwell insert in serum free DMEM. The bottom well was filled with DMEM with 10% FBS and 10 ng/ml NGF, and the insert was placed into this well to create a chemoattractant gradient. Cells without any hydrogel barrier were incubated for 24 h and cells with a hydrogel barrier were incubated for 2 wk to allow for invasion through the hydrogels and attachment on the opposite side of the membrane. Throughout the entirety of the culture time, cells were washed with 1X PBS, and both serum free media and chemoattractant media were replaced every 72 h. Following culturing, media was removed, inserts were washed 2x in PBS, and cells were fixed with 4% PFA for 20 min. Inserts were washed 2x in PBS and permeabilized in 100% methanol for 20 min. Inserts were washed 2x in PBS and stained with 0.2% crystal violet for 20 min. The crystal violet was washed off along with any excess, and the gel along with any noninvasive cells were removed by wiping the top of the transwell membrane with a cotton swab. The inserts were left to air dry and were imaged under brightfield conditions using an inverted microscope. Cell counts were quantified through the use of ImageJ.

4.2.8. Schwann Cell Migration

Rat SCs were seeded in a 6 well plate format but adjusted to fit the custom nature of the assay. KOS/COL hydrogels were prepared as mentioned previously. Following complete hydrogel curing, a 6 mm biopsy punch was used to create 2 different circular cutouts in the gel. These cutouts were aspirated out of the initial gel, and the gel was washed with 1X PBS to remove any underlying gel debris. Following the gel defect formation, gels were conditioned with serum free DMEM overnight. Chemoattractant media was placed into one of the gel cutouts and allowed to diffuse through the gel overnight. Rat SCs were then seeded at a density of 20,000 cells/cutout in serum free media and were left to attach for 1 h. Plates were washed multiple times with 1X PBS to remove any unattached cells, and serum free media was placed in the entire well of the 6 well plate. Cultures were carried out for 72 h. At the end of the culture period, cells were fixed with 4% PFA for 20 min, washed with 1X PBS, permeabilized with 0.1% triton, washed with 1X PBS, and stained with DAPI (1:100) to assess migration through the gel. Distances between the gel cutouts were between 2-3 mm in length. A detailed representation of this assay is illustrated by **Figure 4.1**.

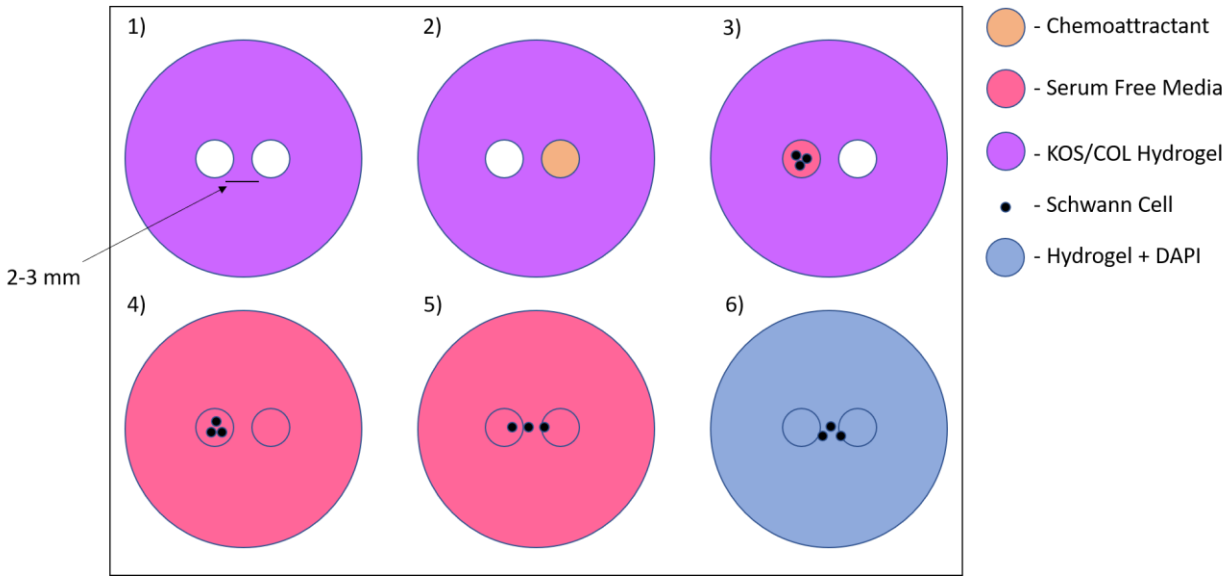

Figure 4.1: Illustration of one well of the custom migration assay in sequential steps. 1) Two cutouts are made from the biopsy punch leaving a 2-3 mm hydrogel gap, and the gel is conditioned in serum free media overnight. 2) The right cutout is filled with chemoattractant media and incubated at 37 °C overnight to allow for diffusion into the gel. 3) SCs are seeded at 20,000 cells/cutout. 4) After 1 h for cell adherence and washing steps, the entirety of the well is filled with serum free media. 5) The cells are cultured for 1 week with media changes every 2-3 days. 6) Cells are fixed, permeabilized, and stained with DAPI for imaging.

4.2.9. Statistical Analysis

All quantitative results are reported as means ± standard deviation unless otherwise stated. Statistical analyses were carried out in JMP 13.0.0 using one-way analysis of variance (ANOVA) and Tukey's post hoc tests to determine significance. Statistical significance was defined as $p < 0.05$.

4.3. Results

4.3.1. Cell Viability

Cell viability measurements using an alamarBlue assay revealed similar results across all groups, with cells on 80/20 hydrogels being slightly more proliferative. At 24 h, no statistically significant difference in relative fluorescence was observed between 80/20 and COL groups, but statistically significant difference was observed at both 48 and 72 h time points (80/20 relative

fluorescence values of 0.994 ± 0.02, 1.05 ± 0.02, and 1.04 ± 0.01 for 24, 48, and 72 h, respectively).

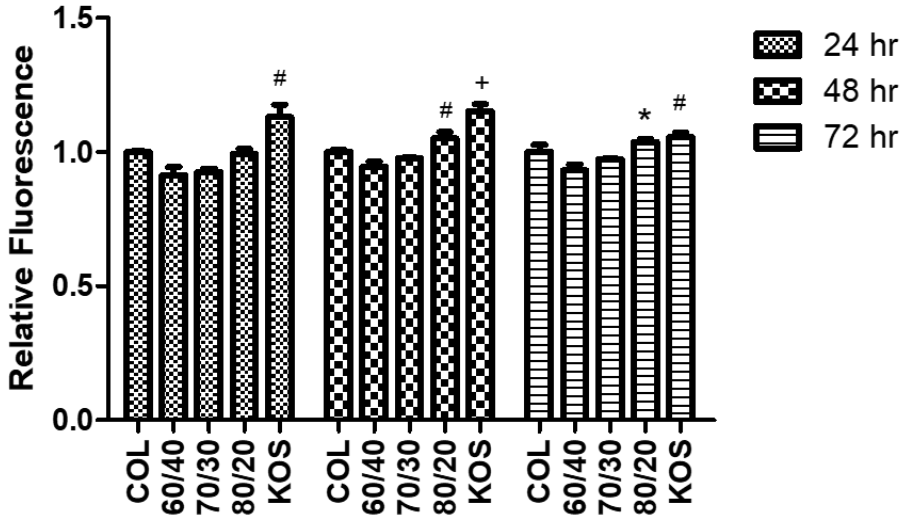

Figure 4.2: Viability profiles of SCs seeded a1 top COL hydrogels, KOS/COL hydrogels, and KOS coatings (n = 3, mean ± SD). * signifies $p < 0.05$, # signifies $p < 0.01$, and + signifies $p < 0.001$ compared to the COL controls.

4.3.2. Focal Adhesion Immunochemistry

Focal adhesion staining revealed that SCs are able to attach to KOS/COL hydrogels through integrin receptors. Each hydrogel formulation along with a COL hydrogel and TCP control was observed for cell adhesion through both F-actin (**Figure 4.3**) and vinculin (**Figure 4.4**) immunofluorescence, which is quantified in **Figure 4.5**. No statistically significant difference was observed among any of the groups from the quantified results, which suggests that KOS/COL hydrogels allow for a similar amount of cellular adhesion as the TCP and COL controls.

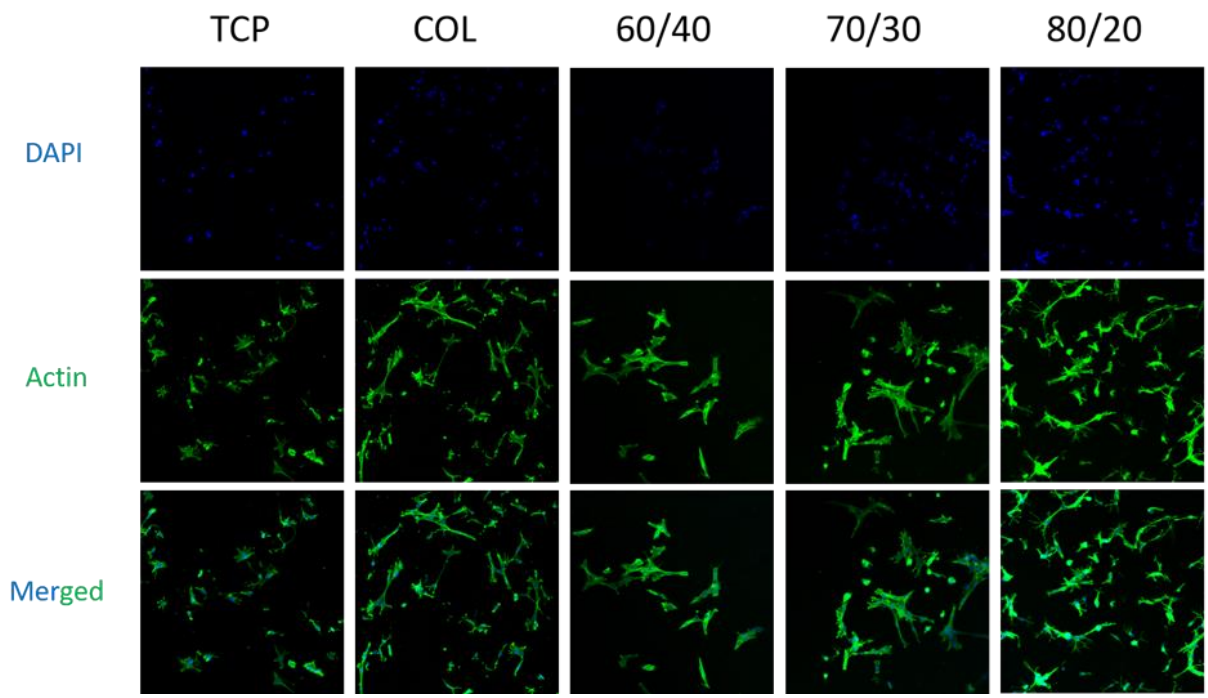

Figure 4.3: Immunofluorescence images of F-actin (green) and DAPI (blue) from SCs seeded atop TCP, COL hydrogels, and KOS/COL hydrogels

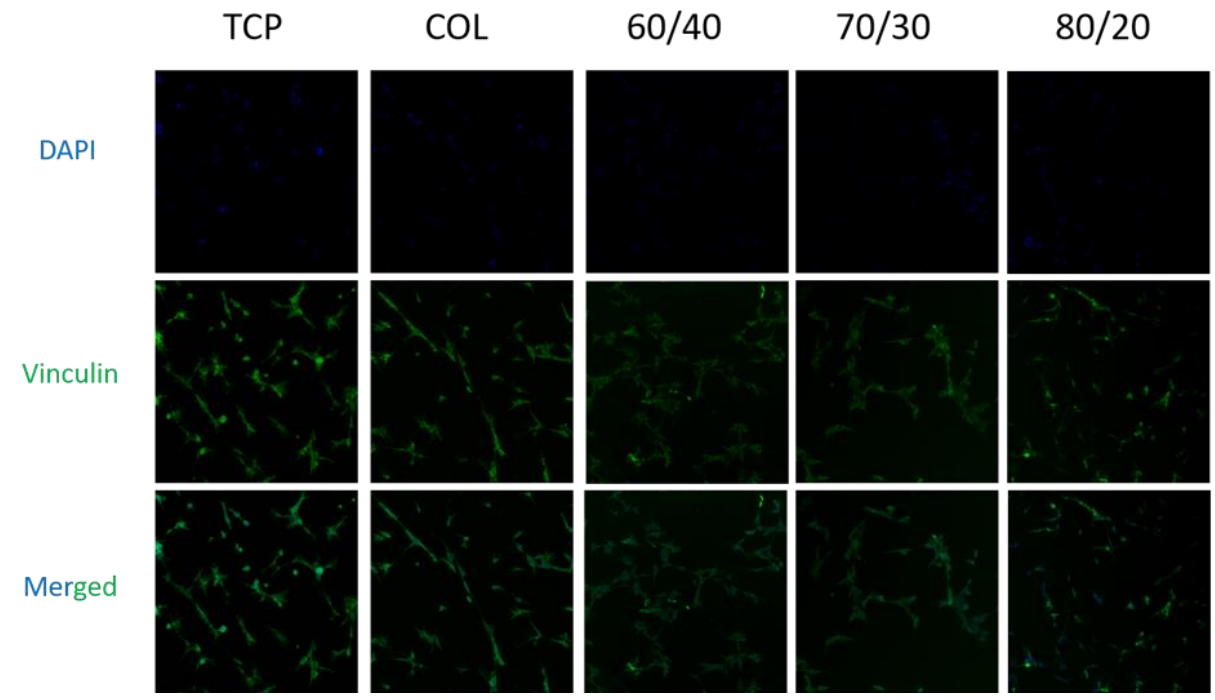

Figure 4.4: Immunofluorescence images of vinculin (green) and DAPI (blue) from SCs seeded atop TCP, COL hydrogels, and KOS/COL hydrogels

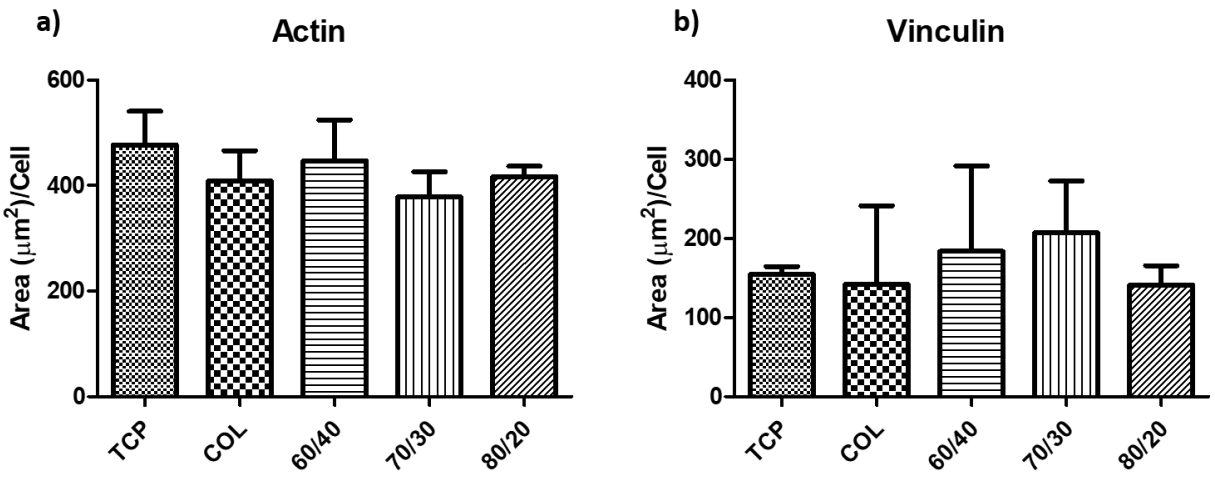

Figure 4.5: Immunofluorescence intensity of F-actin **(a)** and vinculin **(b)** from SCs seeded atop TCP, COL hydrogels, and KOS/COL hydrogels (n = 3 for TCP and all KOS/COL groups, n = 2 for COL in Actin; n = 3 for all groups in Vinculin. Mean ± SD).

4.3.3. Schwann Cell Invasion

Transwell invasion assays revealed that hydrogel barriers have a significant effect on the ability of SCs to migrate. Without a barrier, SCs were able to easily traverse through the porous PET membrane, and this migration was maximized when the chemoattractant of 10% FBS and 10 ng/ml NGF was introduced to the culture system. In addition, as samples increased in KOS content and decreased in COL content, the migratory capability of SCs increased. As seen from **Figure 4.6a** and **Figure 4.6b**, minimal to no SC migration was observed with 60/40 hydrogels, and 80/20 hydrogels allowed for the greatest amount of migration compared to the 60/40 and 70/30 groups ($p < 0.05$). 1 mg/ml COL hydrogels with chemoattractant were shown to exhibit the greatest amount of migration and were statistically significant to all other KOS/COL hydrogel groups.

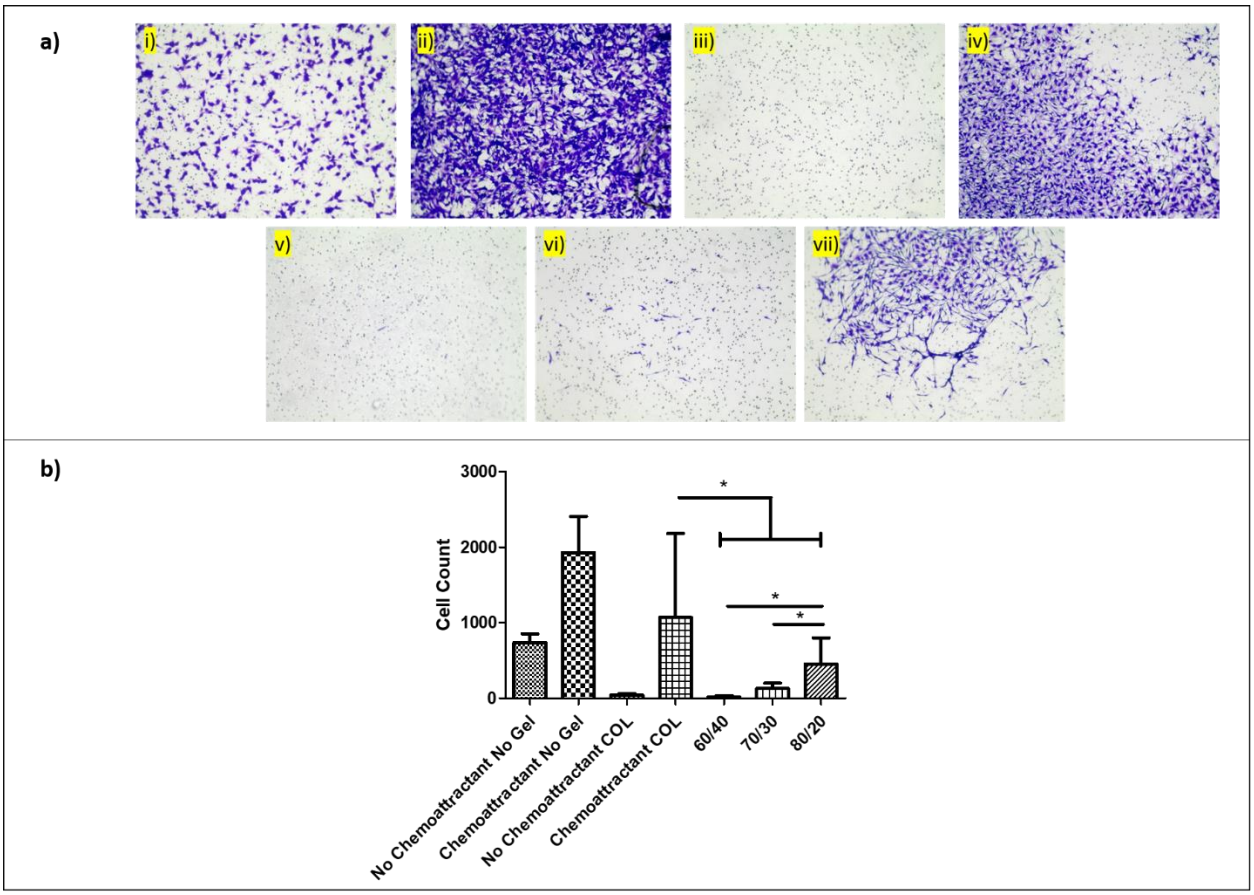

Figure 4.6: Transwell invasion assay images of rat SCs through no gel, COL hydrogel, and KOS/COL hydrogel groups. **a)** cells that traveled through the membrane are shown in violet; **i)** No chemoattractant no gel **ii)** Chemoattractant no gel **iii)** No chemoattractant COL **iv)** Chemoattractant COL **v)** 60/40 **vi)** 70/30 **vii)** 80/20. **b)** cell counts from each group (n = 3 for 60/40, and 70/30. n = 2 for every other group. Mean ± SD. * indicates $p < 0.05$).

4.3.4. Schwann Cell Migration

Figure 4.1 illustrates a detailed depiction of the custom migration assay in a stepwise manner. In this assay, the objective is to obtain an understanding of the migration rate of SCs through the KOS/COL hydrogel by allowing chemoattractant to diffuse into a gel barrier that separates the chemoattractant reservoir well and the cell well. Following diffusion, the SCs are in contact with a chemoattractant gradient in which they can migrate.

Figure 4.7 illustrates a 70/30 KOS/COL hydrogel that SCs migrated through over the course of 72 h. In the first image, the outlines of both wells that were created from the biopsy punch can be easily visualized due to the lack of genipin autofluorescence. In this set of images,

it can be seen that SCs are migrating through the gel barrier and following the chemoattractant gradient with cells reaching a distance between 721-906 μm.

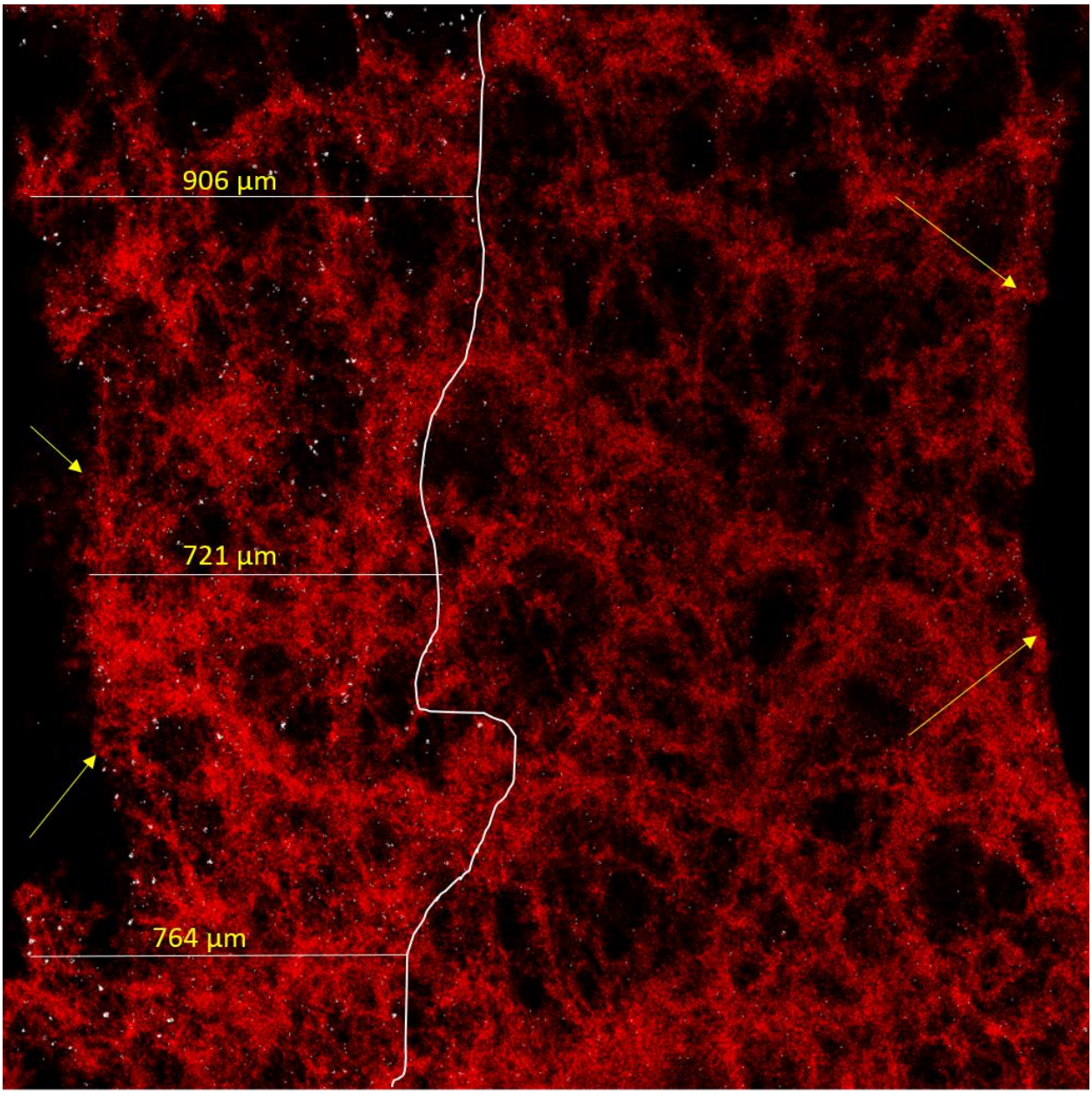

Figure 4.7: Image of SC migration through a 70/30 gel barrier between hydrogel cutouts stained with DAPI (converted to white for better visualization). The red is indicative of genipin autofluorescence. Yellow arrows indicate the edges of the two wells were made using the biopsy punch with the left being the well where cells were seeded and the right being the well where chemoattractant was placed. The white line indicates the boundaries were SCs migrated.

4.4. Discussion

In trying to determine the feasibility of a biomaterial to serve as a conduit luminal filler for peripheral nerve regeneration, there are not many studies that attempt to obtain results in an *in vitro* manner before transitioning into an animal study. This study aims to provide an *in vitro* perspective on the ability for a KOS/COL blended biomaterial to support SC growth and migration through this material matrix. As mentioned previously, the concentrations of KOS used in prior peripheral nerve regeneration studies were high with total protein content at concentrations between 15-20 wt% [23,24,32]. Luminal fillers that have such high concentrations can be inhibitory to cellular migration as the matrix is too dense for cells to traverse [29,30]. Attempting to use a less concentrated, KOS-based biomaterial for the purpose of aiding in peripheral nerve regeneration aims to build off the prior work done with pure KOS luminal fillers, and also offers an *in vitro* perspective that has been lacking from prior work.

Cell viability assays showed promising results as the 80/20 KOS/COL material allowed for greater levels of viability, which was statistically significant compared to the COL control group. These cells were seeded atop the gel, so the ability to promote cell viability in 3D was not assessed, but this is an adequate starting point because when *in vivo*, SCs migrate from the injured nerve stumps and migrate toward the center of the defect. In this environment, they are on the surface of the luminal filler material. In addition, the manufacturing process of the KOS/COL material requires using an amine-reactive crosslinking molecule known as genipin, which can also act as a fixative, so attempting to encapsulate cells within this hydrogel during the curing process would not have been advantageous [45,46].

Focal adhesion staining revealed that SCs were able to adequately bind to KOS/COL hydrogels just as well as they could to TCP and COL substrates from quantification of both actin

and vinculin staining. F-actin is known to play a pivotal role in cell migration as it is F-actin that provides mechanical forces to change cellular shape in addition to generating movement to invade surrounding ECM [47]. F-actin production is an important factor that contributes to the ability of SCs to migrate in a peripheral nerve regeneration environment. Actin inhibition in Sprague-Dawley rats has been explored through the application of an actin polymerization inhibitor known as cytochalasin D. At concentrations of 1000 nM, the length of regenerated nerve fibers, compound muscle action potential (CMAP) amplitude, and the migratory distance of SCs was seen to decrease compared to the dimethyl sulfoxide (DMSO) control group [42]. From the present work, KOS/COL hydrogel material does not appear to inhibit F-actin expression compared to control groups.

Transwell invasion assays revealed that SCs are able to migrate through COL controls along with the KOS/COL blends. Initial studies using this assay revealed that time along with hydrogel concentration are important factors when trying to gauge the migratory capabilities of SCs through hydrogel materials. The generally accepted rate of peripheral nerve regeneration is 1 mm/day, but this does not take into account any sort of luminal filler material that aids in guiding SCs and axons [48]. When casting the hydrogels, it was determined that their height was about 1 mm based on the transwell insert dimensions and the volume of gel added. When conducting initial studies over the course of 1 and 3 days, no discernable migration through any KOS/COL group nor COL control was observed. From these preliminary results, it was decided to observe migration over a longer period of time (2 wk). From the cell count data, the COL group with the chemoattractant was seen to perform better than any of the KOS/COL groups. It is important to note that the KOS/COL control groups had 150% more total protein content than the COL control. The COL group was comprised of a lesser total protein content because of the need to

have a positive control among the hydrogel groups with chemoattractant. Aiming to create KOS/COL hydrogels at lesser concentrations than 0.25 and 0.5 wt% is desirable when trying to control migration rate, and this has been shown in prior studies with COL hydrogels at differing concentrations with bone mesenchymal stem cells (BMSCs) [49,50]. Future work with this primarily includes optimizing assay time along with keeping the total protein content of all hydrogel groups the same.

The custom migration assay revealed that SCs are able to traverse through the KOS/COL matrix but at slower migration rates than anticipated. After 72 h, SCs were observed to travel a maximum of 906 μm into the matrix. This assay, however, has its shortcomings. For example, overflowing of the punched out wells with either chemoattractant or a cell suspension is an issue that was encountered multiple times, which required optimization of optimal media volume, incubation times, and biopsy punch dimensions. Another problem that was encountered was determining how long to allow cells to attach in their respective well before liquid that resided in the hydrogel diluted the added media. For future studies aiming to gauge migration rate through these gels, an improved experiment would be to keep the transwell invasion assay format but altering the standard invasion assay protocol in a way that would allow for better visualization of SCs in the matrix without the deficiencies. For example, removing the transwell membrane and freezing the hydrogel after a set time point, then slicing the gel in half and observing thin slices across the cross-sectional area would allow for better visualization and circumvent many of the previously mentioned problems. For both this custom migration assay and the transwell invasion assay, no pure KOS hydrogels were used. Pure KOS hydrogels do not have well-documented hydrolytic stability when immersed in media as they undergo near complete dissolution in this

type of setting in as little as 1 wk [33]. Due to this hydrolytic instability, these hydrogels would not have been able to last the duration of these assays.

4.5. Conclusions

This study aimed to assess the capability of a KOS/COL blended material to serve as a conduit luminal filler in for peripheral nerve regeneration. Experiments associated with this objective were all carried out in an *in vitro* manner to provide insight before transitioning into a potential *in vivo* study. We hypothesized that a KOS/COL blended material would allow for adequate SC infiltration and migration along with allowing SC adhesion and viability. From the conducted studies, it was shown in some cases that KOS/COL material promotes more cell viability than COL hydrogel controls. In addition, SCs were shown to be able to attach to KOS/COL material as seen from focal adhesion immunofluorescent staining, and the expression of actin and vinculin was not seen to decrease in comparison to COL and TCP control groups. Finally, SC invasion and migration was observed to increase as the KOS concentration of KOS/COL material increased. The overall material protein concentration, however, is a point of interest that needs to be investigated further. The results from this study revealed that KOS/COL exhibits the potential to serve as a luminal filler and justifies the pursuit of *in vivo* testing.

4.6. Acknowledgements

The authors thank Dr. Scott Verbridge for the use of the Zeiss LSM 800 confocal microscope. Funding was provided by Virginia Tech Biomedical Engineering and Mechanical (BEAM) departmental and overhead funds.

References

[1] Gordon, T., & Gordon, K. (2010). Nerve regeneration in the peripheral nervous system versus the central nervous system and the relevance to speech and hearing after nerve injuries. *J Commun Disord, 43*(4), 274-285. doi:10.1016/j.jcomdis.2010.04.010

[2] Huebner, E. A., & Strittmatter, S. M. (2009). Axon regeneration in the peripheral and central nervous systems. *Results Probl Cell Differ, 48*, 339-351. doi:10.1007/400_2009_19

[3] Faroni, A., Mobasseri, S. A., Kingham, P. J., & Reid, A. J. (2015). Peripheral nerve regeneration: experimental strategies and future perspectives. *Adv Drug Deliv Rev, 82-83*, 160-167. doi:10.1016/j.addr.2014.11.010

[4] Ide, C. (1996). Peripheral nerve regeneration. *Neurosci Res, 25*(2), 101-121.

[5] Chen, Z. L., Yu, W. M., & Strickland, S. (2007). Peripheral regeneration. *Annu Rev Neurosci, 30*, 209-233. doi:10.1146/annurev.neuro.30.051606.094337

[6] Burnett, M. G., & Zager, E. L. (2004). Pathophysiology of peripheral nerve injury: a brief review. *Neurosurg Focus, 16*(5), E1.

[7] Ribeiro-Resende, V. T., Koenig, B., Nichterwitz, S., Oberhoffner, S., & Schlosshauer, B. (2009). Strategies for inducing the formation of bands of Bungner in peripheral nerve regeneration. *Biomaterials, 30*(29), 5251-5259. doi:10.1016/j.biomaterials.2009.07.007

[8] Siemionow, M., & Brzezicki, G. (2009). Chapter 8: Current techniques and concepts in peripheral nerve repair. *Int Rev Neurobiol, 87*, 141-172. doi:10.1016/S0074-7742(09)87008-6

[9] Pabari, A., Lloyd-Hughes, H., Seifalian, A. M., & Mosahebi, A. (2014). Nerve conduits for peripheral nerve surgery. *Plast Reconstr Surg, 133*(6), 1420-1430. doi:10.1097/PRS.0000000000000226

[10] Gao, Y., Wang, Y. L., Kong, D., Qu, B., Su, X. J., Li, H., & Pi, H. Y. (2015). Nerve autografts and tissue-engineered materials for the repair of peripheral nerve injuries: a 5-year bibliometric analysis. *Neural Regen Res, 10*(6), 1003-1008. doi:10.4103/1673-5374.158369

[11] Ray, W. Z., & Mackinnon, S. E. (2010). Management of nerve gaps: autografts, allografts, nerve transfers, and end-to-side neurorrhaphy. *Exp Neurol, 223*(1), 77-85. doi:10.1016/j.expneurol.2009.03.031

[12] Arslantunali, D., Dursun, T., Yucel, D., Hasirci, N., & Hasirci, V. (2014). Peripheral nerve conduits: technology update. *Med Devices (Auckl), 7*, 405-424. doi:10.2147/MDER.S59124

[13] Muheremu, A., & Ao, Q. (2015). Past, Present, and Future of Nerve Conduits in the Treatment of Peripheral Nerve Injury. *Biomed Res Int, 2015*, 237507. doi:10.1155/2015/237507

[14] Deal, D. N., Griffin, J. W., & Hogan, M. V. (2012). Nerve conduits for nerve repair or reconstruction. *J Am Acad Orthop Surg, 20*(2), 63-68. doi:10.5435/JAAOS-20-02-063

[15] Reid, A. J., de Luca, A. C., Faroni, A., Downes, S., Sun, M. Z., Terenghi, G., & Kingham, P. J. (2013). Long term peripheral nerve regeneration using a novel PCL nerve conduit. *Neuroscience Letters, 544*, 125-130. doi:10.1016/j.neulet.2013.04.001

[16] Klein, S., Vykoukal, J., Felthaus, O., Dienstknecht, T., & Prantl, L. (2016). Collagen Type I Conduits for the Regeneration of Nerve Defects. *Materials, 9*(4). doi:ARTN 219

[17] Xie, F., Li, Q. F., Gu, B., Liu, K., & Shen, G. X. (2008). In vitro and in vivo evaluation of a biodegradable chitosan-PLA composite peripheral nerve guide conduit material. *Microsurgery, 28*(6), 471-479. doi:10.1002/micr.20514

[18] Oh, S. H., Kim, J. H., Song, K. S., Jeon, B. H., Yoon, J. H., Seo, T. B., . . . Lee, J. H. (2008). Peripheral nerve regeneration within an asymmetrically porous PLGA/Pluronic F127 nerve guide conduit. *Biomaterials, 29*(11), 1601-1609. doi:10.1016/j.biomaterials.2007.11.036

[19] Madduri, S., Papaloizos, M., & Gander, B. (2010). Trophically and topographically functionalized silk fibroin nerve conduits for guided peripheral nerve regeneration. *Biomaterials, 31*(8), 2323-2334. doi:10.1016/j.biomaterials.2009.11.073

[20] Yu, W., Jiang, X., Cai, M., Zhao, W., Ye, D., Zhou, Y., . . . Zhang, Z. (2014). A novel electrospun nerve conduit enhanced by carbon nanotubes for peripheral nerve regeneration. *Nanotechnology, 25*(16), 165102. doi:10.1088/0957-4484/25/16/165102

[21] Sarker, M., Naghieh, S., McInnes, A. D., Schreyer, D. J., & Chen, X. (2018). Strategic Design and Fabrication of Nerve Guidance Conduits for Peripheral Nerve Regeneration. *Biotechnol J, 13*(7), e1700635. doi:10.1002/biot.201700635

[22] Chen, M. B., Zhang, F., & Lineaweaver, W. C. (2006). Luminal fillers in nerve conduits for peripheral nerve repair. *Ann Plast Surg, 57*(4), 462-471. doi:10.1097/01.sap.0000237577.07219.b6

[23] Pace, L. A., Plate, J. F., Mannava, S., Barnwell, J. C., Koman, L. A., Li, Z., . . . Van Dyke, M. (2014). A human hair keratin hydrogel scaffold enhances median nerve regeneration in nonhuman primates: an electrophysiological and histological study. *Tissue Eng Part A, 20*(3-4), 507-517. doi:10.1089/ten.TEA.2013.0084

[24] Apel, P. J., Garrett, J. P., Sierpinski, P., Ma, J. J., Atala, A., Smith, T. L., . . . Van Dyke, M. E. (2008). Peripheral Nerve Regeneration Using a Keratin-Based Scaffold: Long-Term Functional and Histological Outcomes in a Mouse Model. *Journal of Hand Surgery-American Volume, 33a*(9), 1541-1547. doi:10.1016/j.jhsa.2008.05.034

[25] Williams, L. R. (1987). Exogenous Fibrin Matrix Precursors Stimulate the Temporal

Progress of Nerve Regeneration within a Silicone Chamber. *Neurochemical Research, 12*(10), 851-860. doi:Doi 10.1007/Bf00966306

[26] Williams, L. R., Danielsen, N., Muller, H., & Varon, S. (1987). Exogenous Matrix Precursors Promote Functional Nerve Regeneration across a 15-Mm Gap within a Silicone Chamber in the Rat. *Journal of Comparative Neurology, 264*(2), 284-290. doi:DOI 10.1002/cne.902640211

[27] Matsumoto, K., Ohnishi, K., Kiyotani, T., Sekine, T., Ueda, H., Nakamura, T., . . . Shimizu, Y. (2000). Peripheral nerve regeneration across an 80-mm gap bridged by a polyglycolic acid (PGA)-collagen tube filled with laminin-coated collagen fibers: a histological and electrophysiological evaluation of regenerated nerves. *Brain Res, 868*(2), 315-328.

[28] Toba, T., Nakamura, T., Lynn, A. K., Matsumoto, K., Fukuda, S., Yoshitani, M., . . . Shimizu, Y. (2002). Evaluation of peripheral nerve regeneration across an 80-mm gap using a polyglycolic acid (PGA) - collagen nerve conduit filled with laminin-soaked collagen sponge in dogs. *International Journal of Artificial Organs, 25*(3), 230-237.

[29] Rosen, J. M., Padilla, J. A., Nguyen, K. D., Padilla, M. A., Sabelman, E. E., & Pham, H. N. (1990). Artificial Nerve Graft Using Collagen as an Extracellular-Matrix for Nerve Repair Compared with Sutured Autograft in a Rat Model. *Annals of Plastic Surgery, 25*(5), 375-387. doi:Doi 10.1097/00000637-199011000-00006

[30] Rosen, J. M., Padilla, J. A., Nguyen, K. D., Siedman, J., & Pham, H. N. (1992). Artificial Nerve Graft Using Glycolide Trimethylene Carbonate as a Nerve Conduit Filled with Collagen Compared to Sutured Autograft in a Rat Model. *Journal of Rehabilitation Research and Development, 29*(2), 1-12. doi:Doi 10.1682/Jrrd.1992.04.0001

[31] Wang, K. K., Nemeth, I. R., Seckel, B. R., Chakalis-Haley, D. P., Swann, D. A., Kuo, J. W., . . . Cetrulo, C. L., Jr. (1998). Hyaluronic acid enhances peripheral nerve regeneration in vivo. *Microsurgery, 18*(4), 270-275.

[32] Lin, Y. C., Ramadan, M., Van Dyke, M., Kokai, L. E., Philips, B. J., Rubin, J. P., & Marra, K. G. (2012). Keratin gel filler for peripheral nerve repair in a rodent sciatic nerve injury model. *Plast Reconstr Surg, 129*(1), 67-78. doi:10.1097/PRS.0b013e3182268ae0

[33] Potter, N. A., & Van Dyke, M. (2018). Effects of Differing Purification Methods on Properties of Keratose Biomaterials. *Acs Biomaterials Science & Engineering, 4*(4), 1316-1323. doi:10.1021/acsbiomaterials.7b00964

[34] Szot, C. S., Buchanan, C. F., Freeman, J. W., & Rylander, M. N. (2011). 3D in vitro bioengineered tumors based on collagen I hydrogels. *Biomaterials, 32*(31), 7905-7912. doi:10.1016/j.biomaterials.2011.07.001

[35] Topp, K. S., & Boyd, B. S. (2006). Structure and biomechanics of peripheral nerves: nerve

responses to physical stresses and implications for physical therapist practice. *Phys Ther, 86*(1), 92-109. doi:10.1093/ptj/86.1.92

[36] Borschel, G. H., Kia, K. F., Kuzon, W. M., Jr., & Dennis, R. G. (2003). Mechanical properties of acellular peripheral nerve. *J Surg Res, 114*(2), 133-139. doi:10.1016/s0022-4804(03)00255-5

[37] Chang, H. M., Shyu, M. K., Tseng, G. F., Liu, C. H., Chang, H. S., Lan, C. T., . . . Liao, W. C. (2013). Neuregulin facilitates nerve regeneration by speeding Schwann cell migration via ErbB2/3-dependent FAK pathway. *PLoS One, 8*(1), e53444. doi:10.1371/journal.pone.0053444

[38] Liu, Q. Y., Miao, Y., Wang, X. H., Wang, P., Cheng, Z. C., & Qian, T. M. (2019). Increased levels of miR-3099 induced by peripheral nerve injury promote Schwann cell proliferation and migration. *Neural Regen Res, 14*(3), 525-531. doi:10.4103/1673-5374.245478

[39] Qian, T. M., Zhao, L. L., Wang, J., Li, P., Qin, J., Liu, Y. S., . . . Zhou, S. L. (2016). miR-148b-3p promotes migration of Schwann cells by targeting cullin-associated and neddylation-dissociated 1. *Neural Regen Res, 11*(6), 1001-1005. doi:10.4103/1673-5374.184504

[40] Qin, J., Wang, L., Zheng, L., Zhou, X. Y., Zhang, Y. D., Yang, T. T., & Zhou, Y. M. (2016). Concentrated growth factor promotes Schwann cell migration partly through the integrin beta 1-mediated activation of the focal adhesion kinase pathway. *International Journal of Molecular Medicine, 37*(5), 1363-1370. doi:10.3892/ijmm.2016.2520

[41] Chaudhry, N., Bachelin, C., Zujovic, V., Hilaire, M., Baldwin, K. T., Follis, R. M., . . . Filbin, M. T. (2017). Myelin-Associated Glycoprotein Inhibits Schwann Cell Migration and Induces Their Death. *Journal of Neuroscience, 37*(24), 5885-5899. doi:10.1523/Jneurosci.1822-16.2017

[42] Wang, Y., Shan, Q., Pan, J., & Yi, S. (2018). Actin Cytoskeleton Affects Schwann Cell Migration and Peripheral Nerve Regeneration. *Front Physiol, 9*, 23. doi:10.3389/fphys.2018.00023

[43] Anderson, P. N., Nadim, W., & Turmaine, M. (1991). Schwann-Cell Migration through Freeze-Killed Peripheral-Nerve Grafts without Accompanying Axons. *Acta Neuropathologica, 82*(3), 193-199. doi:Doi 10.1007/Bf00294445

[44] Maniwa, S., Iwata, A., Hirata, H., & Ochi, M. (2003). Effects of neurotrophic factors on chemokinesis of Schwann cells in culture. *Scand J Plast Reconstr Surg Hand Surg, 37*(1), 14-17.

[45] Sung, H. W., Chang, Y., Liang, I. L., Chang, W. H., & Chen, Y. C. (2000). Fixation of biological tissues with a naturally occurring crosslinking agent: fixation rate and effects of pH, temperature, and initial fixative concentration. *J Biomed Mater Res, 52*(1), 77-87. doi:10.1002/1097-4636(200010)52:1<77::aid-jbm10>3.0.co;2-6

[46] Yoo, J. S., Kim, Y. J., Kim, S. H., & Choi, S. H. (2011). Study on genipin: a new alternative natural crosslinking agent for fixing heterograft tissue. *Korean J Thorac Cardiovasc Surg, 44*(3), 197-207. doi:10.5090/kjtcs.2011.44.3.197

[47] Stricker, J., Falzone, T., & Gardel, M. L. (2010). Mechanics of the F-actin cytoskeleton. *Journal of Biomechanics, 43*(1), 9-14. doi:10.1016/j.jbiomech.2009.09.003

[48] Seddon, H. J., Medawar, P. B., & Smith, H. (1943). Rate of regeneration of peripheral nerves in man. *J Physiol, 102*(2), 191-215. doi:10.1113/jphysiol.1943.sp004027

[49] Chieh, H. F., Sun, Y., Liao, J. D., Su, F. C., Zhao, C., Amadio, P. C., & An, K. N. (2010). Effects of cell concentration and collagen concentration on contraction kinetics and mechanical properties in a bone marrow stromal cell-collagen construct. *J Biomed Mater Res A, 93*(3), 1132-1139. doi:10.1002/jbm.a.32606

[50] Hesse, E., Hefferan, T. E., Tarara, J. E., Haasper, C., Meller, R., Krettek, C., . . . Yaszemski, M. J. (2010). Collagen type I hydrogel allows migration, proliferation, and osteogenic differentiation of rat bone marrow stromal cells. *J Biomed Mater Res A, 94*(2), 442-449. doi:10.1002/jbm.a.32696

Chapter 5

Conclusions and Future Steps

Nils A. Potter

Virginia Polytechnic Institute and State University, Department of Biomedical Engineering and Mechanics, School of Biomedical Engineering and Sciences, Blacksburg, VA 24061

5.1. Overall Project Conclusion

Natural biomaterials have distinct advantages over synthetic polymers, most notably biological recognition and/or acceptance in living systems. But natural biopolymers exhibit deficiencies as well, most often those associated with mechanical strength. Making improvements to natural biomaterials are paramount when trying to use them in a tissue regeneration environment. Improvements to such biomaterials can result from a variety of approaches including alteration of the extraction/purification method of the biomolecule itself, direct synthesis (e.g. recombinant DNA technology), chemical modification (including crosslinking), and blending with either natural or synthetic polymers.

This dissertation primarily explores improving the mechanical strength of keratin biomaterials, while preserving its inherent biochemical and biological characteristics (e.g. enzyme-mediated degradation resistance, cell compatibility, cellular recognition). Specifically, oxidized keratin or keratose (KOS), which is one of the mechanically weakest keratin derivatives in use as a biomaterial. In the present work, methods for increasing the mechanical strength of hydrogels made from KOS obtained from human hair fibers through improvement in extraction and purification methods were explored. A higher purity KOS resulted that differed significantly from samples made using conventional techniques, which was then blended with collagen (COL) to leverage inherent electrostatic interactions and improve mechanical strength even further. Finally, in a proof-of-concept study, a KOS/COL blend was investigated for potential use in a peripheral nerve regeneration application.

This work succeeds in determining the effect that different purification methods have on KOS as a bulk material, and afforded techniques to blend KOS with COL to produce molecular coordination that generated mechanically strong hydrogel networks. This outcome allowed for

formulation of hydrogels that could be used as a luminal filler matrix for peripheral nerve repair conduits, which were shown to support Schwann cell infiltration, migration and growth, thus suggesting utility in a medical device application.

5.2. Effects of Differing Purification Methods on Properties of Keratose Biomaterials

The first aim of the project was focused on investigating the effects that differing dialysis conditions have on KOS characteristics both as a bulk material, in solution, and as a hydrogel construct. The extraction process for KOS includes many steps including oxidation of hair fibers, solubilization of cortical proteins, solids separation, removal of process reagents and low molecular weight oxidation/hydrolysis by-products, and lyophilization. Other studies on the extraction of KOS mostly focus on utilization of different extraction solutions but do not explore the effect of dialysis conditions (namely, dialysate composition) during the purification step, particularly as these relate to resulting material characteristics. In the keratin literature, the dialysate of choice is almost always pure water. The results from this study revealed that KOS dissolved in water favors a propensity for aggregation, likely resulting from the inherent capacity of keratin for self-assembly. From this finding, it was hypothesized that KOS would undergo aggregation during the dialysis/ultrafiltration step, which would lead to retention of low molecular weight contaminants as well as increased fouling of the ultrafiltration membrane, thereby increasing the effective molecular weight cutoff and exacerbating the contamination problem. This hypothesis was confirmed through size-exclusion chromatography when the material extracted using water as a dialysate was shown to have a higher retention time than material extracted using phosphate buffer solution suggesting that the overall molecular weight of water dialyzed KOS was lower than phosphate buffer dialyzed KOS. It was further established that increased peptide content resulting from dialysis had a significant effect on mechanical and

degradation properties with water dialyzed KOS resulting in weaker hydrogels but less prone to enzymatic degradation than the phosphate buffer dialyzed KOS. In conclusion, we determined that selection of dialysate for KOS extraction is of great importance and can have a significant effect on the final KOS product.

5.3. Fabrication and Characterization of a Novel Keratose/Type I Collagen Biomaterial

The second aim of the project was to leverage the potential for molecular coordination associated with COL (alkaline isoelectric point) with KOS (acidic isoelectric point) to create a blended material that would be better suited for tissue regeneration purposes. Past *in vivo* studies have used KOS hydrogels at concentrations between 15-20 wt%. This high solids content may not be optimal for cell infiltration and the downstream remodeling that accompanies most tissue regeneration approaches. Improvements to extraction methods along with the addition of chemical crosslinking of the network structure, have aided in lowering the concentration needed to attain mechanically stable, pure KOS hydrogels to between 8-12 wt%, but this is still considered high. This study succeeded in creating and characterizing a KOS/COL blend that allowed for the formation of a mechanically stable hydrogel that did not result in any material separation at concentrations as low as 0.5 wt% total protein content. In addition, other characterization techniques such as scanning electron microscopy for microarchitecture investigation, differential scanning calorimetry for thermal stability determination, enzymatic degradation, and cell viability studies were conducted. We were able to conclude that the formation of a KOS/COL blend allows for the creation of a mechanically strong hydrogel that includes KOS on a scale of 3-4 mg/ml (0.3-0.4 wt%) while still maintaining beneficial cell compatibility.

5.4. Schwann Cell Behavior and Interaction with a Keratose/Type I Collagen Material

The third aim of this project was to assess the effects that this KOS/COL blend had on Schwann cells (SCs) for the purpose of investigating its potential use as a peripheral nerve conduit luminal filler. As mentioned previously, KOS material used as a hydrogel construct was formulated at high concentrations to maintain structural integrity in previous studies. When introducing this high-solids-content material into a peripheral nerve regeneration environment, it can be more difficult for cells to migrate through the matrix or remodel it after initial stages of tissue regeneration. From this work, the use of a KOS/COL blend in an *in vitro* setting revealed that SCs experienced similar, and in some cases better, viability when compared to control COL hydrogels. In addition, SCs were able to form focal adhesions to the KOS/COL material, an important indication that normal cell physiology can result following attachment to the substrate. In cell migration studies, SCs were found to be able to migrate through a KOS/COL hydrogel layer as seen in invasion assays in the presence of a chemoattractant. This, however, revealed that SC migration is heavily dependent on time as well as hydrogel concentration. In the custom migration assay, the SC migration distance could be assessed, but the migration rate was low and variable. Other methods for gauging SC migration rates through these gels are being considered for future studies. The general accepted rate of peripheral nerve regeneration is 1 mm/day, but this does not take into account the added obstacle of SCs attempting to migrate within a luminal filler, a necessary starting point for the nerve regeneration process. Migration through these gels was shown to be significantly slower than this accepted rate, but this was expected given the added obstacle and the lack of trophic factors that would be present in an *in vivo* environment.

5.5. Research Importance and Future Work

Natural biomaterials are widely used in the field of tissue engineering primarily due to their cell and tissue compatibility after implantation compared to other polymer, ceramic, or

metallic-based biomaterials. Compared to other natural biomaterials, keratin is easily extractable and can be produced for a relatively low cost. These qualities are highly advantageous from both a fiscal and a feasibility perspective. In addition, keratin biomaterials have shown promising results in *in vitro* and *in vivo* environments, but further improvements to these materials can be made through modifications to extraction methods as well as combining with other natural biomaterials. This dissertation successfully revealed the effect purification methodologies have on keratin extraction and the resulting bulk biomaterial properties. This research paves the way for further keratin research by offering more pure keratin biomaterials for use in tissue engineering applications.

In addition, this dissertation was successful in creating a blended KOS/COL material and observing the effect this has as a potential peripheral nerve conduit luminal filler application in an *in vitro* setting. KOS hydrogels have been used in numerous tissue regeneration settings but have demonstrated poor bulk qualities (i.e. degradation rate, mechanical stability) even at high concentrations, and anything below these concentrations will not form a stable hydrogel network. This research resulted in the creation of a hydrogel with minimal chemical crosslinking that incorporates KOS into a hydrogel network by taking advantage of COL's self-assembly characteristics at concentrations significantly lower than previously reported.

Finally, this dissertation was also successful at assessing the potential of this KOS/COL blend for implementation as a conduit luminal filler in peripheral nerve regeneration. The KOS/COL blend displayed properties similar to, and in some cases better than, control groups in terms of cell viability and focal adhesion-mediated cell attachment. SCs were able to migrate through KOS/COL hydrogels, but COL controls were shown to allow for increased migration.

This, however, was more than likely due to the disparities in total protein content as the KOS/COL materials were 150% more concentrated than the COL controls.

Future work that builds off this dissertation can be divided into two distinct groups: 1) continuation of the characterization of keratin and further optimizing the extraction method, and 2) continuation of using the KOS/COL material as a peripheral nerve luminal filler in an *in vivo* study.

Numerous extraction methods have been explored when extracting keratin proteins from a variety of sources including skin, wool, hooves, nails, and hair. For keratin extraction from human hair and wool, the most commonly investigated aspect of extraction methodologies is the use of different extraction solvents. The research performed in this dissertation aimed to look at the effect of other steps such as purification (i.e. the dialysis step) to remove the lower molecular weight components from the extraction solution. Further exploration into the dialysis step and investigation of methods that completely mitigate membrane cartridge fouling is paramount, and this work sets the foundation for that research.

In any translational research program, a major milestone is performing an *in vivo* study that is predicated on *in vitro* data, and the *in vitro* work in the present project sets the stage for such endeavors. The next step in gauging the efficacy of KOS/COL as a peripheral nerve conduit luminal filler is implementing this material in an *in vivo* setting. KOS has been used in prior *in vivo* studies as mentioned previously, but the hydrogel material used in these studies contained a solids concentration on the order of 15-20 wt%. Because the subject KOS/COL blend is able to incorporate KOS into the system but not at a high level, it allows for adequate cell viability, attachment, and migration, and is therefore a strong candidate to continue on into *in vivo* studies in either a rat or non-human primate animal model.